UNIVERSITÀ DEGLI STUDI FIRENZE

DOTTORATO DI RICERCA IN

SCIENZE CHIMICHE

CICLO XXIX

COORDINATORE Prof. PIERO BAGLIONI

Synthesis and application of novel materials for cleaning and protection of historical documents

Settore Scientifico Disciplinare CHIM/12

Dottorando

Dott. Maria Diletta Pianorsi

_____

(firma)

Tutore

Prof. Rodorico Giorgi

_____

(firma)

Coordinatore

Prof. Piero Baglioni

_____

(firma)

Anni 2013/2016

ABSTRACT

The cleaning of cultural heritage artifacts is a delicate conservation practice that aims to bring the surface to a state that resembles as close to its original status. However, cleaning is an irreversible treatment and thus requires high control and selectivity to avoid risks for the original materials.

Solvent/water sensitive paper artworks are usually soiled by a wide range of contaminants, such as deposits of pollutants, grime, aged adhesives and waxy coatings, which are confined in the surface layer typically characterized by the co-presence of art media (e.g. inks, dyes and pigments).

In order to avoid the drawbacks of traditional cleaning methods, here organic solvents were confined into chemical organogels specifically developed for the cleaning of paper-based artifacts.

The organogels synthesized and studied during this work are based on poly(methyl methacrylate) network (PMMA), a polymer characterized by suitable features, i.e. mechanical strength, adhesiveness, optical transparency and low environmental toxicity. Diethyl carbonate (DEC) and methyl ethyl ketone (MEK) were used as solubilizing and porogenous agents during the organogels synthesis and also as loaded cleaning fluids for the removal of aged pressure sensitive tapes (PSTs) and waxes from paper-based artifacts.

The physico-chemical and mechanical characterization were carried out on several PMMA formulations in order to investigate the synthesis parameters that affect the final properties of the organogels. Attenuated Total Reflection Fourier Transform Infrared Spectroscopy (ATR-FTIR), gravimetric analysis, Thermogravimetry (TGA), Differential Scanning Calorimetry (DSC), Scanning Electron Microscopy (SEM), Small-Angle X-ray Scattering (SAXS) and rheological measurements were performed.

Finally, the best performing organogel formulations were used for the cleaning of contemporary and historical artworks. The PMMA-DEC system was employed for the detachment of PSTs from Federico Fellini's drawing entitled "*Anniversario. 14 Maggio 1957-14 Maggio 1987"*. The PMMA-MEK formulation was applied for the removal of wax spots from the printed book entitled "*In officio et Missa solemni pro defunctis*", of the mid-19th century.

The results of the cleaning treatments were checked through optical microscopy and ATR-FTIR analysis.

PART II – Fundamentals

CHAPTER 3
Gels

CHAPTER 4
Polymers blends

CHAPTER 7
Organogels characterization: methods and instrumental conditions

CHAPTER 8
Results and discussion

PART IV – Cleaning of contemporary and historical paper artworks

CHAPTER 9
Cleaning of paper artworks

INTRODUCTION

Introduction

Cleaning is a conservative procedure that aims to bring the surface to a state that resembles as close to the original appearance of the work of art, indeed it represents the first step in restoration practice. The cleaning simplifies any other conservative actions and it must be specifically tailored for each artifact, which is unique for definition. For this purpose, conservation topics are continuously demanding innovative materials and techniques capable of providing efficient long-term preservation of cultural heritage artifacts.

Traditional methods for the removal of unwanted layers or contaminant coatings may be potentially aggressive and cause irreparable damage to the surface of artworks. Restorers adopted preferentially the use of “free” organic solvents for the removal of undesired materials. However, recently studies have shown that traditional solvents exhibit two main disadvantages: poor selectivity and poor controllability in terms of solubilization power and penetration within the layers of the works of art.

In this context, in the last decades novel cleaning systems have been developed. For example, nanostructured fluids has given the opportunity to discontinue the use of neat solvents: water-based systems, such as microemulsions and micellar solutions, are efficient in the swelling, solubilization and removal of hydrophobic coatings. Water-based systems are straightforward and optimal for several applications yet, in some cases, some limitations can persevere. Wherever the artifact is composed of water-sensitive materials (e.g. cellulose-based materials), then water-based systems can become potential stressing agents to the physicochemical stability of substrate. The interaction of water with the

hydrophilic materials may cause mechanical stresses by swelling or solubilization processes and then may cause irreparable damages.

The use of confining systems, able to restrict the penetration of cleaning agents into the artifact surface offers an increased control of the treatments. Currently, conservators and restorer have adopted new cleaning tools based on gel technology. For example, thickeners (e.g. cellulose ethers and polyacrylic acids), solvent gels and polysaccharide gels (e.g. agar-agar and gellan gum) are commonly used. However, these systems present important drawbacks related to the presence of gel residues after treatments and evident spreading of the confined liquid is still observed, even if minimized with respect to the free system.

In the past ten years, the studies carried out at CSGI (Center for Colloids and Surface Science) have largely contributed to the development of innovative gelled systems, able to be effective and versatile and, at the same time, to overcome some of the main drawbacks related to the use of the mentioned "traditional gels".

Highly viscous polymer dispersions (e.g., rheoreversible polyallylamine based organogels, viscoelastic polyvinyl alcoholborate based gels) and chemical hydrogel based on semi-interpenetrating polymer networks (SIPNs) (p(HEMA)/PVP semi-IPN hydrogels) were largely studied and applied for conservation purpose.

Beside chemical hydrogels, another important class of chemical gel, named as organogel, presents a series of attractive features to be further investigate. Organogels are characterized by the presence of organic solvent, which is used both for synthesis and as cleaning fluid loaded within the polymeric matrix. These systems showed to be useful in the cleaning of artworks because they

allow the controlled delivery of fluids, the decrease in solvent evaporation, and the easy residue-free removal from artistic surfaces.

The aim of this thesis was the development of new cleaning systems based on chemical organogels in order to improve traditional cleaning technology by reducing the given drawbacks. In particular, these systems are tailored for the cleaning of water/solvent sensitive paper-based artifacts.

The organogel systems synthesized, characterized and applied during this project are mainly designed for the removal of waxy layers and for the detachment of pressure sensitive tapes (PSTs) from paper supports. Due to their cohesive force, chemical gels can be easily removed from any surface without breaking or leaving residues. The retentiveness of the organogel network can be adjust tuning the amount of cross-linker and the monomer-solvent phase ratio during the synthesis, which is carried out through the free radical polymerization of monomer in pure solvent. Solvent used for the gel preparation can be changed in order to targeting the removal of different coatings from surface of works of art. In particular, the properties of poly(methyl methacrylate) (PMMA) as polymer network and the main features of diethyl carbonate (DEC) and methyl ethyl ketone (MEK), as solvents used for the synthesis of organogels and as cleaning fluid loaded within gels, were studied.

Diethyl carbonate, a typical alkyl carbonate, is one of the most studied solvent mainly for its properties of nontoxicity and biodegradability. DEC was selected during this work as potential cleaning agent for conservation of paper artifacts. In fact, DEC was used both for synthesis of polymeric network and as confined solvent in order to develop innovative PMMA organogels for the removal of pressure sensitive tapes from paper works of art.

2-Butanone, well known as methyl ethyl ketone, is an organic solvent characterized by satisfactory boiling point, good solubility, volatility and stability.

It is widely used in various range of applications, for example as an extraction medium for fats, oils, paraffin waxes and resins and it is also employed in surface coatings, adhesives, printing inks. In this framework, PMMA organogel was synthetized and loaded with MEK, and specifically designed for the selective removal of degraded waxy coatings from the surface of water sensitive surfaces, such as ancient inked paper.

The ability of the PMMA-DEC organogels to match the established conservation issues has been investigated in partnership with Opificio delle Pietre Dure (Florence). Laboratory tests have been performed on paper samples on which different kinds of PSTs (ordinary tape, masking tape, magic tape) and inks (from felt-tip pens and ball-point pens) were applied. Application of PMMA organogels succeed in the removal of PSTs even in case of inks soluble in solvents: dramatic spread of inks is avoided thanks to the retentiveness of gels.

The PMMA-MEK organogels were applied on a 19th century inked book in order to remove spots of paraffin wax that hindered the readability and aesthetic appearance of the artifact. The PMMA-MEK system allowed a safer and more gradual release of solvent on paper surface and led to the gradual swelling and detachment of the wax contaminant. After the cleaning intervention, the gel is removed without leaving polymer residues on the surface, as confirmed by ATR-FTIR analysis.

This dissertation is divided in four parts: conservation issues, fundamentals, experimental and cleaning of contemporary and historical paper artworks.

The conservation issues part is an overall introduction to the cleaning treatment in conservation practice and it reports a description of paper-based cultural heritage artifacts.

Chapter 1 is focused on a comparison between the most used cleaning treatments and the recent innovative cleaning tools developed in order to overtake drawbacks of the traditional cleaning.

In chapter 2 the chemical composition of paper documents and a short history of papermaking processes are described. Moreover, a description of the main unwanted layers and contaminants that can be found on the surface of archival works of art, their physical-chemical properties and the conservative issues are discussed.

In the fundamentals part, the theoretical background of cleaning systems is described based on an in-depth investigation of the relevant literature.

In chapter 3 gels are explained throughout their physico-chemical features. Due to the variety of gel systems, which are the physico-mechanical condition between liquids and solids, a detailed overview on the gel definition is presented as well as the types of classification. Last, examples of gels used as retentive tools for the cleaning of cultural heritage artifacts are detailed.

In chapter 4 the concept of polymer blends is introduced, in order to provide the reader with the basic thermodynamic concepts regarding the interaction that may occur in a blended polymer system and advantages that can be attained through blending process.

Chapter 5 is dedicated to gels having a liquid phase composed totally by organic solvents and for this reason defined “organogels”. Physico-chemical characteristics are detailed considering their structural and mechanical properties. Moreover, the properties of poly(methyl methacrylate) (PMMA) as polymer network and the main features of solvents (diethyl carbonate and methyl ethyl ketone), used for the synthesis of PMMA organogels, are reported.

In the experimental part, the research work is presented in three chapters, whereas the first two concern the synthesis and the physico-chemical

characterization of the developed gel systems, while the last concern the discussion over the obtained results

In chapter 6, the synthesis method is detailed and the compounds used are explained with reference to the literature.

Chapter 7 is dedicated to the physico-chemical characterization of the selected organogel systems. Methods and instrumental conditions are detailed. In particular, a description of Scanning Electron Microscopy (SEM), Small Angle X-ray Scattering (SAXS) and rheological measurement techniques is reported.

In chapter 8, the results of physico-chemical and mechanical characterization of the selected systems are discussed. The presence of unreacted monomer in the polymer network was assessed with Attenuated Total Reflection Fourier Transform Infrared Spectroscopy (ATR-FTIR).

The PMMA network's affinity with the solvent liquid phase is evaluated with evaporation and release cycles through gravimetric measurements and also with calorimetric analysis. In particular, Thermogravimetric Analysis (TGA) was used to check the equilibrium solvent content of the gels, while Differential Scanning Calorimetry (DSC) was employed to determine the fraction of free solvent.

Scanning Electron Microscopy (SEM) was employed to study the macroporosity and the morphology of organogels network; moreover, the mesoporosity and the nanoscale structure of the gel systems were investigated with Small Angle X-ray Scattering (SAXS) to detail the average mesh size and the inhomogeneities domains. The viscoelastic behavior of PMMA systems was checked with mechanical analysis based on rheological measurements.

The final part, cleaning of contemporary and historical paper artworks, reports the application of the selected PMMA-DEC and PMMA-MEK organogel systems for the removal of pressure-sensitive tapes and wax spots, respectively, from paper artifacts.

In chapter 9, the first part is dedicated to a briefly description of paper artworks and the assessment of conservation issues. The physical-chemical characterization of papers, PST and wax was performed through ATR-FTIR technique and optical microscopy.
In the second part of chapter, the cleaning treatments performed on the selected paper artworks through the application of innovative chemical organogels are described and the results will be discussed.

This thesis is the result of a three-year research route performed in the context of the project “Apprendistato di Alta Formazione e Ricerca”, which involved the achievement of professional training at Book Restoration Laboratory of Certosa di Firenze, and the development of research activities at University of Florence.

PART I

Conservation issues

CHAPTER 1

Innovative tools for cleaning of cultural heritage artifacts

1.1 Introduction

Conservation of cultural heritage involves several procedures that allow the long-term protection of artifacts using minimal interventions, suitable materials and reversible methods.

The challenge for conservators worldwide is to achieve compromises between the preservation of original appearance and material properties and the reversibility of treatments. For this purpose, conservation issues are constantly demanding innovative tools capable of providing efficient long-term preservation of works of art.

Within the procedures carried out during conservation treatments, cleaning is one of the most controversial, delicate and potentially harmful operation; the principal aim is to bring the surface of artifact to a state that resembles as close to its original appearance. A correct cleaning operation requires to set-up specifically treatments for each typology of artifact, which is unique for definition.

This chapter is focused on a comparison between the cleaning treatments most used in the last decades and the recent innovative cleaning tools developed in order to overtake the drawbacks of the traditional cleaning.

1.2 Cleaning cultural heritage artifacts

Cleaning is a fundamental step to perform before other interventions on artifact, since it allows the access to the multi-layer artistic surface; it permits to

remove degraded compounds, which could interact with the materials of the artwork that need to be preserved.

Indeed, the term “cleaning” typically refers to the actions related to the removal of grime and soil from the surface, but also to the partial or complete removal of degraded layers such as aged and yellowed varnishes, adhesives or other potentially harmful materials. Since the treatment is irreversible, there are many risks for the artwork: usually the materials to be removed and those belong to the artifact consist in complex layered structures of few hundred of microns, thus a very high control over the cleaning action is required.

However, as reported before, cleaning is a fundamental step to restore the original esthetical features and to improve the readability of the artwork. On the other hand, as stated by Bonsanti, cleaning treatment represents “…*the condition for the access to the surface of the artifact…*” necessary for any further intervention: “… *if there is no access to the artifact, also the conditions for other structural and conservative interventions are generally missing…*” (Bonsanti, 2002).

Through the centuries cleaning was performed using a great variety of materials, such as soaps, alimentary products (wine, vinegar, lemon juice) or even bio fluids (saliva, urine or blood).

In the last decades, the traditional cleaning methods involved principally the use of neat organic solvents for the treatments of artifacts. Anyhow, the main concerns related to the use of this substances are due to the lack of control on solvents penetration within the treated substrate, which can lead to solubilization or leaching of binding medias and thus to detrimental effects. Moreover, the use of some organic solvents implies drawbacks related to their high toxicity, i.e. the issue of operators safety and working environment.

Nowadays, much attention is addressed towards more innovative systems such as gels, thickeners and aqueous cleaning systems to deal with the above-mentioned questions.
The use of aqueous cleaning methods and/or solvents confined within polymeric matrices, such as gels, has been proposed as the more effective way.

It must be noticed that correct cleaning operation requires to set-up specifically tailored treatments for each artifact, by taking into account its organic or inorganic composition (i.e. cellulosic, collagenous, metallic, mineralogical), its conservation condition and the stratigraphic distribution of the surface. Based on these concepts, diagnostic analyses of the artifact, along with historical-artistic researches, should precede the cleaning intervention in order to evaluate the most suitable, effective and less aggressive cleaning methodology to use.
Furthermore, the desired level at which the cleaning action should be stopped has to be defined, based on the definition of *patina* (Brandi, 1977), its historical value and/or the protective role that it may have.
The term *patina* and the related historical-artistic implications, has been object of debates for centuries between two factions: who sustained its drastic, integral removal to re-establish the original aspect with bright and vivid colors/surfaces; those who, on the other hand, defended its authenticity and then assume necessary its preservation (Brandi, 1997; Conti, 2001; Baldinucci, 1681).
Currently, as concern the Italian concept of conservation and restoration, is generally accepted that cleaning methodologies must be differentiate according to the material and to its conservative conditions, and that the patina has not to be completely removed, by performing a selective, gradual and controllable cleaning action.

1.3 Traditional cleaning: “free” organic solvents

Among the “traditional” materials for the cleaning of works of art, organic solvents are probably those considered the more useful tools by restorers. The ease of handling and predictability of their action, the low cost and the fair effectiveness make organic solvents the most common cleaning agents in restoration.

As reported in the previous section, some drawbacks are related to the use of “free” organic solvents, i.e. the risks for the treated artifact and the potential hazard to the health of the operators. In fact, the most common undesired effects during a cleaning treatment can involve, for example, the swelling of binding media, chromatic alterations and the transport and re-deposition of dissolved matter through the porous matrices. These concerns depend on a lack of control in cleaning process, due to impossibility of monitoring penetration and spreading of the solvent within the treated matrix.

Cleaning with solvents is usually achieved according to the principle of “like dissolves like”, choosing a solvent that is considered to have adequate polarity for the solubilization of the undesired material, without affecting the underlying layers. However, rarely the substrate results completely inert.

The selection of suitable solvent is based on the definition of its solubility parameters (Hansen, 2007; Teas, 1968) and on practical tests for the determination of polarity of the substances to be removed, as for instance the Feller test (Cremonesi, 1998; Feller, 1976). Conservators can also use interactive digital programs, such as the “*Triasol*” (Cremonesi, 1999).

The final evaluation of selectivity performed by operators with a simple visual analysis is obviously unable to detect possible undesired consequences on a microscopic or molecular level. The evaluation of cleaning efficiency can be carried out through specific diagnostic analysis; for instance, Burnstock and

Learner evidenced through electron microscope analysis erosion phenomena of the treated surface after removal of aged mastic varnish by means of alkaline substances (Burnstock and Learner, 1992). Furthermore, the removal of oxidized varnishes frequently requires the use of highly polar solvents that are known to cause swelling and leaching of low-molecular weight components of the binding medium, causing stiffening and embrittlement of the surface layers. This effect has been reported on both oil and tempera paint films (Khandekar et al., 1994; Phenix and Sutherland, 2001).

Besides the risks related to the preservation of the artifact, it must to be considered the high toxicity of many organic solvents, that means that is difficult grant safe working conditions in restorer's workshops. The increased awareness on safety of the working environment resulted in looking for alternative products able to be effective and, at the same time, less harmful for the operators.

1.4 Innovative cleaning tools

In order to avoid the above problems related to the use of neat organic solvents, novel systems have been recently developed by the Center for Colloid and Surface Science research group (CSGI).

The research performed at CSGI, in the field of cleaning of works of art, is mainly focused on the formulation and assessment of innovative tools, specifically tailored for each artifacts typology (i.e. organic or inorganic).

In the last few years several surfactant-based cleaning fluids, such as microemulsions and micellar solutions, have been formulated for cultural heritage conservation (Baglioni et al., 2014(b), 2012 (a); Giorgi et al., 2010; Carretti et al., 2003, 2007). These systems exhibit significant advantages with respect to traditional cleaning methods, mostly since they are water-based systems. Microemulsions and micellar solutions promote the solubilization

and/or the swelling of grime and polymer coatings, causing their detachment from the artistic substrates; furthermore, the hydrophilic barrier, provided by the fluids continuous phase (water), avoids the penetration of the detached hydrophobic material within the porous matrix of the substrate. Moreover, the impact on health of operators is drastically reduced because of the low content of organic solvents.

At the same time, the research work at CSGI was focused on the confinement of cleaning fluids and organic solvents within a gel matrix (polymer network) that release them onto the surface of the work of art in a controlled way. The confinement within a polymeric network introduces several advantages such as the slow release of solvents, solutions or emulsions across the gel-artifact interface, the decrease of evaporation rate of confined fluids/solvents, and the better control over the diffusion of cleaning systems and dissolved grime through the artifact layers.

These requirements resulting in the development of several gel formulations with key features, such as improved mechanical properties (i.e. easy handling and lack of gel residues) and high retentiveness (i.e. control of cleaning action).

The following sections will provide a briefly description of the main innovative formulations for the cleaning of cultural heritage artifacts.

1.4.1 Nanostructured systems

Aqueous methods allow to reduce the toxicity of the cleaning systems, to control the cleaning efficiency and the interaction with the substrate by varying the properties of the system. In the last decades, Wolbers has been one of the major promoters of the use of aqueous methods for cleaning painted surfaces (Wolbers, 2000); his approach is based on the addition of other compounds to

water (used as a solvent), as for instance acids and alkalis, surfactants, chelating agents or enzymes.

In this way, cleaning systems can be modified by modulating some parameters such the solutions viscosity, the pH and the ionic strength in order to obtain aqueous system becomes able to interact also with materials originally not soluble in water. As for solvents, interactive digital programs were created to provide practical guidelines for the testing of the suggested aqueous cleaning systems (Stavroudis et al., 2005).

A significant contribution to aqueous cleaning methods was introduced by the developments of nanostructured cleaning fluids, since the first application in the late 1980s (Borgioli et al., 1995). Nowadays several systems have been developed and successfully applied, as reported extended in literature (Baglioni et al., 2014, 2012; Carretti et al., 2007, 2003).

Microemulsion is surfactant-based colloidal system that has been widely used for the cleaning of cultural heritage artifacts. This system is defined as a "*liquid, stable and homogeneous, optically transparent, isotropic and 'spontaneously' formed system, comprising two liquids mutually insoluble…stabilized by at least a monolayer of amphiphilic molecules (surfactants)*" (Danielsson and Lindman, 1981).

In an oil-in-water microemulsion water represents the continuous phase where the organic solvent (oil) is dispersed, thanks to formation of micro- or nano-sized micelles stabilized by the presence of a surfactant (figure 1.1).

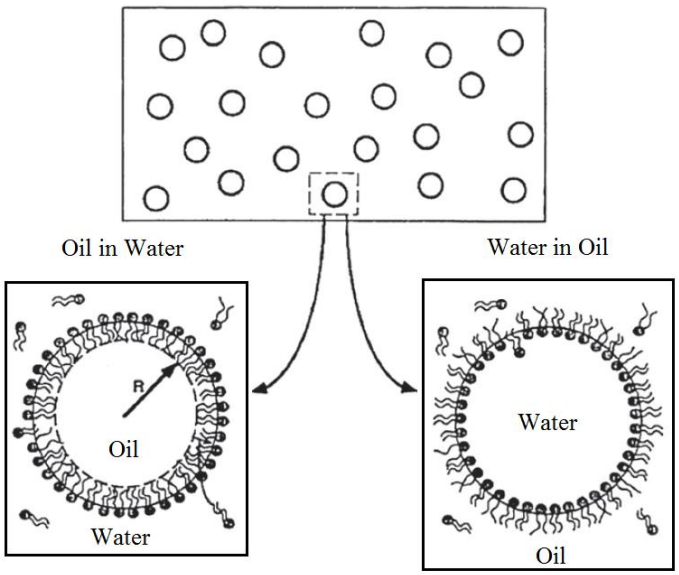

Figure 1.1. Representation of direct (o/w) and inverse (w/o) microemulsions. (Readapted from Evans and Wennerström, 1999).

Oil-in-water microemulsions are thermodynamically stable and optically transparent; the continuous phase (i.e. water) represents the major component (75-99%), while the quantities of organic components (i.e. solvents and surfactants) are reduced (0,5-15%).

The main advantages related to the use of microemulsions with respect to conventional cleaning systems are reported:

- Oil-in water formulations require very small amounts of solvents and the presence of aqueous medium permits a general reduction of the evaporation rate; thus, a consistent depression of toxicity and environmental impact is achieved.
- Diffusion of solubilized material (organic coatings, wax, etc.) within the porous matrix of artifact can be limited since the hydrophilic aqueous phase surrounds the removed hydrophobic material; hydrophilic phase acts as a barrier and may prevent re-deposition into the substrate porosity.

- Owing to their small size, nano-droplets within a microemulsion are characterized by a huge exchange surface area; such extended interface maximizes the interaction with the detrimental layer facilitating its swelling/solubilization.

The application of aqueous solutions and water-based systems is generally discouraged on water-sensitive substrates as canvas, preparation layers, paper artworks, leather bookbinding, gypsum or wood. Swelling phenomena induced by water absorption in these hydrophilic materials can lead to mechanical stress and thus the embrittlement of substrate or the solubilization of water-soluble components. However, aqueous methods applied in a confined form are successfully used for the cleaning of water-sensitive artifacts, such as collagenous materials. A recent research is focused on the cleaning of historical leather samples by confining an oil-in-water (o/w) nanostructured fluid in a highly retentive chemical hydrogel, which allows the controlled release of the cleaning fluid on sensitive surfaces (Baglioni et al., 2016).

1.4.2 Polymeric systems

The confinement of cleaning systems within gel network permits to minimize drawbacks related to the use of free fluids/solvents. In this way, the release of cleaning agents occurs gradually onto the treated substrate; the controlled release allows to address the task of removing undesired layers without affecting the materials pertaining to the artifact, either chemically or physically.

A gel can be defined as a three-dimensional solid network immersed in a fluid or, in a larger sense, as a soft material where the interconnected polymer chains entrapping a liquid. The polymer is called “gelator” or “gellant”.

The term “hydrogel” is used when the liquid phase is water, while “organogel” is a gel that confines organic solvents.

Another criterion used for classification of gels take into account the type of interactions that build the network between the polymer chains. In “physical gels” the interactions are secondary bonds, i.e. non-covalent interactions between the macromolecular chains. Instead, in “chemical gels” the polymer network is formed by covalent bonds (e.g. cross-links between polymer chains), which are more than ten times stronger than a hydrogen bond. In this case, the three dimensional network can be considered as a single huge molecule (figure 1.2).

In chapter 3 a comprehensive overview of the gel and the ‘gel-like’ systems will be reported.

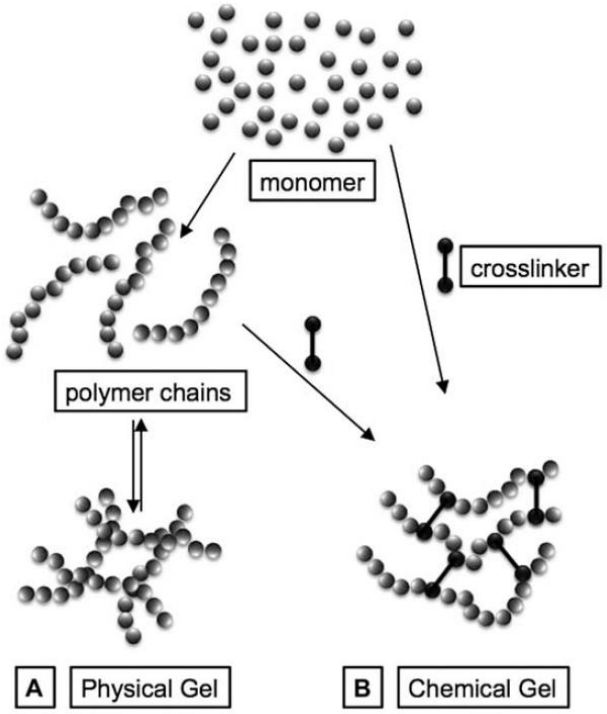

Figure 1.2. (A) gel formation through physical association of polymer chains (physical gel); (B) gel made by polymerization and crosslinking (chemical gel). Readapted from Baglioni and Chelazzi, 2013.

Advantages entailed by the confinement of cleaning fluids within gels or highly viscous matrices can be summarized as follows:

- The increase in viscosity drastically lowers the degree and the rate of penetration into the porous substrate thus, the cleaning action is selectively limited at the interface between the artifacts surface and the environment.
- High viscosity reduces the mobility of solutes inside the gel phase thus, the rate of solubilization is much lower with respect to solubilization with a free fluid phase; lower solubilization kinetics allow higher control on the cleaning action.
- Interaction of the liquid phase with gel network results in a drastic decrease of evaporation rate, with a strong reduction of toxicity issues.
- Gel systems are very versatile; in fact, they can be used as carriers for both organic solvents and aqueous fluids (i.e. enzymes, chelating agents, microemulsions, etc.).
- Gels can be used on a great variety of supports; although the use of gels was introduced specifically for the cleaning of easel paintings, nowadays they have found application on the treatment of wide array of painted supports, such as glass (Valentin et al., 1996), metals (Tomozei and Balta, 1998), feathers (Da Silveira, 1997), leather (Baglioni et al., 2016).

A brief but comprehensive overview of the classes of gels currently used in restoration and the most recent developments in these field will be provided in chapter 3 (see sections 3.3 and 3.4).

1.5 Final remarks

It is important to recall that since cultural heritage artifacts are unique, each case study exhibits specific characteristics and a universally valid cleaning procedure does not exist.

It is important to know that an efficient gel system for restoration practice requires specific characteristics, summarized as follows:

- High retention features are necessary to grant low diffusivity rates of the cleaning system within the artifacts matrix and thus, permit a controlled cleaning action. Moreover, the reduction of fluid volatility leads to a decrease of toxicity.
- Ease of handling and residue-free removal are usually achieved by enhancing mechanical or elastic properties of polymeric system. As a general rule, the stronger are interactions between the macromolecules forming the gel network, the more enhanced are gels mechanical features owing to stronger cohesive forces. In fact, the synthesis of chemical gels represents a possible strategy to avoid residues.
- Good adhesion properties are necessary to grant a homogeneous interaction and thus a uniform cleaning action. Being mechanically adjustable, physical gels usually provide better adhesion; this feature is especially required on irregular or molded surfaces.
- Versatility is a paramount characteristic, in terms of adaptability to different cleaning issues, that is, the removal of the various classes of detrimental materials that might be found on artifacts surfaces. From a practical point of view, this means that an organogel must be able to load and retain an array of solvents, while a hydrogel must be able to be used in association with different aqueous cleaning fluids.

- Chemical inertness towards the original materials composing the artifact is necessary.

It is improbable that a single gel formulation displays these features all together: the most appropriate choice for each case study will be dictated, case-by-case, by the specific needs and characteristics of the artifact.

References

Baglioni, M.; Bartoletti, A; Bozec, L.; Chelazzi, D.; Giorgi, R.; Odlyha, M.; Pianorsi, D.; Poggi, G.; Baglioni, P. 2016. Nanomaterials for the cleaning and pH adjustment of vegetable-tanned leather. Appl. Phys. A 122, 114.

Baglioni, P.; Berti, D.; Bonini, M.; Carretti, E.; Dei, L.; Fratini, E.; Giorgi, R. 2014. Micelle, microemulsions, and gels for the conservation of cultural heritage. Adv. Colloid Interface Sci., Special Issue in honor of Bjorn Lindman 205, 361–371.

Baglioni M.; Giorgi, R.; Berti, D.; Baglioni, P. 2012 (a). Smart cleaning of cultural heritage: a new challenge for soft nanoscience. Nanoscale 4, 42–53.

Baglioni M.; Berti, D.; Teixeira, J.; Giorgi, R., Baglioni P. 2012 (b). Nanostructured surfactant-based systems for the removal of polymers from wall paintings: a small-angle neutron scattering study. Langmuir 28, 15193–15202.

Baldinucci, F. 1681. Vocabolario toscano dell'Arte del disegno.

Bonsanti, G. 2002. Storia ed Etica della Pulitura, in: Colore E Conservazione: Materiali E Metodi Nel Restauro Delle Opere Policrome Mobili. Presented at the CESMAR7, Il Prato, Piazzola sul Brenta, pp. 14–15.

Borgioli, L.; Caminati, G.; Gabrielli, G.; Ferroni, E. 1995. Removal of hydrophobic impurities from pictorial surfaces by means of heterogeneous systems. Sci. Technol. Cult. Herit. 4, 67–74.

Brandi, C. 1997. Teoria del restauro. Einaudi. Torino.

Burnstock, A.; Learner, T. 1992. Changes in the surface characteristics of artificially aged mastic varnishes after cleaning using alkaline reagents. Stud. Conserv. 37, 165–184.

Burnstock, A.; White, R. 1990. The Effects of Selected Solvents and Soaps on a

Simulated Canvas Painting. In Cleaning, Retouching and Coatings, ed. Mills, J.S. and Smith, P., London: International Institute for Conservation of Historic and Artistic Works, pp. 111-118.

Carlyle, L.; Townsend, J.H.; Hackney, S. 1990. Triammonium Citrate: an Investigation into its Application for Surface Cleaning in Dirt and Pictures Separated, ed. Hackney, S., Townsend, J. and Eastaugh, N. London: United Kingdom Institute for Conservation, pp.44-48.

Carretti, E.; Giorgi, R.; Berti, D.; Baglioni, P. 2007. Oil-in-Water nanocontainers as low environmental impact cleaning tools for works of art: two case studies. Langmuir 23:6396–6403.

Carretti E.; Dei L.; Baglioni, P. 2003. Solubilization of acrylic and vinyl polymers in nanocontainer solutions. Application of microemulsions and micelles to cultural heritage conservation. Langmuir 19, 7867–7872.

Conti, A. 2001. Manuale di restauro. Einaudi Editore.

Cremonesi, P. 1999. Un approccio più scientifico alla pulitura dei dipinti: Triansol, il triangolo delle solubilità, un software per il restauro. Progetto Restauro 6, 42–45.

Cremonesi, P. 1998. Un approccio più scientifico alla pulitura dei dipinti: il test di solubilità di Feller. Progetto Restauro, 38–42.

Da Silveira, L. 1997. A note on the poultice cleaning of feathers using Laponite RD gel. Stud. Conserv. 42, 11–16.

Danielsson, I.; Lindman, B. 1981. The definition of microemulsion. Colloid Surface 3, 391–392.

Evans, D.F.; Wennerström, H. 1999. The colloidal domain: where physics, chemistry, biology, and technology meet (2nd ed.). Wiley, New York.

Feller, R.L. 1976. The Relative Solvent Power Needed to Remove Various Aged

Solvent Type Coatings, in: Conservation and Restoration of Pictorial Art. Bromelle and Smith, London.

Giorgi R.; Baglioni, M.; Berti, D. et al. 2010. New methodologies for the conservation of cultural heritage: micellar solutions, microemulsions, and hydroxide nanoparticles. Acc. Chem. Res. 43, 695–704.

Hackney, S.; Townsend, J.; Eastaugh, N. 1990. Dirt and Pictures Separated. London: United Kingdom Institute for Conservation.

Hansen, C.M. 2007. Hansen Solubility Parameters: A User's Handbook, Second Edition. CRC Press.

Hedley, G.; Odlyha, M.; Burnstock, A.; Tillinghast, J. and Husband, C. 1990. A Study of the Mechanical and Surface Properties of Oil Paint Films treated with Organic Solvents and Water. In Cleaning, Retouching and Coatings, ed. Mills, J.S., and Smith, P., London: International Institute for Conservation of Historic and Artistic Works, pp. 98-106.

Khandekar, N.; Dorge, V.; Khanjian, H.; Stulik, D.; de Tagle, A. 2002. Detection of residues on the surfaces of objects previously treated with aqueous solvent gels. In ICOM-CC 13th Triennial meeting Rio de Janeiro, pp. 352-359.

Khandekar, N.; Phenix, A.; Sharp, J. 1994.Pilot study into the effects of solvents on artificially aged egg tempera films. The Conservator 18, 62–72.

Khanjian, H.; Dorge, V.; de Tagle, A.; Maish, J.; Considine, B.; Miller, D.; Khandekar, N. 2002. Scientific investigation of surface cleaning processes: quantitative study of gel residue on porous and topographically complex surfaces. In ICOM-CC 13th Triennial meeting Rio de Janeiro, pp. 245–251.

Phenix, A.; Sutherland, K. 2001. The cleaning of paintings: effects of organic solvents on oil paint films. Rev. Conserv. 2, 47–60.

Stavroudis, C.; Doherty, T; Wolbers, R. 2005. A New Approach to Cleaning I: Using Mixtures of Concentrated Stock Solutions and a Database to Arrive at an Optimal Aqueous Cleaning System. WAAC Newsl. 27, 17–28.

Teas, J.P. 1968. Graphic analysis of resin solubilities. J. Paint Technol. 40, 19–25.

Tomozei, M.; Balta, Z. 1998. La restauration d'une plaque de corselet (Iran, 17éeme siécle), in: Metal 98: Proceedings of the International Conference in Metals Conservation. Draguignan- Figanières. James & James, London, pp. 27–29.

Valentin, N.; Sanchez, A.; Herraez, I. 1996. Analyses of Deteriorated Spanish Glass Windows, Cleaning Methods using Gel Systems, in: Preprints of the ICOM Committee for Conservation. Presented at the IIth triennal meeting in Edinburgh, Scotland, James & James, London, pp. 851–856.

Wolbers, R. 2002. Cleaning Painted Surfaces: Aqueous Methods. London: Archetype Publications.

Wolbers, R. 2000. Aqueous Methods for Cleaning Painted Surfaces. London: Archetype Publications.

CHAPTER 2

Historical paper documents and unwanted substances: a briefly review

2.1 Introduction

Historical paper documents such as books, manuscripts and drawings represent the most abundant historically valuable heritage (Wouters, 2008). According to their physico-chemical properties, these artefacts are composed of water sensitive materials, starting from their cellulose-based support up to the presence of coloring matter over a thin surface layer, which can make them also solvent sensitive.

The natural ageing of these artifacts depends on several factors, some of them connected to environmental conditions, and others associated with the papermaking technique. During the last decades, the conservative issues related with natural ageing of paper documents were widely studied (Barrow, 1974; Smith, 1987; Daniels, 1996; Plossi and Zappalà, 2007), as the vast amount of literature evidenced.

Besides the natural ageing, historical collections and archives are typically contaminated by deposits of soiling and detrimental materials, such as aged adhesives or natural polymeric coatings (i.e. wax residues), which can modify the appearance and readability of the artifacts. The presence of these unwanted substances may be due to improper handling or to past restoration interventions.

In the first part of this chapter the chemical composition of paper documents and a short history of papermaking processes are shortly described. The

degradation pathways due to chemical, physical and biological processes are only mentioned, since their influence on the cleaning issues discussed in this dissertation is minimal.
The second part of the chapter is dedicated to a detailed description of the main unwanted layers and contaminants that can be found on the surface of archival works of art. The physical-chemical properties and the conservative issues of these materials are discussed.

2.2 Paper manufacturing among centuries

Cellulose is the main component of a paper document but since the last 19th century, several substances have been commonly added in papermaking processes to provide a sheet with ideal properties. (Bower, 1997; Hunter, 1978). The chemical composition of paper mainly depends on the origin of the fibers, on the chemical treatment of the raw material during pulping and on the additional treatments that may be necessary to refine the quality and improve the properties of the final product. Furthermore, the presence of fillers and additives for the sizing of sheets could affect the features of paper.
During the Middle Ages the major fiber sources were cotton (figure 2.1), linen or other textile fibers obtained from old rags; however, at the end of 15th century, the invention of printing machines caused an increase in the demand of paper support. In order to provide large amounts of pure cellulose the paper industry developed to accelerate the mechanical, and even chemical, treatment of textile rags. The Hollander beater (1680 AD) is the most known facility used to produce paper pulp from cellulose-containing plant fibers, as well as the first continuous papermaking machine invented by Louis-Nicolas Robert (1799 AD).

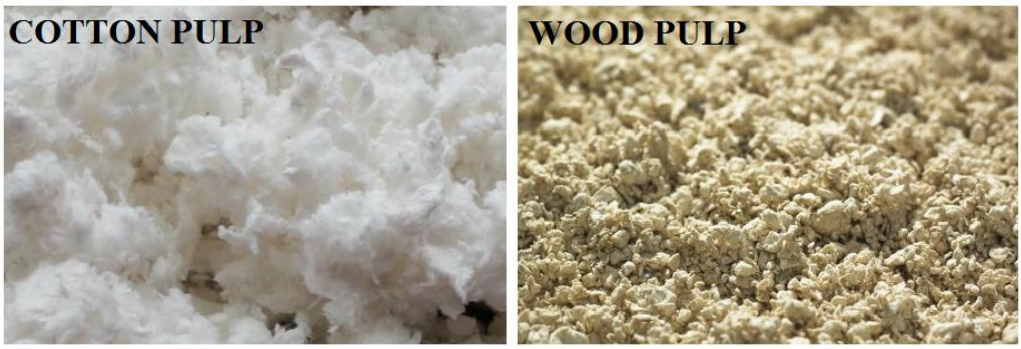

Figure 2.1.Comparison between cotton and wood pulps (digital images).

In the second half of the 19th century, paper production processes were drastically changed by using wood as the raw material to obtain cellulose. In wood pulp (figure 2.1), the fibers are bound together by a polymeric complex composed of lignin linked to hemicellulose. On the contrary, cellulose obtained from cotton plants is relatively pure and characterized by isolated and long linter fibers.

In order to produce high quality paper, wood pulp is highly processed to removal of both hemicellulose and lignin; in fact, the latter is the principal degradation source of cellulosic-based materials. The stability of paper is abundantly reduced during the delignification process known as Kraft method (developed by Carl Dahl in 1884), which is chemically aggressive and promotes the depolymerization of cellulose. In fact, this method is based on the action of alkaline compounds at high temperatures (ranging from 150 to 180 °C) that contributes to alkaline degradation of cellulose.

Beside the changes in production processes, some modifications also occurred in terms of the additives used for the sizing of paper. Sizing is performed to reduce the hydrophilic nature of cellulose and to retard the penetration rate of aqueous fluids, such as inks. While in the European Middle Ages sizing involved the use of animal glue (invented in Fabriano, Italy), producing an excellent

material in terms of chemical and physical stability, at the beginning of the 19th century, the procedure was replaced by addition of aluminum sulfate and amphiphilic rosin (colophony) to pulp during paper production (internal sizing). This sizing method provided great economic advantages and it was used until the beginning of the 20th century when, unfortunately, it was found to be one of the main causes of paper degradation. In fact, the resin acids are responsible for inducing acid-catalyzed hydrolysis. In modern times, acid sizing has been replaced by alkaline sizing paper technology.

2.2.1 Physico-chemical characteristics of paper

Natural cellulose, the main constituent of paper, is a network of chains characterized by entanglement and hydrogen bonds. Cellulose is a carbohydrate produced by plants to construct the highly tensile tissue in cell walls. Pure cellulose is obtained from plant fibers, such as cotton, jute, flax and hemp; moreover, highly vascular plants, such as trees, contain roughly 40–50% cellulose, 15–25% hemicelluloses and 20–30% lignin (Roberts, 1996; Plossi and Zappalà, 2007), are used.

Cellulose is a linear semi-crystalline polysaccharide whose degree of crystallinity ranges between 50 and 90%. The glucose units are linked through a β(1–4)-glycosidic bond, giving long chains that form crystallites. The β position of the –OH on C1 determines a 180° rotation of the following glucose unit around the 1–4 axis of the pyranoside ring; in that way, the steric encumbrance between two units is reduced (figure 2.2). For this reason, the repeating monomeric unit of cellulose is usually given as a disaccharide, formed by two glucose molecules, formally named cellobiose.

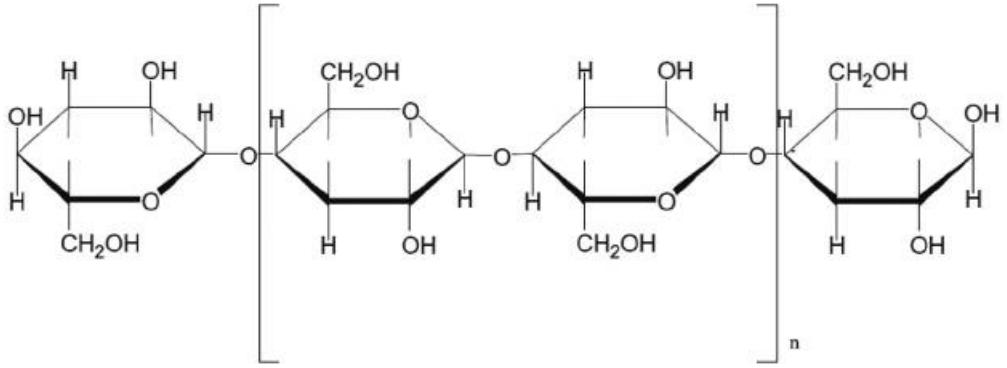

Figure 2.2. Chemical structure of cellulose (Takhur et al., 2014).

The molecular weight of cellulose ranges from $0.5x10^6$ to $2.5x10^6$ g/mol, with the average molar mass reaching $1.5x10^6$ g/mol, or even higher in native cellulose.

The degree of polymerization (*DP*) is the ratio between the molecular weight of the cellulose molecule and the weight of a glucose unit, i.e. the average number of monomer units present in a cellulose chain. The *DP* of native cellulose varying upon the fibers source and can ranges between 9000 and 15000, as well as polydispersity, which is less in cotton and linen cellulose than wood cellulose. The *DP* is an important value because is related to mechanical behavior of fibers: higher the degree of polymerization, higher the mechanical strength.

Despite the scarcer solubility of cellulose in water, its high hygroscopicity is due to the presence of –OH groups, which give hydrogen bonds with the H_2O molecules. Generally, the interaction between cellulose and water molecules depends on the temperature and on relative humidity: cellulose can absorbs water at ambient conditions up to 6–7% of its weight.

Moreover, the supramolecular structure is due to the formation of intramolecular hydrogen bonds between glucose units or intermolecular hydrogen bonds between different chains (figure 2.3). Hydrogen bonding, helped by dipole and Van der Waals interactions, promotes the alignment in parallel strands, resulting in a highly regular sequence and rigid molecular chains.

The chains, characterized by an average distance of 0.54 nm, partly form highly crystalline domains. In pure cotton the crystalline regions cover 70–80% of the cellulose, while the rest exhibits amorphous structure.

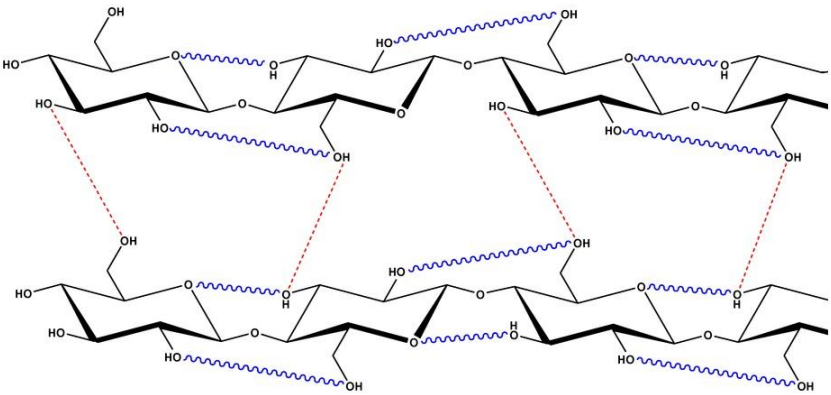

Figure 2.3. Intramolecular (blue lines) and intermolecular (red lines) hydrogen bonds in a cellulose molecule (readapted from Terzopoulou et al., 2015).

The ultrastructure of native cellulose is a random aggregation of elementary fibrils (2–4 nm in cross-section and 100 nm in length) assembled into microfibrils of 10–30 nm width and then grouped into macrofibrils (100–400 nm wide) structured in different cell wall layers (figure 2.4) (Roberts, 1996).

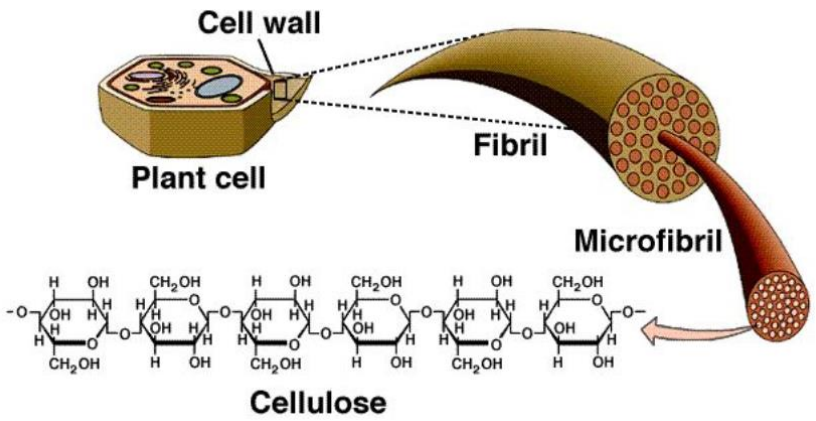

Figure 2.4. Arrangement of fibrils, microfibrils and cellulose in cell wall (Moore et al., 1998).

This structuring of cotton fibers and wood implies the presence of interfaces, pores and channels ranging from 1 to 5 nm in width, that determine the accessibility and swelling properties of the fibers.

2.2.2 Degradation of historical documents

As reported in the previous section, paper is based on natural organic materials (principally cellulose) and thus is susceptible to several degradation phenomena. Chemical, physical and biological processes may cause irreversible structural changes in the constituting fibers, principally resulting in discoloration and embrittlement.

The stability and durability of paper are influenced both on material composition and on environmental conditions. Besides structural properties (i.e. fibers type and length and crystallinity of cellulose), the presence of fillers (e.g. calcium carbonate, clay and others), functional groups (e.g. aldehydes, ketones or carboxylic groups formed during papermaking), acidic components (e.g. sizing agents), and metal ion impurities (e.g. iron and copper ions) can lead the stability of paper. Furthermore, some environmental factors, such as temperature, relative humidity (RH%), oxygen and light exposition, air pollutants (e.g. O_3, NOx, SO_2), and microorganisms (fungi and bacteria), promote the degradation both in a direct and an indirect way.

Hydrolysis and oxidation are the main chemical processes responsible for reducing the mechanical strength of paper.

The mechanism of hydrolysis and oxidation processes will not be reported here, since their effect on cleaning processes is outside the framework of this thesis.

2.3 Unwanted layers and contaminants

Besides natural ageing of paper due to environmental and physical-chemical alterations, the presence of unwanted substances on the paper surface may cause a series of irreversible degradation processes.

In the context of the thesis aim, pressure sensitive tapes (PSTs) and waxes are investigated along with their specific conservation issues. The removal of these materials represent a challenge for paper conservator worldwide. Due to their nature, PSTs and waxy compounds establish strong interactions with the cellulosic fibers; the adhesive forces between these materials and the paper fibers are stronger than the cohesive ones among the fibers themselves.

The inevitable aging of pressure sensitive tapes may cause alteration of paper support (distortion, tearing, darkening) because of chemically interaction (cross-linked) with cellulose chains and their removal, without affecting the support, become difficult. Moreover, PSTs can stain materials, modify inks and adhering to other items.

Otherwise, wax is known as inert material, in terms of chemical stability, particularly petroleum derived waxes (Bahadori et al., 2013). Apart from that, the presence of wax on paper-based artifacts can promotes degradation owing to release of oily and fatty compounds within cellulose fibers. These processes result in mechanical stresses (crack and brittleness), and may causes staining and transparency of substrate. Furthermore, coatings or spots of wax can obscure surface details and tend to attract dust and lint. Unfortunately, the research on conservation issues concerning wax is humble, especially in the field of paper restoration. For this reason, the development of new cleaning system for the removal of waxes from paper surface appeared to be interesting.

2.3.1 Pressure sensitive tapes (PSTs)

Pressure sensitive tapes (PSTs) are so called because light pressure causes it to stick quickly to most surfaces. In fact, with pressure the physical forces between the adhesive and the surface can build up.

Basically, the most used PST is a single sided tape, which is composed of four layers (figure 2.5):

1) An adhesive mass, which is usually composed of a synthetic or natural rubber and more recently of acrylic polymer. It may contain a variety of softeners, antioxidants, plasticizers, and curing agents.

2) The backing, or carrier, which can be foil, crepe paper, cellophane, cellulose acetate, plasticized polyvinyl chloride, or any of a number of other flexible materials. It may be reinforced with glass or other fibers.

3) The primer situated between the adhesive and backing, which insures good adhesion between the two. It is composed of natural or synthetic elastomers and contains some tackifiers to increase the tack and the stickiness of the adhesives' surface (Tse, 1989).

4) The release coat applied to the side of the backing. In this way, the roll can be unwound without leaving any residual adhesive.

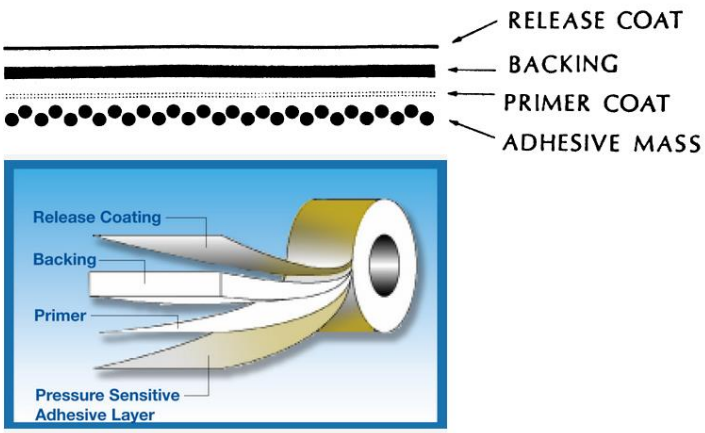

Figure 2.5. Components of a typical single sided pressure sensitive tape (Smith et al., 1984).

Within this thesis only the main characteristics of pressure sensitive tapes are reported, in order to better understand the conservation issues due to interaction between these material and paper substrates.

PST was first developed in 1845 by a surgeon who produced a kind of surgical tape applying a natural rubber adhesive to strips of cloth (Bemmels, 1962). For the first time, in 1925, Minnesota Mining and Manufacturing Company (3M) produced a new tape, so called Masking Tape (MT), composed by a paper backing with a rubber adhesive and combined with various oils and resins to make it tacky. Rapidly, the pressure-sensitive adhesive industry began to grow and new tapes and applications were developed. The adhesive components were changed and in the 1950s, cellulose acetate and its copolymers came into use as backings, and adhesives were principally composed by synthetic polymers combined with resins.

The advantage and facility of using tape to mount, hang and mend raised questions, in particular in the conservation community, about the stability, removability, and long-range effects of the materials involved. In this context, during the 1970s, were developed "archival" pressure sensitive tapes, well known as Filmoplast® P and Filmoplast® P90. The adhesive on both tapes is an acrylic ester that is laid on from a water-based dispersion.

Nowadays, world demand of pressure sensitive tapes is projected to increase 5% annually to 50.2 billion square meters in 2018 (Freedonia®, 2016).

Aging of PST: conservation issues of historical documents

The tapes most frequently encountered on archival materials and paper artworks were masking tape and cellophane tape, characterized by rubber or acrylic adhesive.

Oxidation is the main degradation process that affects the adhesive component of tapes, as extensively studied by Feller and Encke (Feller and Encke, 1982).
Oxidation leads fairly abrupt change in adhesive consistency and color. The adhesive mass gets sticky and oily, because of the breaking up of the rubber polymer and starts to change color. In this way, several components of the adhesive penetrate the paper fibers, and the support becomes translucent (Smith et al., 1984). Moreover, the oily adhesive mass can affects certain media, i.e. printing, typing, and ballpoint pen inks, causing them to bleed. Removal of PST in these conditions is still possible, but is very difficult.
When degradation process is advanced and the adhesive is fully penetrate into the paper fibers, the carrier may fall off, the adhesive residues crosslinked and becoming hard, brittle and highly discolored. In this condition, the residues and the stain created are very difficult, sometimes impossible, to remove.
The acrylic adhesives are characterized by a different aging behavior, because of their chemical composition: each acrylic adhesive is homogeneous polymer that coated the backing in its final pre-crosslinked form. If the acrylic adhesive components penetrate into paper porosity, the traditional removal can be only carried out with mechanical actions. In fact, the acrylic pressure-sensitive adhesives are not soluble in any of the solvents used in paper conservation, because of this pre-crosslinked condition (Smith et al., 1984).

Traditional removal methods of ageing PST

The conservators should be familiar with a variety of tape removal methods. Here, the most commonly procedures are reported.

- Dry method: the removal is achieved by first taking off the carrier with scalpel, microspatula or sand paper and then the adhesive layer. Removal of the carrier can be carried out either mechanically or with solvents.

Mechanical techniques are preferred, where possible, because they expose the entire adhesive layer and enable uniform access to it during subsequent operations in which solvents may be involved.

- Immersion: the entire artifact is immersed in a bath of solvent, which acts upon the tape to remove the carrier, if it has not been previously removed. In this way, it is possible to remove the surface adhesive and any components that have migrated into the paper. The proper choice of solvent, established by solubility tests on adhesives and artistic techniques, allows the conservator to remove selectively the undesirable tape and adhesive without altering other parts of the object.
- Poultice: this methods consists in the use of an absorbent support filled with solvent. The absorbent can be selected from a wide variety of materials, such as clays, siliceous materials or cellulosic materials (cellulose powder, filter paper, or torn-up blotters). These two components work like a mudpack. The absorbent prevents the solvent from evaporating too fast while keeping it close to the surface of the adhesive. During drying the softened adhesive is removed from the surface.
- Suction table: the advantage of suction is that it limits solvent spread. If the tape lies over solvent-soluble artistic technique, the conservator is able to achieve a local removal without bleed of color or solubilization of inks. Another advantage is the less mechanical action involved.

Drawbacks of traditional removal methods

Although recognized as the preferred method, dry mechanical cleaning shows some limits related to scarce selectivity and invasiveness of the procedure, which can damage the paper surface. Moreover, dry method involves mechanical stresses that can alter the integrity of support.

Immersion treatment is not without risk. Inks that were stable during testing may start to move during the treatment. Furthermore, the cellulose matrix is subjected to an aggressive chemical treatment that can lead to physical, chemical and mechanical alterations of paper, with the consequent loss of its properties.

Likewise, the poultice method exhibits disadvantages. For example, poultice wreckages can lie in the porous matrix of paper. This debris are particularly evident against dark paper or pigments and the only way to remove them is a mechanical action. Another disadvantage is that lateral movement of solvent and solvent-carried adhesive can occur, creating tidemarks in the paper.

The traditional cleaning techniques exhibit a unique fundamental drawback: the use of free organic solvents. As mentioned before (chapter1, section 1.3) the treatments with neat solvents not assure a complete removal of the unwanted layers without causing risk to the artifact.

2.3.2 Waxes

Waxes are hydrophobic organic compounds consisting of long alkyl chains. They include higher alkanes and lipids, which are insoluble in water but soluble in organic, nonpolar solvents. These compounds are malleable solids near ambient temperatures, typically with melting points above 40 °C.

The classification of waxes is based on their nature: natural waxes are produced by plants and animals; synthetic waxes are long-chain hydrocarbons (alkanes or paraffin) that lack substituted functional groups.

Natural waxes

This waxes are synthesized naturally by a wide range of plants and animals.

Natural waxes may contain unsubstituted hydrocarbons, such as higher alkanes, but can also include fatty acids, primary and secondary long chain alcohols, ketones and aldehydes.

- *Animal waxes*

  These waxes typically consist of esters derived from a variety of carboxylic acids and fatty alcohols. The most known is beeswax, which is composed mainly by ester myricyl palmitate (an ester of triacontanol and palmitic acid). The melting point is 62-65 °C.

  The main constituent of spermaceti, a waxy substance originated in the head cavities of the sperm whale, is cetyl palmitate, another ester of a fatty acid, and a fatty alcohol. Lanolin is a wax obtained from wool, consisting of esters of sterols (Riemenschneider and Bolt, 2005).

- *Plant waxes*

  In plant waxes the mixtures of unesterified hydrocarbons predominate over esters (Baker, 1982). The composition depends on species and on geographic location of the organism.

  Plants secrete waxes into and on the surface of their cuticles as a way to control evaporation, wettability and hydration (Wolfmeier and al., 2002). The vegetation's waxes are mixtures of substituted long-chain aliphatic hydrocarbons, containing alkanes, alkyl esters, fatty acids, primary and secondary alcohols, diols, ketones and aldehydes (Baker, 1982). The most known plant wax is carnauba, which contains the ester myricyl cerotate. Obtained from the Brazilian palm *Copernicia prunifera*, carnauba is used for many applications (i.e. food coatings, car and furniture polish, floss coating, etc.).

Synthetic wax (petroleum-derived wax): paraffin

Paraffin wax is characterized by long-chain hydrocarbons, produced by distillation from petroleum. It is a heterogeneous material, which has a softening range, usually between 45 and 67 °C, rather than a specific melting point (Mills and White, 1994). Paraffin waxes are composed by mixtures of saturated n- and iso- alkanes and naphthenes. A typical alkane paraffin wax chemical composition comprises hydrocarbons with the general formula C_nH_{2n+2}. The degree of branching has an important influence on the properties. Paraffin is soluble in aromatic hydrocarbons such as white spirit, benzene, toluene, and xylene (Johnson, 1984).

Paraffin wax (figure 2.6) is used in many fields, for example lubrication, electrical insulation, in food industry, in candles and cosmetics, as non-stick and waterproofing coatings.

Figure 2.6. Paraffin wax droplets.

Paraffin was first produced in the 1850s, and candle-making production was rapidly increased, because this material burned more cleanly and reliably than others waxes, and was cheaper to produce. Paraffin candles are odorless, and bluish-white in color. Nowadays, millions of tons of paraffin waxes are produced annually.

Waxes in conservation field

Waxes are not ideal for use in conservation field because they are subject to photo-oxidation, which causes cross-linking, embrittlement, and discoloration (Horie, 2010). Additionally, wax is not an efficient water vapor barrier and water can cause wax coatings to swell (Price et al., 1997). Wax coatings can obscure surface details, tend to attract dust and lint (Moffett, 1996), and are incompatible with most adhesives (Koob, 1984). Furthermore, wax coatings have been shown to be ineffective at stabilizing archaeological iron (Keene 1984; Johnson 1984). Wax is difficult to remove from objects and its presence severely limits an objects repeatability. Attempts at removing wax coatings, involving the use of boning water have been shown to be ineffective (Johnson, 1984), and room temperature solvents were also found to incompletely dissolve wax (Johnson, 1984; Moffett, 1996).

Despite these drawbacks, paraffin wax has been used for over one hundred years as a consolidant for corroded iron (Plenderleith, 1956), ivory (Petrie, 1904; Packard, 1971), textiles (Newell, 1933), zoological specimens (Noble and Jaeckle, 1926), corroded copper alloy (Fink, 1933), frescoes and stonework (Heaton, 1921).

Unfortunately, the wax coatings have frequently caused damage, e.g. terracotta (Tomba, 2007), wall paintings (Ballantyne and Hulbert, 1993) and polychromy on wood (Froysaker, 2006) and their complete removal is difficult or, maybe, impossible (Berger and Zeliger, 1975; Hatchfield and Koestler, 1987). The use of waxes as consolidant material has been largely abandoned except on lead (Green, 1990) and wood (Jensen et al., 1994).

Paraffin wax was widely used in the 19th and 20th centuries as a lifting material on archaeological sites (Greene, 2003) by pouring the molten liquid over objects.

Moreover, wax has been used for temporary protection for fugitive pigments on paper during aqueous treatments.

Besides the use of waxy compounds in conservation treatments, in some particular events, such as the “reading by candle light”, the presence of wax on historical paper documents is attributed to an erroneous handling of the candles. For example, on some especially formal or festive occasion, lighted candles are set about the collections area and there was the possibility of their dripping hot candle wax onto paper documents.

Traditional dry cleaning

As discussed before, dry cleaning is used for the removal of dust, dirt, foreign materials, etc. from the paper surface for aesthetic reasons and/or to facilitate the preservation of the artefact. Normally, dry cleaning must precede aqueous treatments, because dirt can be transferred by water into the paper matrix and become fixed there (American Institute for Conservation—Book and Paper, 2013). Dry cleaning is made up by use of hard brushes, scalpels and tweezers. Moreover, specific commercial products for the surface cleaning of paper have been developed, such as special sponges and dust-absorbing materials.

Wax drops are a kind of soiling which can be generally classified as stain and it may be an important historical evidence. On the other hand, in many books the most handled pages have more traces of stains, which can alter the readability or, in the worst case, can produced degradation processes. For example, the presence of wax drops may produce transparent spots on the sheets, a discoloration of cellulose, fading or color changes of dyes or pigments, and yellowing and embrittlement of paper support. Moreover, the discoloration and embrittlement may be irreversible since removal of discolored component drastically alter transparency of sheet.

Cleaning is often a disruptive treatment, which may cause abrasion of the paper surface, force foreign materials into the paper matrix and cause media damage. The dry cleaning of paper is discussed by several authors, including Banks (1969), Appelbaum (1987), Nordstrand (1987), Batterham (1998), Cumming and Colbourne (1998).

References

American Institute for Conservation. Book and Paper. 2013. Online version: http://cool.conservation-us.org/coolaic/sg/bpg/annual/

Appelbaum, B. 1987. Criteria for treatment: reversibility. J. Am. Inst. Conserv. 26, 65–73.

Baglioni, P.; Berti, D.; Bonini, M.; Carretti, E.; Dei, L.; Fratini, E.; Giorgi, R. 2014. Micelle, microemulsions, and gels for the conservation of cultural heritage. Adv. Colloid Interface Sci., Special Issue in honor of Bjorn Lindman, 205, 361–371.

Bahadori, A.; Nwaoha, C.; Clark, M.W. 2013. Dictionary of Oil, Gas, and Petrochemical Processing. CRC Press: Boca Raton, FL.

Baker, E.A. 1982. Chemistry and morphology of plant epicuticular waxes. In The Plant Cuticle. Ed. Cutler, Alvin, Price. Academic Press.

Ballantyne, A.; Hulbert, A. 1993. 19th and early 20th century restorations of English mediaeval wall paintings: problems and solutions. Past restorations of mural paintings. In M. Stefanaggi (Ed.), Les anciennes restaurations en peinture murale. International Institute for Conservation, pp. 143–151.

Bemmels, C.W. 1962. Adhesive Tapes. Handbook of Adhesives, Irving Skeist ed. Robert E. Krieger Publishing Company, Huntington, New York, pp. 584-592.

Banks, P.N. 1969. Paper cleaning. Restaurator 1, 52–66.

Barrow, W. J. 1974. Permanence/Durability of the Book–VII. Physical and Chemical Properties of the Book Papers, 1507–1949. W. J. Barrow Research Laboratory Inc., Richmond, VA.

Batterham, I. 1998. The Walter Burley Griffm design drawings of the city of

Canberra: conservation work at the National Archives of Australia. Restaurator 19, 115–134.

Berger, G.A.; Zeliger, H.I. 1975. Detrimental and irreversible effects of wax impregnation on easel painting. In 4th triennial meeting, Venice, 1975. International Council of Museums Committee for Conservation.

Bower, P. 1998. Proceedings of the 4th International Conference of the Institute of Paper Conservation, London 1997, ed. J. Eagan, The Institute of Paper Conservation, Haddon Leigh, NJ.

Cao, B.; Heise, O. 2005. Analyzing contaminants in OCC: Wax or not wax? Pulp & Paper Canada 106, 82-86.

Cumming, L.; Colbourne, J. 1998. The conservation of Mrs Marton, an eighteenth-century pastel and gouache portrait by Daniel Gardner. Pap. Conserv. 22, 38–47.

Daniels, V.D. 1996. The chemistry of paper conservation. Chem. Soc. Rev, 25, 179-186.

Feller, R.L.; Encke, D.B. 1982. Stages in deterioration: The examples of rubber cement and transparent mending tape: Science and Technology in the Service of Conservation: Preprints of the Contributions to the Washington Congress, 3-9 September 1982, London, pp. 19-23.

Fink, C.G. 1933. The care and treatment of outdoor bronze statues. Technical Studies in the Field of the Fine Arts, 2, 34.

Freedonia®, World Pressure Sensitive Tapes-Demand and Sales Forecasts, Market Share, Market Size, Market Leaders.
[www document]. URL: http://www.freedoniagroup.com/World-Pressure-Sensitive-Tapes.html (accessed 05/11/2016).

Froysaker, T. 2006. The removal of a previous wax-resin treatment and the re-

consolidation of the polychrome wooden cavalry group, c. 1150 in Urnes stave church. Beiträge zur Erhaltung von Kunst und Kulturgut 2, 7–1.

Green, L. 1990 .A re-evaluation of lead conservation techniques at the British Museum. M. Járo, ed., pp. 121–130. In Conservation of metals: Problems in the treatment of metal–organic and metal–inorganic composite objects: International restorer seminar, Veszprém, Hungary, 1989., Központi Muzeumi Igazgatóság. (Hungary).

Greene, V. Conservation of a lyre from Ur: a treatment review. Journal of the American Institute

for Conservation, 42, 261–278, 2003.

Hatchfield, P.B.; Koestler, R.J. 1987. Scanning electron microscopic examination of archaeological wood microstructure altered by consolidation treatments. Scanning Microscopy, 1, 1059–1069.

Heaton, N. 1921. The preservation of stone. Journal of the Royal Society of Arts, 70, 124–139.

Horie, C.V. 2010. Materials for conservation: Organic consolidants, adhesives and coatings. Ed. Butterworth-Heinemann, Elsevier, 2 ed.

Hunter, D. 1978. Papermaking–The history and Technique of an Ancient Craft, Dover Publications Inc., New York.

Jensen, P.; Bojesen Koefoed, I.; Meyer, I.; Straetkvern, K. 1994. The cellosolve–petroleum method. In Fifth meeting, Portland, 1993. Proceedings, 523–535. Working Group on Wet Organic Archaeological Materials ICOM Committee for Conservation.

Johnson, R. 1984. The removal of microcrystalline wax from archaeological ironwork. Adhesives and consolidants, ed. Brommelle et al. London: International Institute for Conservation of Historic and Artistic Works.107–9.

Mills, J.; White, R. 1994. The organic chemistry of museum objects. 2 ed. London: Butterworth-Heinemann.

Moffett, D. 1996. Wax coatings on ethnographic metal objects: Justifications for allowing a tradition to wane. Journal of the American Institute for Conservation 35, 1-7.

Moore, R.; Clark, D.; Votopich, D. 1998. Botany Visual Resource Library. The McGraw-Hill.

Newell, L.C. 1933. Chemistry in the service of Egyptology. Journal of Chemical Education, 10, 259–266.

Noble, G.K.; Jaeckle, M.E. 1926. Mounting by paraffin infiltration. American Museums Novitiates, 233.

Nordstrand, O.K. 1987. The conservation treatment of paper. Restaurator 8, 133–139.

Packard, E. 1971. Consolidation of decayed wood sculpture. In Conference on Conservation of Stone and Wooden Objects, New York, 1970. International Institute for Conservation.

Petrie, W.M.F. 1904. Methods and aims in archaeology. Macmillan.

Plenderleith, H. J. 1956. The conservation of antiquities and works of art: Treatment, repair and restoration. Oxford University.

Plossi, M.; Zappalà, A. 2007. Libri e Documenti. Le scienze per la conservazione e il restauro. ed. Laguna, Biblioteca Statale Isontina, Gorizia.

Price, C.; Hallam, D.; Heath, G.; Creagh, D.; Ashton, J. 1997. An electrochemical study of waxes for bronze sculpture. In Metal 95, 233-241. Ed. James & James, London.

Riemenschneider, W.; Bolt, H.M. 2005. Esters, Organic. Ullmann's Encyclopedia of Industrial Chemistry. Ed. Wiley-VCH Verlag GmbH & Co. KGaA.

Roberts, J.C. 1996. The Chemistry of Paper, RSC paperbacks, London.

Smith, R. D. 1987. Conservation of Library and Archive Materials and the Graphic Arts, ed. G. Petherbridge, Butterworth, London.

Smith, M.A.; Jones, N.M.M.; Page, S.L.; Dirda, M.P. 1984. Pressure-Sensitive Tape and Techniques for Its Removal from Paper. Journal of the American Institute for Conservation (JAIC), 23, 101-113.

Terzopoulou, Z.; Kyzas, G.Z.; Bikiaris. D.N. 2015. Recent Advances in Nanocomposite Materials of Graphene Derivatives with Polysaccharides. Materials, 8, 652-683.

Thakur, V.K.; Thakur, M.; Gupta, R. 2014. Review: Raw Natural Fiber-Based Polymer Composites. Int. J. Polym. Anal. Ch., 19, 256–271.

Tomba, F. 2007. L'apparato decorativo in terracotta del chiostro piccolo della Certosa di Pavia: Conseguenze di un intervento sperimentale di consolidamento del dopoguerra. pp. 531–538.. In G. Biscontin& G. Driussi (Eds.), Il consolidamento degli apparati architettonici e decorativi: conoscenze, orientamenti, esperienze: atti del convegno di studi, Bressanone, 2007.

Tse, M.F. 1989. Studies of triblock copolymer-tackifying resin interactions by viscoelasticity and adhesive performance. J. Adhes. Sci. Technol., 3, 551–570.

Wolfmeier, U.; Schmidt, H.; Heinrichs, F.L.; Michalczyk, G.; Payer, W.; Dietsche, W.; Boehlke, K.; Hohner, G.; Wildgruber, J. 2002. Waxes. In Ullmann's Encyclopedia of Industrial Chemistry. Ed. Wiley-VCH, Weinheim.

Wouters J. 2008. Coming Soon to a Library Near You? Science, 322, pp. 1196-1198.

PART II

Fundamentals

CHAPTER 3

Gels

3.1 Definition

The extensive literature available, the large amount of publications, the wide range of application and the studies coming from different backgrounds (i.e. physical, chemical, biological, engineering, medical, etc.) contributed to define the concept of gel.

During the last century the scientific community proposed several definitions and classifications, to allow the identification of phenomenological characteristics common to all gel systems, independently of their composition and molecular structure. The principal features taken into account to formulate a definition of gel were principally the macroscopical behavior, the microscopical structure and rheological performance.

According to the International Union of Pure and Applied Chemistry (IUPAC) terminology, the general definition of gel is "*non-fluid colloidal network or polymer network that is expanded throughout its whole volume by a fluid*", (Alemán et al., 2007).

Gels can be described as soft materials made up by colloidal solid particles dispersed in large amounts of fluid producing a semi-solid network system, which still showing solid-like behavior.

The concept of gel is closely related to colloid chemistry, but owing to the variability of the characteristics of gel systems and the various fields of application, the classification criteria depend on the reference theoretical

background and on specifically synthesis procedure (e.g. source of the gelator, structure, functional groups, etc.).

As reported by Lloyd, gels are "*build up of two components, one of which must be a liquid, and the other of which, the gelling substance proper, often spoken as the gelator, is a solid*" (Lloyd, 1926). Moreover, Lloyd highlights that also mechanical properties characterize the condition of gel: "*The gel itself has the mechanical properties of a solid, i.e. it can maintain its form under the stress of its own weight, and under any mechanical stress it shows the phenomenon of strain*". Almdal proposed a definition based on the following phenomenological characteristics: gels consist of two or more components one of which is a liquid, present in substantial quantity and they are soft, solid, or solid-like materials; the solid-like characteristics of gels are further defined in terms of the dynamic mechanical properties (Almdal et al., 1993).

Significant milestones were set by the development of statistical approaches for the prediction of the gel point and the modeling of gel formation, such as the "classical statistical theory" postulated by Flory and Stockmeyer, and the "percolation model" described by Zallen and Stauffer (Flory, 1953; Stauffer et al., 1982; Zallen, 2008).

Considering the intrinsic complexity and the vast array of gel classes, this dissertation is focused on gels made up by polymers.

Gels may be considered as colloidal systems due to the dimension of the interconnected long polymer chains, organic molecules or colloidal particles that entrap a fluid. The definition of colloidal systems covers a wide range of different materials though, to define specifically the gel condition one must consider its structure, its phenomenology and its mechanical behavior.

One of classification criteria used for the description of polymeric gels is based on IUPAC recommendations (Alemán et al., 2007). A gel system formed by

polymers is described as "*a covalent polymer network, e.g., a network formed by crosslinking polymer chains or by non-linear polymerization*"; or "*a polymer network formed through the physical aggregation of polymer chains, caused by hydrogen bonds, crystallization, helix formation, complexation, etc., that results in regions of local order acting as the network junction points*".

3.2 Classification

The continuously new developed gel typologies and the different theoretical backgrounds make difficult a well-defined classification of gel systems.

As well as for gel definition, gels classification depends on the discriminating characteristics taken into account, for example the medium in which they were obtained, the basis of the network structure, the thermal behavior; the type of bonds in the three-dimensional network etc. Some examples of the above gel systems, along with a short description, are presented in table 3.1.

Depending on the addressed subject of this thesis, only some classifications useful for a better understanding of the systems developed in this work will be well defined.

The classification based on chemical gels and physical gels, is the most commonly used. In this case, the discriminating characteristic is the nature of the interactions that build the gel structure, as described in the next section.

CATEGORY	SUB-CATEGORY	DESCRIPTION
Source	Natural	Found in nature. Solutions of biological proteins (fish-glue) or polysaccharides (gelatin; pectin; agarose; carrageenan).
	Synthetic	Man-made to meet specific purposes (contact lenses; drug delivery systems; bone tissue; etc.).
	Hybrid	Mixture of natural and synthetic source polymers.
Medium	Hydro-	Three-dimensional networks constituted by hydrophilic polymers, generally covalently or ionically cross-linked, which interact with aqueous solutions.
	Organo-	Polymers made from an oil-medium, such as an organic solvent.
	Xero-	Are the result of a freezedrying process that produce a porous solid with partially collapsed porosity. They must not be considered as gels, according to Almdal's definition.
	Aero-	Prepared as liquid gels which liquid phase has been replaced by a gas by means of the supercritical drying technique. They must not be considered as gels, according to Almdal's definition.
Thermal response	Thermoset	Gels with permanent cross-links. They do not melt when subject to high temperatures. These materials have improved mechanical properties, chemical resistance, heat resistance and structural integrity.
	Thermoplastic	Become more fluid when heat is applied. They are thermoreversible gels.
Crosslinking	Chemical	Polymer network constituted by permanent bonds, i.e. covalent bonds.
	Physical	Polymer network constituted by weak interactions that can be removed and reformed without any irreversible effects.

Table 3.1. Classification of gels. Examples and description (Buwalda et al., 2014; Fratini et al., 2013).

The fundamental characteristic that differentiates chemical and physical gels is the nature of the bonds between the polymer chains that build the gel structure. Chemical gels are characterized by "strong bonds", such as covalent bonds and ionic bonds, while the typical interactions in physical gel are "weak bonds" like dipole-dipole interactions, the London dispersion forces and hydrogen bonds. The different characteristics of these bonds affect the macroscopic behavior of the two type of gel. Covalent bonds are not reversible and are characterized by a high energy of bonding. On the other hand, "weak bonds" are relatively weak intermolecular forces between molecules or between different chemical groups of the same molecule.

In the context of this thesis topic, importance will be addressed to chemical organogels.

3.2.1 Chemical gels

Chemical gels are composed of cross-linked polymer networks that are built by covalent bonds (figure 3.1 a). The polymer network forms a macromolecule with a very high molecular weight (M_w). The permanent nature of the covalent bonds (from 200 up to 650 kJ mol^{-1}) connecting polymer chains is responsible for the thermoset nature of these materials: only over a critical temperature the bonds can be irreversibly broken. Their behavior is similar to solids; in fact, chemical gels are able to load high amounts of liquid without undergoing polymer solubilization. Due to their cohesive force, chemical gels can be easily removed from any surface, without breaking or leaving residues. This behavior is a very important characteristic for the cleaning of cultural heritage artifacts (Fratini et al., 2013).

3.2.2 Physical gels

Physical gels are polymeric systems gelled by the presence of non-covalent interactions between chains, such as hydrophobic, electrostatic, and Van del Waals forces, or the rather stronger hydrogen bonds (figure 3.1 b). Due to the weak nature of this kind of bonds, less energy is necessary to break them (around 1-120 kJ mol^{-1}) in respect to covalent ones, but they are easily reformed in certain conditions. Therefore, physical gels are also thermoreversible: by increasing the temperature over a given threshold, the single molecules are dispersed again in the solvent bulk phase and a ‘sol’ is obtained; by cooling back to the original temperature a sol-gel transition occurs and the system turns back into the gelled form. Common examples of natural source physical gels are the ones based on polysaccharides and proteins. Moreover, physical gels can be molded and may grant a perfect adhesion to the surface, which are good

characteristics for the cleaning of artifacts although residues problems can arise (cellulose ethers, polyacrylic acids and polysaccharides-based gels) (Fratini et al., 2013).

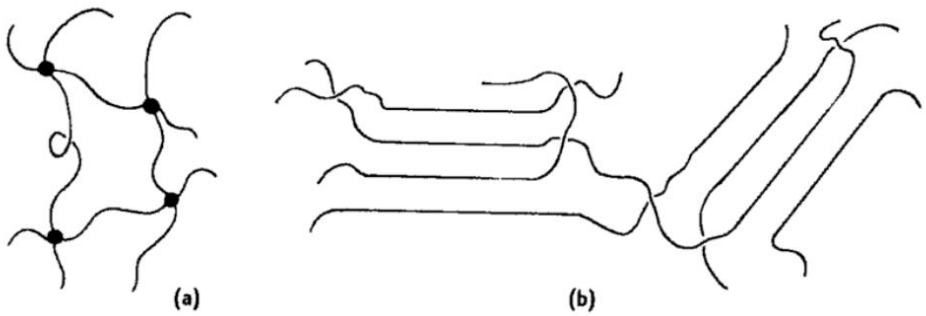

Figure 3.1. Example of polymer structures for: (a) chemical gel with cross-linking points; (b) physical gel with crystalline junctions (Sperling, 2006).

3.3 Characteristic parameters

Gels network structure is in direct relationship with the affinity of the system with the liquid phase, that is, the ability of embedding and retaining considerably large amounts of solvent. In order to understand the application features of a chemical gel it is fundamental to introduce some characteristic parameters of these systems.

3.3.1 Structural properties

There are some parameters characterizing the network of a chemical gel:

- The polymer volume fraction in the swollen state ($v_{2,s}$);
- The Equilibrium Solvent Content (ESC);
- The gel porosity;
- The average molecular weight of the polymer chain (M_c);

- The mesh size (ξ).

Figure 3.2 illustrates schematically the swelling of a hydrogel and the corresponding change of the mesh size.

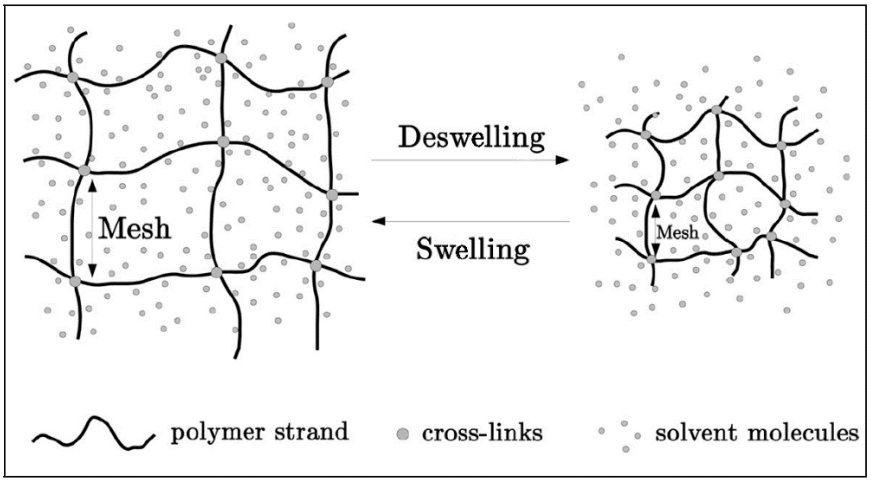

Figure 3.2. Schematic representation of the swelling-deswelling behavior of a gel and the corresponding change in mesh size.

Polymer volume fraction

The polymer volume fraction in the swollen state refers to amount of the liquid fraction absorbed and retained by the gel, thus it specifies the affinity between gel and solvent.

A direct measurement of volume fraction (Fratini et al., 2013) is from the volume of the dry polymer, V_p, and the swollen gel volume, V_g as follows:

$$V_{2,s} = \frac{V_p}{V_g} = \frac{1}{Q} \tag{3.1}$$

where *Q* is the volumetric swollen ratio.

As higher is the *Q* value, the higher the polymer affinity to the solvent. Therefore, $V_{2,s}$ is strictly connected to the molecular affinity between a specific polymer and

a specific solvent. Knowing the $V_{2,s}$ or the reciprocal *Q*, of the macromolecules, it is possible to tune the gel's affinity to a specific solvent by adding different monomers or different polymers to the formulation.

Equilibrium Solvent Content (ESC)

A parameter related to polymer volume fraction is the Equilibrium Solvent Content (ESC) (Fratini et al., 2013), calculated as follows:

$$\mathrm{ESC} = \frac{W_w - W_d}{W_w} \cdot 100 \tag{3.2}$$

where W_w and W_d are the weights of swollen gel and dry gel, respectively. Furthermore, the ESC is proportional to the gel's porosity. In fact, gels having an increased porosity, i.e. the pore volume to polymer volume ratio is high, can load high amounts of solvent. For this reason, liquid medium is added during gel formation to create polymer voids, thus, for obtaining gels with high solvent affinity. The decrease of ESC over time or after de-solvation/re-solvation cycles, can be directly associated to some collapse of pores.

Gel porosity

The examination of the gel porosity is an important analysis to consider, since it offers relevant information on the retention/release capacity of the gel system. Porosity ε is defined as the fraction of the apparent volume of the sample of the sample which is attributed to the pores detected by the method used (Rouquerol. et al., 1994; Bear, 1972):

$$\varepsilon = \frac{V_p}{V} \tag{3.3}$$

The value of the fraction ε depends on the method used to determine the apparent volume *V*, which excludes interparticle voids (geometrical determination, fluid displacement) and on that used to assess the pore volume V_p, (adsorption and capillary condensation, fluid displacement, ultrasonics, etc.). According to the IUPAC, the pore size can be classified in three different classes (Rouquerol et al., 1994):

I) *Micropores*: pore widths of up to 2 nm.
II) *Mesopores*: the width lies between 2 and 50 nm.
III) *Macropores*: pore widths greater than 50 nm.

This classification accounts only for the porosity in the nanometer scale, considering that macropores cover all the greater sizes. There are several techniques for porosity quantification described in the literature (Rouquerol et al., 1994). The Scanning Electron Microscopy (SEM) is useful for the examination of the macroporosity (Jacop, 1999).

Molecular weight

Synthetic and natural polymers have a molecular weight distribution that differs depending on the method of synthesis and on the fractionation procedure.

A method to obtain a measure of the polydispersity in molecular weight is to determine the average molecular weight between two consecutive cross-links, M_c. One approach is to calculate the number average molecular weight, M_n, as follows (Holmberg et al., 2002):

$$M_n = \frac{\sum N_i M_i}{\sum N_i} \tag{3.4}$$

where N_i is the number of molecules with mass M_i.

M_n can be determined by freezing point depression, osmosis or chemical analysis of end groups. An alternative molecular weight average is the weight average molecular weight, M_w, where w is the weighting factor for each molecular weight species, and is thus defined by:

$$M_w = \frac{\sum w_i M_i}{\sum w_i} = \frac{\sum N_i M_i^2}{\sum N_i M_i} \tag{3.5}$$

M_w is sensitive to high molecular weight species and is always larger than M_n. For a monodisperse polymer $M_w \approx M_n$, so the ratio of the weight average to the number average molecular weights is a measure of the degree of polydispersity (Holmberg et al., 2002).

M_c can define the degree of cross-linking of the polymer network, X, as follows (Fratini et al., 2013):

$$X = \frac{M_0}{2M_c} \tag{3.6}$$

where M_0 is the molecular weight of the repeating units in the polymer chains. The M_c value in chemical gels cannot vary with different swelling degrees as occurs for the mesh size ξ, due to the chemical permanent topology.

Mesh size and inhomogeneities

The mesh size ξ of the network is defined by the distance between two consecutive cross-linking points and depends on the swelling degree of the polymeric system. Since there is a distribution of distances in a polymeric

network, due to the random nature of the gelation process, the average ξ values are accounting for a 3D network system. Average mesh size is the same as the measure of the average porosity in the nanometer scale (Fratini et al., 2013).
Inhomogeneities in polymer gels are non-relaxing frozen polymer concentrations, which is dependent on the crosslinking density. The increase of inhomogeneities domains can lead to gel turbidity and can cause inhomogeneous responses in swelling and shrinking, as well as in rheological properties. According to Ikkai (Ikkai et al., 2005), there are three types of inhomogeneities in polymer gels, as illustrated in figure 3.3.

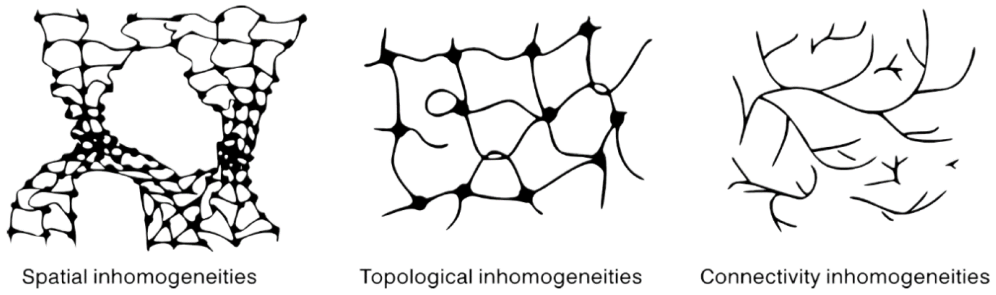

Figure 3.3. Types of inhomogeneities in gels (Ikkai et al., 2005).

The spatial inhomogeneities represent non-uniform spatial distributions of crosslinks. Topological inhomogeneities denote the defects on the topology of the polymer network (e.g. loops, trapped entanglements, dangling chains). The connectivity inhomogeneities are in relationship with the sizes and spatial distributions of clusters. Spatial inhomogeneities and mesh sizes can be examined through small-angle scattering techniques (SAXS).

3.3.2 Mechanical properties

To better understand the definition of gel, in this paragraph are reported mechanical properties gel, according to Almdal (Almdal et al., 1993), in which

some measurable parameters are given. In fact, Almdal give a precise definition based on experimental data obtained from rheological measurements: the elastic fraction (storage modulus *G'*) is always predominantly higher that the viscous one (loss modulus, *G''*), over a wide range of frequencies.

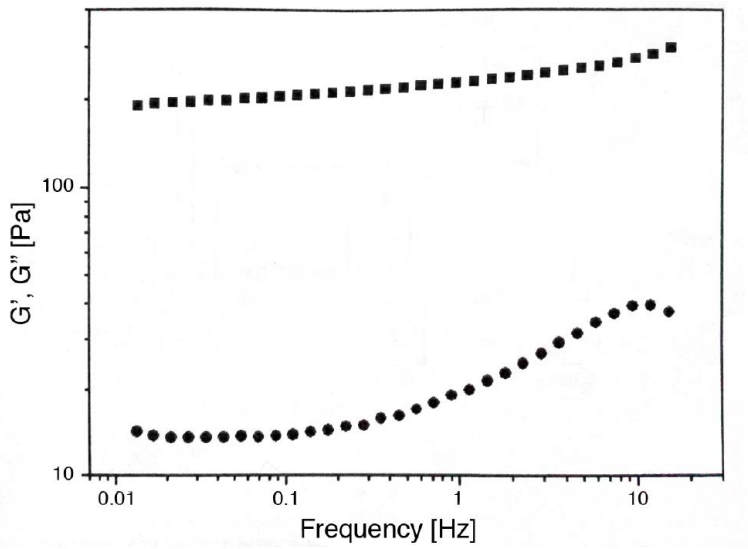

Figure 3.4. Example of frequency sweep of a gel composed by polyacrylic acid (1 w/w%), 1-propanol (20 w/w%) and water. Storage modulus *G'* (▪) and loss modulus *G"* (●) (Fratini et al., 2013).

For what concerns the borderline between solid-like gels and solids, a further recommendation was given; materials with moduli in the order of 10^8 Pa should not be considered gels, as they are too rigid. According to this definition, materials such as xerogels, aerogels and highly cross-linked polymers with low swollen degree must not be addressed as gels.

From a mechanical point of view, gels are viscoelastic materials characterized by contemporary mechanical behaviors typical of liquids and solids. As discussed before, the elastic fraction always prevails over the viscous behavior in gels. Two important parameters to consider for studying the mechanical properties of gels are the elastic modulus and the viscosity. The elastic modulus, *E*, also known as

Young's modulus, is defined as the fraction between the applied tensile stress, *T*, and the relative length of elongation, L_R (Fratini et al., 2013):

$$E = \frac{T}{L_R} = \frac{F/A}{\Delta L/L_0} \tag{3.7}$$

where *F* is the applied force over an area *A* and L_0 is the initial length.

The elastic modulus *E* decreases with the increasing of mesh size ξ, and thus is dependent of the swelling degree, and with increasing in M_c, consequently with decreasing of crosslinking density.

The viscosity η is defined as the resistance of fluids to external mechanical stresses. When a perturbation is applied, the fluid starts to flow; this displacement is influenced by many factors, such as temperature, pH and the magnitude of the applied stress. However, the most important features that influence on gel viscosity is the chemical nature of the fluid and the molecular interactions between the fluid's components. Therefore, gel viscosity can be tailored as well.

Rheology of viscoelastic materials is detailed in chapter 7 (section 7.7).

3.4 Gels for cleaning of cultural heritage

In the field of conservation of cultural heritage artifacts, cleaning with gels is a topic that has been receiving increasing interest in the last decades from a wide group of conservators and restorers. Actually, gel-cleaning practice permits to deal with most of the recently debated issues regarding the cleaning procedure of cultural heritage artifacts.

Gels have the essential role of carrying a cleaning agent and containing its penetration into the artifacts substrate, thus, controlling the removal of unwanted layers from the surface.
The aim of the following paragraphs is to introduce an overview on gels whose use in restoration procedures is already well established and on the most recent developments in gel-technology research will also be provided.
References for the different materials will be given in each section, however for a more detailed and all-embracing description of the systems resulting from developments in nanoscience for conservation, the reader is referred to two recent publications (Baglioni et al., 2015; Baglioni and Chelazzi, 2013).

3.4.1 Conventional gel systems

In the past decades, conservators devised several methods for the confinement of solvents to increase the control over the cleaning process.
The most part of gelators traditionally used for the preparation of thickened or gelled systems for the cleaning of artistic substrates. Restorers commonly refer to the overall typologies of confining systems with the term ‘gel’ since they all display the macroscopic appearance of gels; however, some of the systems that will be described in this section do not correspond to definition of gels in its strict sense but, for simplicity, we will adopt the terminology in use among restorers.

Different cleaning systems were devised in order to attain better control over the cleaning action, using thickeners and gellants, mainly constituted by water-soluble polymers. The application of these systems allows to reduce some of the drawbacks related to the use of cleaning mechanical methods (e.g. friction with a soaked cotton swab) and free solvent (toxicity, scarce selectivity and control).

Some of the common products used in restoration procedures, are reported as follow.

- *Cellulose ethers*: e.g. Klucel®, a hydroxypropyl cellulose; Tylose®, a hydroxyethyl cellulose.

  This materials are widely used to thicken water and polar solvents (e.g. alcohols), which can form physical gels. The preparation procedure consists in dispersing the polymer into the liquid phase by stirring at room temperature or under heating, then letting equilibrate for at least one day. The obtained jam-like system can be applied on the surface to be cleaned, as showed in figure 3.5, with a consistence ability to fill and follow also rough surfaces. However, residues remain on the treated surfaces owing to the prevalence of adhesive forces over cohesive ones. The subsequent removal often implies the use of invasive or mechanical methods, which are often aggressive for the original substrate, thus nullifying the advantages of using a confining system (Casoli et al., 2014). The presence of cellulosic residues might increase the possibility of microbial proliferation on the surface, depending on the hydrophilicity of the substrate and on storage conditions

  Furthermore, the retention features of those systems are usually unsatisfactory, and high solvent evaporation rates can lead to the formation of dry films of solid material on the treated surface.

Figure 3.5. Application and removal of Klucel® (Baglioni et al., 2015).

- *Polyacrylic acid*: e.g. Carbopol®; Pemulens®.

  Synthetic polymer introduced in the late 1980's along with the development of 'solvent gels' by Wolbers (Wolbers et al., 1998).

  'Solvent gels' formulations, i.e. solvents in their thickened state, are one of the most used retentive cleaning tools, based on the combination of the gellant (i.e. polyacrylic acid), characterized by the presence of many carboxylic groups, and a non-ionic surfactant (Ethomeen C12 or C15) with weak basic properties. Solvent gels are made by dispersing polyacrylic acid (~ 1% w/w) into the solvent or solvent mixture, then adding the surfactant (10-15 % w/w) under stirring. The further addition of water in small amounts (~ 5% w/w) produces a drastic increase in viscosity, leading to a physical gel formation. Gelation of the system occurs consequently to the partial neutralization of the acidic functions of polyacrylic acid that produces negatively charged carboxylate groups that repel each other through electrostatic interactions. This effect

results in a significant extension of the chains, otherwise in folded conformation, thus forming a gelled network.

As for cellulose ethers, solvent gels release residues on the surface of works of art after cleaning treatment. Thus, mechanical removal and solubilization of the solvent gel deposits, usually carried out through organic solvent blends, are necessary. Several studies have been carried out to investigate on the residue question; for example, Burnstock (Burnstock and Kieslich, 1996) and Stulik (Stulik, 2004) demonstrate that some polyacrylic acid residues can remain after the application of the relative gels.

- *Polysaccharides*: e.g. agar; gellan gum.

  These materials are recently proposed as residual-free and biodegradable substances (Campani et al., 2007; Iannuccelli and Sotgiu, 2010) for surface cleaning purposes. Polysaccharide gellants can be applied on the surfaces to be cleaned either as a highly viscous solution or as so-called 'rigid gels' (see figure 3.6). Their use as 'rigid gels' permits to perform cleaning treatments leaving almost no residues (Gullotta et al., 2014). The procedure to obtain gels of polysaccharide polymers starts with the addiction of the gallant to water (concentrations usually range from 1 to 4% w/w) and then the mixture is heated up to 80°C, leading to random coil conformation of the macromolecules of the gellant. Rearrangement of the molecules upon cooling results in formation of a thermo-reversible highly porous gel structure.

Figure 3.6. Agar gel (2%) loaded with water (Baglioni et al., 2015).

Agar is extracted from cell walls of red seaweed (*Gelidium* and *Gracilara*) and is composed on agaropectin and agarose. Agar gels can be used with chelating agents, enzymes or surfactants at different pH values (Gulotta et al., 2014); recently they have been used also loaded with nanostructured cleaning fluids (microemulsions) for the removal of hydrophobic materials from porous surfaces (Gorel, 2010).

Gellan gum, also branded as Phytagel® and Kelcogel®, is a water-soluble polysaccharide produced by the bacterium *Pseudomonas Elodea*; its repeating unit is a tetrasaccharide consisting of (1-4)-β-D-glucose, (1-4)-β-D-glucuronic acid, (1- 4)-β-D-glucose and (1-4)-α-L-rhamnose.

Inannuccelli and Sotgiu studied the application of gellan gum for the cleaning of paper artifacts, observing that the gels are able to retain the dirt and removal occurs without leaving substantial residues (Iannuccelli and Sotgiu, 2010).

Agar and gellan gum gels allow gentle surface cleaning or controlled humidification also on water-sensitive artifacts such as paper; however, in some cases their water retention features can be not sufficient, as for instance where leaching or loss of components (water-soluble colors or inks) might take place due to excessive wetting (Domingues et al., 2013).

3.4.2 Innovative gel systems

The aim of recent experimentation of new gel formulations was the development of materials with enhanced properties to avoid the drawbacks due to the presence of gel residues on works of art surface. For this purpose, ongoing research has been mainly centered on development of specific key features such as the improvement of mechanical properties (to ensure ease of handling and a completely residue-free treatment) and high retentiveness (to permit a highly controlled cleaning process even on sensitive substrates).

In this context, colloid and soft matter science has produced a significant contribution, designing a large array of advanced gels and 'gel-like' systems. Some examples, mainly developed in CSGI research group, will be reported in this section.

- *Stimuli-responsive gels*.

  These systems can be removed easily and completely after cleaning treatment owing to their responsiveness to either a chemical, physical or mechanical "switch".

  Polyamine (i.e. polyallilamine, PAA, or polyethylenime, PEI) based rheoreversible gels, are able to be changed from a solution-form into a gel-form through a simple chemical action (Carretti et al., 2004, 2003b); in fact, bubbling CO2 the PAA solution converts into a gallant through the formation of polyallylammonium carbamate (PAACO2). This gel, characterized by strong inter-chain interactions, are applied directly onto a painted surface, and after cleaning action, they can be removed by simply adding in situ a small amount of a weak aqueous solution (0.05M) of acetic acid. Decarboxylation reaction promoted by the acetic acid

solution reverts the gel back to a liquid (figure 3.7), which can be soaked up with a cotton swab.

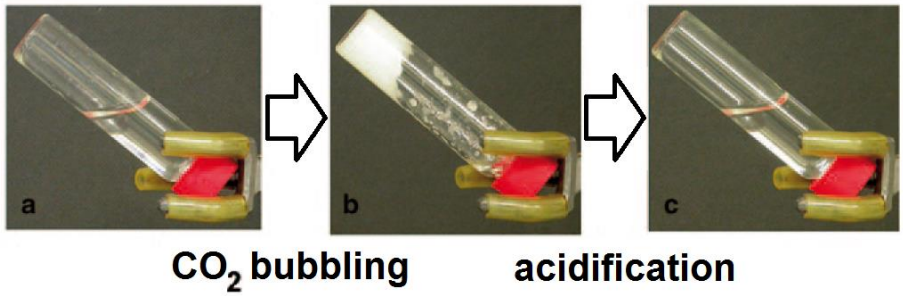

Figure 3.7. Rheoreversible PAA-based gel, able to switch from a solution to a gel through chemical action (Carretti et al., 2004).

Gelled systems of PAA in 1-pentanol were used for the removal of aged varnish from a gilded 19th century frame (Carretti et al., 2005), while PEI based gels proved to be effective on painted surfaces and gilded wood artifacts (Carretti et al., 2010a, 2008, 2005).

Gels responsiveness to external stimuli was further investigated by synthesis of networks able to respond to an external magnetic field. Magnetic nanoparticles were functionalized and then associated with acrylamide-based gels (Bonini et al., 2008, 2007). Acrylamide hydrogels act as confining agents for water or aqueous solutions (e.g. microemulsions), which can be released on the surface in a controlled way. Thanks to magnetic properties, the removal of the gel can be carried out by completely avoiding any direct handling of the gels, by means of a permanent magnet. This feature might be particularly suited in case of artistic surfaces that are extremely sensitive to mechanical stress (figure. 3.8).

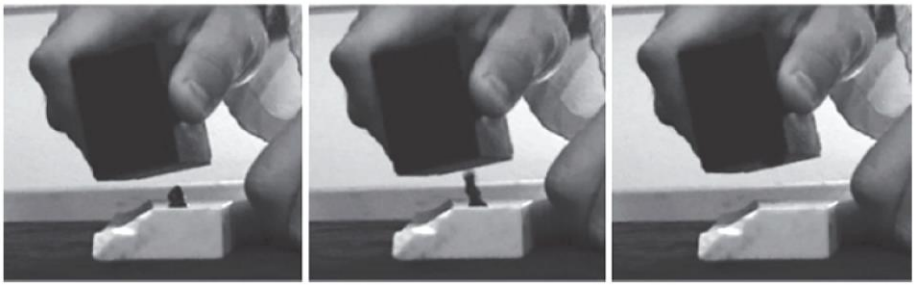

Figure 3.8. Removal of the microemulsion-loaded nanomagnetic gel from a substrate using a permanent magnet (Bonini et al., 2007).

- *"Gel-like" systems*.

  "Gel-like" poly(vinyl alcohol) (PVA, or partially hydrolyzed poly(vinyl acetate), PVAc) based systems for the cleaning of artworks were developed (Carretti et al., 2014, 2010b, 2009).

  These systems cannot be strictly defined as gels, because of their rheological behavior; therefore, they are referred to as Highly Viscous Polymeric Dispersions (HVPD), with a network structure characterized by the presence of entanglements, hydrogen bonds and borax-induced cross-linking. The principal feature of these viscoelastic systems, used as cleaning tools, concerns their removal through a simple peeling action and the absence of residues on the treated surface (figure 3.9).

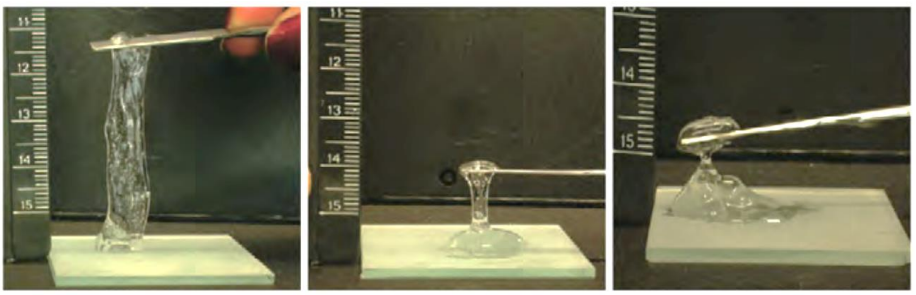

Figure 3.9. Removal of PVA-borax HVPDs with different borax content (left, center); comparison with properties of a traditional polyacrylic acid gel (right) (Carretti et al., 2009).

HVPDs were obtained by adding borax to a PVA aqueous solution. The "gel-like" network is due to the well-known ability of borate ions to cross-

links PVA polymer chains. The nature of cross-links depends on several factors as pH, temperature, concentration of the reagents and chemical composition of the system (Keita et al., 1995; Koike et al., 1995; Wu et al., 1990). Rheological feature of PVA- and PVAc-borax HVPDs permits a safe removal without leaving detectable residues, as assessed by FT-IR measurements.

Moreover, HVPDs are able to load different solvents including ethanol, 1-pentanol, 2-butanol, 1- and 2-propanol, acetone, cyclohexanone, N-methyl-pyrrolidinone and propylene carbonate. The use of partially hydrolyzed PVAc further extends the range of solvents that can be loaded, and allows the preparation of HVPDs with increased quantities of organic solvent (Angelova et al., 2011).

- *Chemical hydrogels*.

  This class of chemical gels are characterized by enhanced retentiveness, permit a safe and effective cleaning give and completely residue-free results. Semi-interpenetrating networks (semi-IPN) were obtained by embedding poly(vinylpirrolidone) (PVP) within a poly(2-hydroxyethylmethacrylate) (p(HEMA)) network (Domingues et al., 2014, 2013).

  Blending p(HEMA) and PVP permits to take advantage of the best features of both polymers, i.e. the good mechanical strength provided by p(HEMA) and the high hydrophilicity characteristic of PVP. Moreover hydrogels characteristics, as for instance water retention properties, can be tuned by varying compositional ratios. Hydrogels are transparent and can be prepared in the shape of elastic foils that can be easily manipulated and removed from surface after cleaning (figure 3.10),

without leaving residues, as assessed through FT-IR analysis. Gels can be loaded by immersion with water or water-based nanostructured fluids (i.e. microemulsions) for the removal of both, hydrophilic surface grime (Domingues et al., 2013) or hydrophobic materials (Domingues et al., 2014). Although gels were originally designed for water-based systems, they are also able to load some polar solvents (e.g. glycols, alcohols, ethanolamine, etc.).

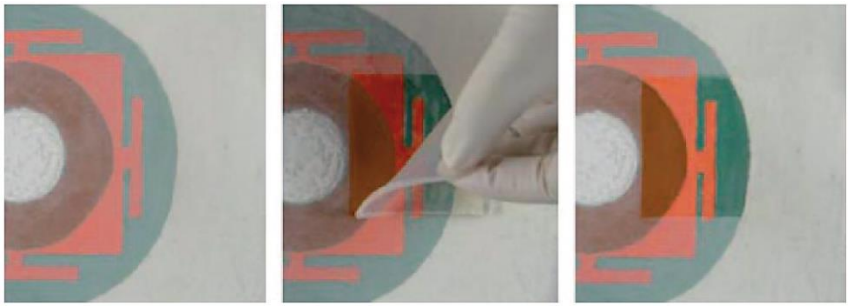

Figure 3.10. Removal of hydrophilic superficial grime using a p(HEMA)/PVP semi-IPN hydrogel loaded with water (Domingues et al., 2013).

- *Chemical organogels*.

  Chemical organogels (i.e. where the confined fluids are organic solvents rather than aqueous systems) can be used as cleaning tools complementary to hydrogels, maintaining good retentiveness and mechanical properties. Rheoreversible organogels have been formulated (Carretti et al., 2005, 2004) allowing to switch their rheological properties with a simple chemical mechanism.

  Besides art conservation, organogels have potential for use in a number of applications, such as in pharmaceuticals (Kumar and Katare, 2005), cosmetics, and food (Pernetti et al., 2007). An example of formation of an undesired thermoreversible network is the occurrence of wax crystallization in crude oil (Visintin et al., 2005).

Organogels are formed by a specific kind of small organic molecules that, in many solvents including water, very efficiently self-assemble into a three-dimensional network and thereby turn the liquid into a gel (Rivas-Orta et al., 2013). The preparation of novel functional organogelators was carried out by organic synthesis starting from simple building blocks such as peptides and carbohydrates, to which functional moieties are attached (Hoekstra et al., 2006). Rational design rules in combination with computer modelling leads to promising molecular structures, which exhibit the desired supramolecular architecture and function .Two features distinguish organogels from gels formed only by polymers: the formation of organogels is fully reversible, and the network structure formed is highly ordered at the supramolecular level (Rivas-Orta et al., 2013).

The confinement of organic solvents, with lower polarity than water, broadens the applicability of gels for the removal of coatings found on the surface of artifacts. Poly(methyl methacrylate) chemical organogels have been prepared using different solvents and applied for the first time for the removal of unwanted adhesives and varnishes from lined canvas and canvas painting samples(figure 3.11) (Baglioni et al., 2015).

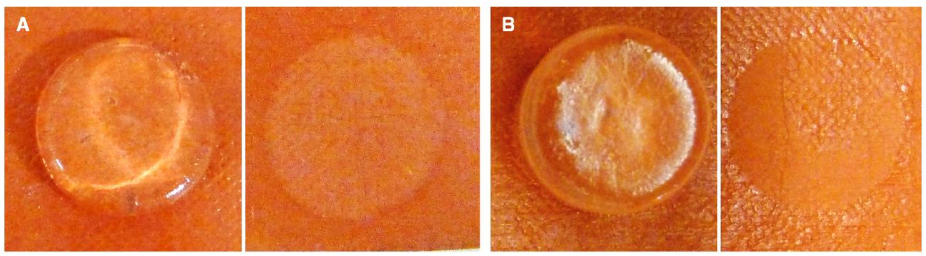

Figure 3.11. Removal of Paraloid B72 from canvas painting models using MMA-Ethyl Acetate gel (A) and MMA-Butyl Acetate gel (B). (Baglioni et al., 2015).

Model samples of varnished canvas paintings were realized applying a preparation layer (using rabbit skin glue in water, CaCO3 and red pigment Fe_2O_3) over natural linen canvas.

The retentiveness of the organogel network can be adjust tuning the amount of cross-linker and the monomer-solvent phase ratio during the synthesis of the gel, which was carried out through the free radical polymerization of monomer in pure solvent.

Changing the solvent used for the gel preparation allows targeting the removal of different coatings such as vinyl acetate and acrylate copolymers or natural terpenic resins.

Furthermore, the PMMA organogels exhibit good optical transparency, which is advantageous for applications on artifacts since the treated surface can be directly observed during the cleaning operation. ATR-IR analysis confirmed that no gel residues are left on the samples' surface after the treatment with the gels (Baglioni et al., 2015).

PMMA chemical organogels may represent a real alternative to the widely used physical ''gel-like'' networks and thickeners for confining cleaning solvents.

References

Alemán, J.V.; Chadwick, A.V.; He, J.; Hess, M.; Horie, K.; Jones, R.G.; Kratochvíl, P.; Meisel, I.; Mita, I.; Moad, G.; Penczek; S.; Stepto, R.F.T. 2007. Definitions of terms relating to the structure and processing of sols, gels, networks, and inorganic-organic hybrid materials (IUPAC Recommendations 2007). Pure Appl. Chem. 79.

Almdal, K.; Dyre, J.; Hvidt, S.; Kramer, O. 1993. Towards a phenomenological definition of the term "gel." Polym. Gels Netw. 1, 5–17.

Angelova, L.V.; Terech, P.; Natali, I.; Dei, L.; Carretti, E.; Weiss, R.G. 2011. Cosolvent gel-like materials from partially hydrolyzed poly(vinyl acetate)s and borax. Langmuir ACS J. Surf. Colloids 27, 11671–11682.

Baglioni, P.; Chelazzi, D.; Giorgi, R. 2015. Nanotechnologies in the Conservation of Cultural Heritage-A compendium of materials and techniques. Springer, Dordrecht.

Baglioni, P.; Chelazzi, D. 2013. Nanoscience for the Conservation of Works of Art: RSC. Royal Society of Chemistry, Cambridge.

Baglioni, M.; Giorgi, R.; Berti, D.; Baglioni, P. 2012. Smart cleaning of cultural heritage: a new challenge for soft nanoscience. Nanoscale 4, 42–53.

Baglioni, P.; Bonelli, N.; Chelazzi, D.; Chevalier, A.; Dei, L.; Domingues, J.; Fratini, E.; Giorgi, R.; Martin, M. 2005. Organogel formulations for the cleaning of easel paintings. App. Phys. A 121 (3), 857-868.

Bear, J. 1972. Dynamics of Fluids in Porous Media; Dover Publications: New York, NY.

Bonini, M.; Lenz, S.; Falletta, E.; Ridi, F.; Carretti, E.; Fratini, E.; Wiedenmann, A.; Baglioni, P. 2008. Acrylamide-Based Magnetic Nanosponges: A New Smart Nanocomposite Material.Langmuir 24, 12644–12650.

Bonini, M.; Lenz, S.; Giorgi, R.; Baglioni, P. 2007. Nanomagnetic Sponges for the Cleaning of Works of Art. Langmuir 23, 8681–8685.

Bonsanti, G. 2002. Storia ed Etica della Pulitura, in: Colore E Conservazione: Materiali E Metodi Nel Restauro Delle Opere Policrome Mobili. Presented at the CESMAR7, Il Prato, Piazzola sul Brenta, pp. 14–15.

Burnstock, A.; Kieslich, T. 1996. A study of the clearance of solvent gels used for varnish removal from paintings. Presented at the Proceedings of 11th Triennial Conference, Edinburgh, Scotland, September 1-6, 1996, James & James, London, pp. 253–262.

Burnstock, A.; Learner, T. 1992. Changes in the surface characteristics of artificially aged mastic varnishes after cleaning using alkaline reagents. Stud. Conserv. 37, 165–184.

Buwalda, S. J.; Boere, K. W. M.; Dijkstra, P. J.; Feijen, J.; Vermonden, T.; Hennink, W. E. 2014. Hydrogels in a Historical Perspective: From Simple Networks to Smart Materials. J. Controlled Release, 190, 254–273.

Campani, E.; Casoli, A.; Cremonesi, P.; Saccani, I.; Signorini, E. 2007. L'uso di agarosio e agar per la preparazione di "gel rigidi." In Quaderni del Cesmar 7. Il Prato Editore, Padova.

Carretti, E.; Grassi, S.; Cossalter, M.; Natali, I.; Caminati, G.; Weiss, R.G.; Baglioni, P.; Dei, L. 2009. Poly(vinyl alcohol)−Borate Hydro/Cosolvent Gels: Viscoelastic Properties, Solubilizing Power, and Application to Art Conservation. Langmuir 25, 8656–8662.

Carretti, E.; Dei, L.; Weiss, R.G.; Baglioni, P. 2008. A new class of gels for the conservation of painted surfaces. J. Cult. Herit. 9, 386–393.

Carretti, E.; Dei, L.; Weiss, R.G. 2005. Soft matter and art conservation. Rheoreversible gels and beyond. Soft Matter 1, 17–22.

Carretti, E.; Dei, L.; Macherelli, A.; Weiss, R.G. 2004. Rheoreversible polymeric

organogels: the art of science for art conservation. Langmuir ACS J. Surf. Colloids 20, 8414–8418.

Carretti, E.; Dei, L.; Baglioni, P. 2003 (a). Solubilization of Acrylic and Vinyl Polymers in Nanocontainer Solutions. Application of Microemulsions and Micelles to Cultural Heritage Conservation. Langmuir 19, 7867–7872.

Carretti, E.; Dei, L.; Baglioni, P.; Weiss, R.G. 2003 (b). Synthesis and Characterization of Gels from Polyallylamine and Carbon Dioxide as Gellant. J. Am. Chem. Soc. 125, 5121–5129.

Casoli, A.; Di Diego, Z.; Isca, C. 2014. Cleaning painted surfaces: evaluation of leaching phenomenon induced by solvents applied for the removal of gel residues. Environmental Science and Pollution Research 21, 13252–13263.

Domingues, J.; Bonelli, N.; Giorgi, R.; Baglioni, P. 2014. Chemical semi-IPN hydrogels for the removal of adhesives from canvas paintings. Appl. Phys. A 114, 705-710.

Domingues, J.; Bonelli, N.; Giorgi, R.; Fratini, E.; Gorel, F.; Baglioni, P. 2013. Innovative Hydrogels Based on Semi-Interpenetrating p(HEMA)/PVP Networks for the Cleaning of Water-Sensitive Cultural Heritage Artifacts. Langmuir 29, 2746-2755.

Fratini, E.; Carretti, E. 2013. Chapter 10. Cleaning IV: Gels and Polymeric Dispersions. In Nanoscience for the Conservation of Works of Art; Baglioni, P.; Chelazzi, D.; O'Brien, P., Eds.; Royal Society of Chemistry: Cambridge, pp 252-279.

Goodwin, W.; Hughes, R. W. 2000. Rheology for Chemists. An Introduction; Roya Society of Chemistry: Cambridge.

Gorel, F. 2010. Assessment of agar gel loaded with micro-emulsion for the

cleaning of porous surfaces. In Conservation, exposition, Restauration d'Objets d'Art.CeROArt.

Gulotta, D.; Saviello, D.; Gherardi, F. et al. 2014. Setup of a sustainable indoor cleaning methodology for the sculpted stone surfaces of the Duomo of Milan. Heritage Science, 1-13.

Hoekstra, D.; Kroesen, B.J.; Kuipers, O.P.; Poolman, B. 2006. University Medical Center Groningen, Bio organicmaterials and devices, Groningen, The Netherlands, 9.

Holmberg, K.; Jönsson, B.; Kronberg, B.; Lindman, B. 2002. Polymers in Solution. In Surfactants and Polymers in Aqueous Solution; John Wiley & Sons: New York, NY.

Ikkai, F.; Shibayama, M. 2015. Inhomogeneity Control in Polymer Gels. J. Polym. Sci. Part B Polym. Phys. 43, 617-628.

Iannuccelli, S.; Sotgiu, S. 2010. Wet treatments of works of art on paper with rigid gellan gels. The Book and Paper Group Annual, American Institute for Conservation, 29, 25-39.

Keita, G.; Ricard, A.; Audebert, R.; Pezron, E.; Leibler, L. 1995. The poly(vinyl alcohol)-borate system: influence of polyelectrolyte effects on phase diagrams. Polymer 36, 49-54.

Koike, A.; Nemoto, N.; Inoue, T.; Osaki, K. 1995. Dynamic Light Scattering and Dynamic Viscoelasticity of Poly(vinyl alcohol) in Aqueous Borax Solutions. 1. Concentration Effect. Macromolecules, 28, 2339–2344.

Kumar, R.; Katare, O.P. 2005. A review. American Association of Pharmaceutical Scientists, Pharmacy Science Technology,6, 298.

Jacop, J. S. 1999. Characterization of Delivery Systems, Microscopy. In Encyclopedia of Controlled Drug Dellivery; Mathiowitz, E., Ed.; John Wiley & Sons: New York, NY; Vol. 1, pp 234–250.

Menard, K. P. 2008. Dynamic Mechanical Analysis: A Practical Introduction. CRC Press: Boca Raton, FL, 2 ed.

Pernetti, M.; Van Malssen, K.F.; Flöter, E.; Bot, A. 2007. Structuring of edible oils by alternatives to crystalline fat. Curr. Opin. Colloid Interface Sci., 12, 221.

Rivas-Orta, V.; Antonio-Cruz, R.; Rivera-Armenta, J.L.; Mendoza-Martínez, A.; Ramírez-Mesa R. 2013. Synthesis and characterization of organogel from poly(acrylic acid) with cellulose acetate. e-Polymers. 10, 1613. DOI: 10.1515/epoly.2010.10.1.1613.

Rouquerol, J.; Avnir, D.; Fairbridge, C.W.; Everett, D.H.; Haynes, J.M.; Pernicone, N.; Ramsay, J.D.F.; Sing, K.S.W.; Unger, K.K. 1994. Recommendations for the Characterization of Porous Solids (Technical Report). Pure Appl. Chem., 66.

Sperling, L.H. 2006. Introduction to Physical Polymer Science. John Wiley & Sons Inc, Hoboken.

Stulik, D. 2004. Solvent Gels for the cleaning of works of art: the residue question. Getty Publications, Malibu.

Visintin, R.F.; Lapasin, R.; Vignati, E.; D'Antona, P.; Lockhart, T.P. 2005. Rheological behavior and structural interpretation of waxy crude oil gels. Langmuir, 21, 6240-6249.

Wolbers, R., Sterman, N., and Stavroudis, C. 1998. Notes for the Workshop on New Methods in the Cleaning of Paintings. The Getty Conservation Institute, Malibu.

Wu, W.L.; Shibayama, M.; Roy, S.; Kurokawa, H.; Coyne, L.D.; Nomura, S.; Stein, R.S. 1990. Physical gels of aqueous poly(vinyl alcohol) solutions: a small-angle neutron-scattering study. Macromolecules 23, 2245–2251.

CHAPTER 4

Polymer blends

4.1 Introduction

In this chapter, will be presented gels having a liquid phase composed totally by organic solvents and for this reason defined “organogels”.
The present chapter has the aim to introduce to the concept of polymer blends in order to provide the reader with the basic thermodynamic concepts regarding the interaction that may occur in a blended polymer system and advantages that can be attained through blending process.

4.2 Polymers in solution

In the last decades the research in the field of polymer blend technology has been largely improved because blending polymers permits to develop new systems with desirable features (Paul and Newman, 1978; Robeson and Robeson, 2007).
The chance to match the requested properties through the combination of different macromolecules is related to blend the polymer properties according to concepts of *additivity* and *synergism* (Paul and Barlow, 1980). When two polymers are mixed together, *additivity* of polymer properties means that in the resulting blend a specific property will be a weighted average in respect to that of the pure components. The averaging of properties permits to tune them in order to obtain a specific requirement. Additivity is the most common

composition correlated relationship in which polymer properties interact in a blend.

Less frequently, in a blend, a specific property of the single components may interact in a *synergic* way. That is, the maximum value of that property is larger than for the single components. On the other hand, if the property exhibits a minimum when plotted versus blend proportions, blended polymers are called "incompatible" (figure 4.1).

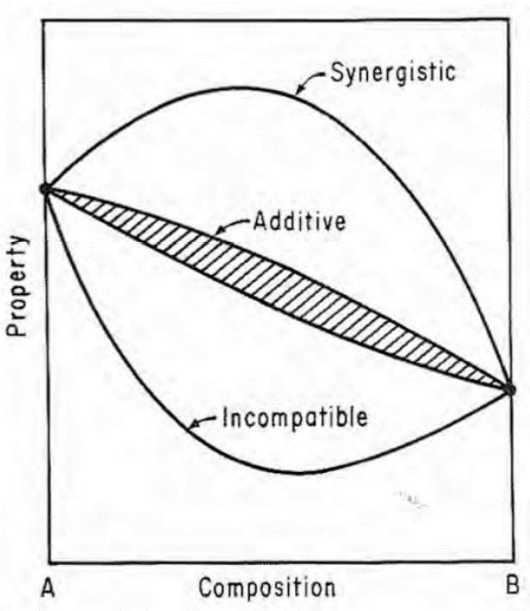

Figure 4.1. Possible effects on properties in relation to component concentration resulting from the blending of two polymers A and B (Paul and Barlow, 1980).

The situation of incompatibility, which often results in poor mechanical properties, is mainly due to limited interfacial adhesion between the components. In fact, the most important limitation for the development of new materials through polymer blending is that most blends of high molecular weight polymers prove to be immiscible. After being mixed together, the blend components tend to separate into phases containing mainly their own kind. Low mechanical properties are often a result of this behavior combined with low

physical attraction between the phase boundaries. Thus, one of the major issues in designing polymer blends is to obtain a system in which a good stress transfer within the multicomponent system is achieved. Actually, polymer incompatibility has not to be confused with immiscibility. If a blend system is able to form miscible amorphous phases, that is, a single-phase system, the components are able to mix at the molecular level. However, strategies have been devised to address the problem of compatibility, with the result that today the vast majority of commercial polymer blends is made up by immiscible polymers. Compatibilization methods are mainly based on a proper control on phase behavior during processing, on functionalization of the polymer chains or on modification of the interface between the immiscible and incompatible components (Hobbs et al., 1988; Liu et al., 2000; Macosko, 2000; Pötschke and Paul, 2003). Compatibilized blends are often labeled as polymer alloys, due to some similarity to heterogeneous systems obtained in metal mixtures.
The basic thermodynamics of polymer solubility will be briefly discussed, as well as the typical phase diagrams of polymer blends.

4.3 Thermodynamics of polymer solvent systems

The theoretical basis to understand polymer behavior in solution was developed independently by Flory and Huggins around the mid-twentieth century (Flory, 1942; Huggins, 1942). The Flory-Huggins theory is based on a simplified model and some assumptions, but it still remains very useful for the theoretical prediction of experimental data.
The theory leads to a modification of the classical expression of the free energy of mixing ΔG_{mix}, by taking into account the different properties of a polymer solution due to the very large size of polymer solute molecules compared to solvent molecules. It also introduces the Flory-Huggins parameter χ, which

permits a quantitative description of the balance of interactions between solvent and polymer segments and predicts if a solvent is either a good or a poor solvent for a given polymer.

We recall the well-known thermodynamic expression of the free energy of mixing:

$$\Delta G_{mix} = \Delta H_{mix} - T\Delta S_{mix} \tag{4.1}$$

The enthalpic and entropic variations of the solution in respect to the pure components are expressed by ΔH_{mix} and ΔS_{mix} respectively.

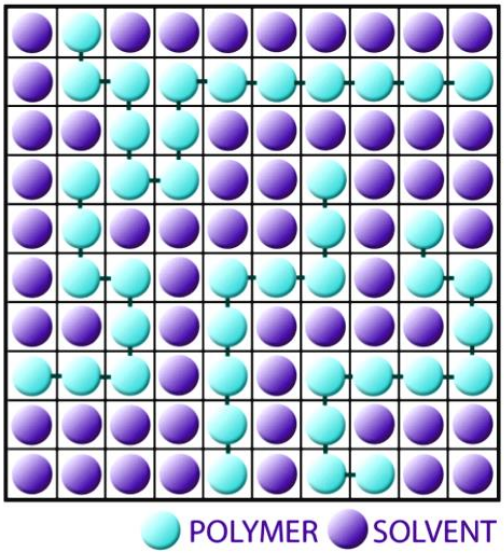

Figure 4.2. Schematic representation of the lattice model for a binary polymer-solvent system.

For what concerns the entropic term of this expression, the Flory-Huggins theory is based on a statistical approach, in which the polymer solution is described as a three-dimensional lattice (figure 4.2). The entire volume is divided in N_0 cells, which can be occupied randomly by solvent molecules or by polymer segments. Each polymer segment is assumed to have the same size as a solvent molecule, thus they can be considered interchangeable within the lattice positions.

Considering a monodispersed polymer, the number of segments x, contained in a polymer chain, is given by the ratio between the molar volumes of the polymer, V_p and the solvent:

$$x = \frac{V_p}{V_s} \tag{4.2}$$

The relation between the number of cells N0 and the number of solvent and solute molecules, respectively N_s and N_p, is:

$$N_0 = N_s + xN_p \tag{4.3}$$

According to Boltzmann, entropy depends on the possible configurations of a system:

$$S = k \cdot ln\Omega \tag{4.4}$$

where Ω is the number of possible arrangements and k the Boltzmann constant. In our case, Ω corresponds to the possible configurations that can arise by placing randomly polymer chains into the lattice and subsequently filling the voids with solvent molecules.

Statistical computations, that will not be discussed here (for in-depth study of this subject the specific literature is recommended), permit to evaluate Ω for a polymer solution. In respect to small molecule solutions there are great limitations in the number of possible configurations due to the dimensions and the covalent bonds between polymer segments.

The expression of the entropy of mixing obtained through the Flory-Huggins theory is:

$$\Delta S_{mix} = -k\left[N_s \cdot lnx\frac{N_s}{N_s + xN_p} + N_p ln\frac{xN_p}{N_s + xN_p}\right] \quad (4.5)$$

Since x is related to the molar volumes (see eq. 4.2), the expression can be changed on a molar basis (i.e. $k = R/N_a$):

$$\Delta S_{mix} = -R\left[n_s ln\phi_s + n_p ln\phi_p\right] \quad (4.6)$$

Where n_s and n_p are the number of moles of each component and ϕ_s and ϕ_p are the volume fractions, respectively, of solvent and polymer, defined in a general form as:

$$\phi_i = \frac{n_i V_i}{\sum_i n_i V_i} \quad (4.7)$$

The expression described in (4.6) is similar to the classical expression of the entropy of mixing for small-molecule solvent-solute systems; the innovation introduced by the Flory-Huggins theory is that volume fractions are here considered rather than molar fractions. In the case of small molecule solutes, the mole fractions and the volume fractions are essentially the same; this makes (4.6) a more general expression for the entropy of mixing.

To calculate the free energy of mixing for the solvent-polymer system, also the enthalpic term needs to be derived. The energy change related to dissolution can be associated to the fact that solvent-solvent and solute-solute interactions are replaced by solvent-solute interactions. If we name w_{ss} the energy related to solvent-solvent interactions and w_{pp} the energy related to polymer-polymer

interactions, the energy associated to dissolution, i.e. to formation of a new interaction solvent-polymer w_{sp}, will be:

$$\Delta w = w_{sp} + \frac{1}{2}\left(w_{ss} + w_{pp}\right) \tag{4.8}$$

Obviously, covalent bonds between chain segments are not included in w_{pp}; only interactions between neighboring molecules are here taken into account. The total enthalpy of mixing will depend on the number of solvent-polymer interactions (i.e. *sp* contacts). The formation probability of a new solvent-polymer contact will depend in our lattice model on the coordination number Z (that is the number of possible adjacent sites to a position in the lattice), and on the contact probability with sites occupied by a solvent molecule. Considering that xN_p is the total number of polymer segments, xN_pZ is the total number of sites near a polymer segment. Since the probability that any of these sites is occupied by a solvent molecule, is approximately equal to solvent volume fraction ϕ_s, the total number of contacts will be:

$$xN_pZ\phi_s = N_sZ\phi_p \tag{4.9}$$

While the enthalpy of mixing will be equal to energy change multiplied by the number of interactions:

$$\Delta H_{mix} = Z\Delta w_{sp}N_s\phi_p \tag{4.10}$$

The χ parameter is introduced to give a measure of the energetic change, in RT units, that occurs when a mole of solvent molecules is removed from pure

solvent ($\phi_p = 0$) and is immersed in a non-infinite amount of polymer ($\phi_p = 1$). The χ parameter is defined as follows:

$$\chi = \frac{Z\Delta w}{RT} \tag{4.11}$$

This dimensionless parameter is material-specific, and it generally has positive values.

By introducing the χ parameter, the expression of the enthalpy of mixing becomes:

$$\Delta H_{mix} = RT\chi n_s \phi_p \tag{4.12}$$

According to (4.12), if χ is generally positive, the dissolution of a polymer in a solvent is generally an endothermic process.

By introducing the expressions for ΔS_{mix} and ΔH_{mix} in (2.1), the free energy of mixing for a polymer-solvent system is obtained:

$$\Delta G_{mix} = RT\left[\chi n_s \phi_p + n_s ln\phi_s + n_p ln\phi_p\right] \tag{4.13}$$

It is now clear that the dissolution of a polymer will occur depending on concentration and on sign and magnitude of χ; χ is inversely related to temperature, so increasing T will thermodynamically favor dissolution. The value assumed by the χ parameter is a measure of the polymer-solvent interactions, as well as for the polymer-polymer interactions, thus it can predict if a solvent is good or poor for a given polymer. In general, the smaller the value of χ the greater the rates of free energy decrease during dissolution.

I) χ<0: negative values may indicate strong polar attractions between polymer and solvent.

II) χ<0.5: selected solvent acts as a good solvent for the given polymer.

III) χ=0: the so-called *theta condition*; polymer chains act as ideal chains, that is, they are not affected by wide range interactions with other polymer chains because they are compensated by the effect of the solvent; such a solvent is called *theta-solvent* and the temperature at which this condition is achieved is the *theta-temperature*.

IV) χ>0: selected solvent is a poor solvent and polymer will not dissolve.

4.4 Phase diagrams for polymer blends

Typically, small molecule mixtures undergo phase separation primarily upon cooling, displaying an Upper Critical Solution Temperature (UCST). One of the most interesting aspects of long-chain molecules mixtures is that many miscible systems show cloud point upon heating, that is, a Lower Critical Solution Temperature (LCST) exists. Examples of phase diagrams displaying UCST and LCST are shown in figure 4.3.

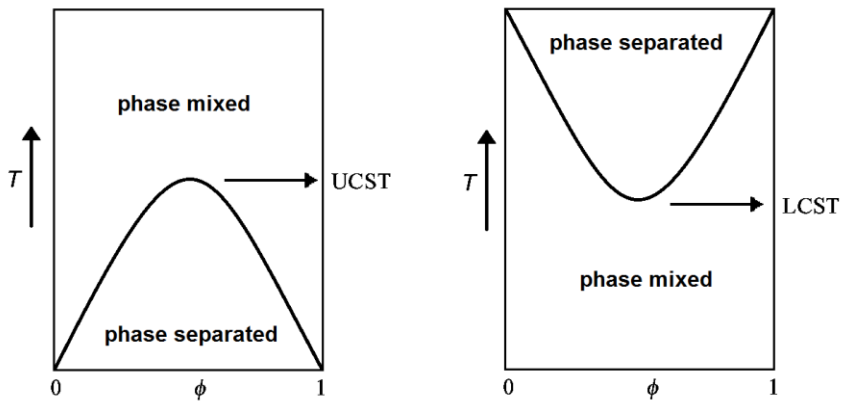

Fig 4.3. Upper critical solution temperature (UCST) and lower critical solution temperature (LCST)-type phase diagrams (Ruzette and Mayes, 2001).

The LCST behavior is not predicted by the classic Flory-Huggins theory, which is a model that does not take into account volume changes during mixing. LCST is related to finite volume variations that occur upon heating, introducing a pressure dependence of the mixing process; and to the not purely enthalpic nature of χ , that introduces additional entropic contributions that result in an increased entropy at high temperatures in the separated phases rather than in the mixed state (Sanchez and Panayiotou, 1993). This behavior can be predicted theoretically only through modification of the original Flory-Huggins model (McMaster, 1973; Prigogine, 1957).

4.5 Phase separation in polymer solution

Phase separation processes within miscible polymer-polymer or polymer-solvent system may occur if they are subject to temperature variation or solvent removal (evaporation or non-solvent addition). Two distinct phenomena can be observed: solid-liquid demixing and liquid-liquid demixing. Solid-liquid phase transitions occur through vitrification or crystallization of one or all the equilibrium liquid phases. Figure 2.6 illustrates a schematic equilibrium phase diagram for a solid-liquid transition in which polymer crystallization occurs.

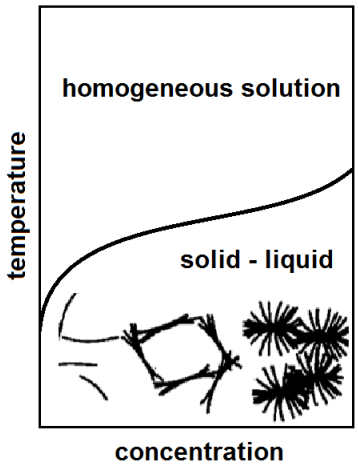

Figure 4.4. Equilibrium phase diagram for a solid-liquid transition. Different morphologies are obtained depending on polymer concentration: single crystals, lamellar stacks, spherulites (Van de Witte et al., 1996).

While solid-liquid demix generally follows the classic mechanism of nucleation and growth, the second phenomena, the liquid-liquid phase transition, is related to the thermodynamic stability of the system. Depending on where the phase boundaries are crossed, nucleation and growth or spinodal decomposition are observed. Figure 4.5 shows a typical phase diagram for a binary polymer-solvent system displaying a liquid-liquid demixing gap. Usually, the boundary of the liquid-liquid demixing gap is called the binodal or cloud point curve. The demixing gap is, in turn, subdivided into a region of spinodal demixing (bounded by the spinodal) and two regions where nucleation and growth is the predominant event. The point of coincidence of binodal and spinodal is the critical point.

The region located between the binodal and the spinodal is the metastable region, where only nucleation and growth can occur. Nucleation is an activated process forming unstable intermediate embryos. Nuclei are formed because of the excess of surface energy of these initial fragments of the new and more

stable phase, while nuclei growth occurs because of the presence of concentration gradients in their immediate vicinity (Cahn, 1965).

The theory of phase separation through spinodal decomposition was described by Cahn (Cahn, 1965). This mechanism involves compositions located in the area enclosed by the spinodal curve, that is, the unstable region. It is best observed through undercooling of compositions that cross the phase boundary directly at the critical point. For all the remaining compositions spinodal decomposition may be observed for very high cooling rates, which prevent demixing while crossing the metastable area. If the fraction of the minor phase is sufficiently high, bicontinuous structures are formed. At the later stages of phase separation, coarsening processes can arise to minimize interfacial energy and in time eventually two fully separated layers may be produced (figure 4.5).

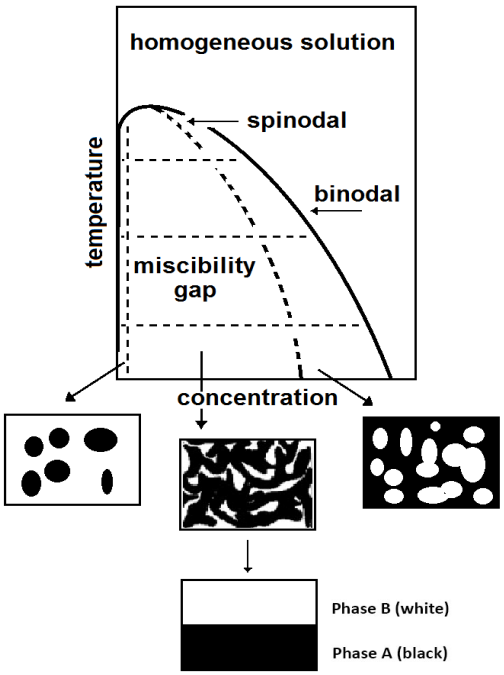

Figure 4.5. Phase diagram for a binary system showing a liquid-liquid demixing gap. Nucleation and growth of *phase A* (black), bicontinuous morphology due to spinodal decomposition, or nucleation and growth of *phase B* (white). Coarsening may produce two fully separated layers (Van de Witte et al., 1996).

References

Cahn, J.W. 1965. Phase Separation by Spinodal Decomposition in Isotropic Systems. J. Chem. Phys. 42, 93–99.

Coleman, J.N.; Khan, U.; Gun'ko, Y.K. 2006. Mechanical Reinforcement of Polymers Using Carbon Nanotubes. Advanced Materials, 18, 689-706.

Fekete, E.; Földes, E.; Pukánszky, B. 2005. Effect of molecular interactions on the miscibility and structure of polymer blends. Eur. Polym. J. 41, 727–736.

Flory, P.J. 1942. Thermodynamics of High Polymer Solutions. J. Chem. Phys. 10, 51–61.

Hildebrand, J.H.; Scott, R.L. 1950. The solubility of nonelectrolytes. Reinhold Pub. Corp.

Hirst, A.R.; Coates, I.A.; Boucheteau, T.R.; Miravet, J.F.; Escuder, B.; Castelletto, V.; Hamley, I.W.; Smith, D.K. J. 2008. Low-molecular-weight gelators: elucidating the principles of gelation based on gelator solubility and a cooperative self-assembly model. Am. Chem. Soc., 130, 9113-9121.

Hobbs, S.Y.; Dekkers, M.E.J.; Watkins, V.H. 1988. Effect of interfacial forces on polymer blend morphologies. Polymer 29, 1598–1602.

Huggins, M.L. 1942. Some Properties of Solutions of Long-chain Compounds. J. Phys. Chem. 46, 151–158.

Jin, Z.; Pramoda, K.P.; Guoqin X.; Suat Hong, G. 2001. Dynamic mechanical behavior of melt-processed multi-walled carbon nanotube/poly(methyl methacrylate) composites. Chem. Phys. Lett., 337, 43-47.

Liu, Q.; Hedberg, E.L.; Liu, Z.; Bahulekar, R.; Meszlenyi, R.K.; Mikos, A.G. 2000. Preparation of macroporous poly (2-hydroxyethyl methacrylate) hydrogels by enhanced phase separation. Biomaterials 21, 2163–2169.

Macosko, C.W. 2000. Morphology development and control in immiscible

polymer blends. Macromol. Symp. 149, 171–184.

Marrs, B; Andrews, R.; Rantell, T.; Pienkowski, D. 2006. Augmentation of acrylic bone cement with multiwall carbon nanotubes. J. Biomed. Mater. Res. A, 77, 269-276.

Paul, D.R.; Barlow, J.W. 1980. Polymer Blends. J. Macromol. Sci. Part C Polym. Rev. 18, 109–168.

Paul, D.R., Newman, S. 1978. Polymer Blends. Academic Press.

Pötschke, P.; Paul, D.R. 2003. Formation of Co-continuous Structures in Melt-Mixed Immiscible Polymer Blends. J. Macromol. Sci. Part C Polym. Rev. 43, 87–141.

Prigogine, I. 1957. The Molecular Theory of Solutions. North-Holland Publishing Company; New York.

Raghavan, S.R.; Douglas, J.F. 2012. The conundrum of gel formation by molecular nanofibers, wormlike micelles, and filamentous proteins: gelation without cross-links?. Soft Matter, 8, 8539-8546.

Robeson, L. 2014. Historical Perspective of Advances in the Science and Technology of Polymer Blends. Polymers 6, 1251–1265.

Robeson, L.; Robeson, L.M. 2007. Polymer Blends: A Comprehensive Review. Hanser Publications, Munich; Cincinnati.

Ruzette, A.G.; Mayes, A.M. 2001. A Simple Free Energy Model for Weakly Interacting Polymer Blends. Macromolecules 34, 1894–1907.

Sanchez, I.C.; Panayiotou, C.G. 1993. Equation of State Thermodynamics of Polymer and Related Solutions. In Models for Thermodynamic and Phase Equilibria Calculations. CRC Press, New York.

Utracki, L.A.; Favis, B.D. 1987. Polymer Alloys and Blends. Industrial Materials Research Institute. Canada, I.M.R.I.

Van de Witte, P.; Dijkstra, P.; Van den Berg, J.; Feijen, J. 1996. Phase separation

processes in polymer solutions in relation to membrane formation. J. Membr. Sci. 117, 1–31.

Winey, K.I.; Vaia, R.A. 2007. Polymer Nanocomposites. MRS Bulletin 32, 314-322.

CHAPTER 5

Organogels and solvents

5.1 Introduction

As briefly discussed in chapter 3 (section 3.4.2), chemical organogels are a class of gel composed of a liquid organic phase (organic solvent) within a three-dimensional, cross-linked network.

Organogels are composed of cross-linked polymer networks that are built by covalent bonds with a very high molecular weight (M_w) and are able to load high amounts of liquid without undergoing polymer solubilization. Due to their cohesive force, chemical gels can be easily removed from any surface, without breaking or leaving residues. The retentiveness of the organogel network can be adjust tuning the amount of cross-linker and the monomer-solvent phase ratio during the synthesis of the gel, which was carried out through the free radical polymerization of monomer in pure solvent. Solvents used for the gel preparation can be changed in order to targeting the removal of different coatings from works of art surface.

This chapter will present an overview on organogels characteristic features to justify its use for the development of a new cleaning system, specifically tailor made for water/solvent sensitive materials, i.e. cellulosic (paper) artifacts.

In particular, the properties of poly(methyl methacrylate) (PMMA) as polymer network and the main features of solvents (diethyl carbonate and methyl ethyl ketone), used for the synthesis of PMMA organogels, will be reported. This chapter provides a fundamental discussion on the knowledge on chemicals,

which constitute innovative cleaning tools developed, assessed, and applied during this work and will be discussed in Experimental section.

5.2 Organogels

As well as gel classification (see chapter 3), in literature there are various definitions of organogel; here we reported two of them:

- Gel is a soft, solid or solid-like material, which contains both solid and liquid components. The solid component (the gelator) is present as a network of aggregates, which immobilizes the liquid component. The solid network prevents the liquid from flowing, primarily via surface tension. The nature of the liquid component defined if gel is a hydrogel (water) or an organogel (solvent) (Murdan, 2005).
- Organogel is a solid system, non-crystalline, thermoreversible (thermoplastic) and viscoelastic. The semi-solid preparation immobilized external apolar phase within spaces of the three-dimensional networked structure; this system is formed due to the physical interactions amongst the self-assembled structures of compounds well-known as gelators (Gang et al., 2011).

Organogels can be classified in various ways (figure 5.1) based on the nature of gelators, solvents and intermolecular interaction (Mujawar et al., 2014).

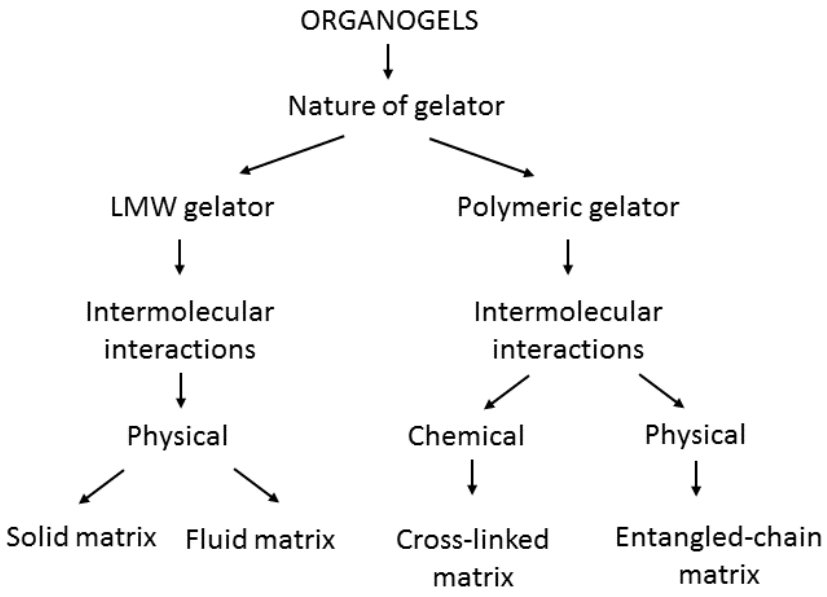

Figure 5.1 Classification of organogel (Mujawar et al., 2014).

For what concerns the nature of gelators, organogel networks can be formed through two different ways: i) formation of gel network by a polymerization reaction, ii) self-assembly process using low molecular weight (LMW) gelators.

In the first case, a precursor solution of monomers is converted into polymeric chains, that grow into covalently-linked network, which immobilizes the solvent. At a critical concentration, called *gel point*, the polymeric matrix starts to exhibit gel-like physical properties, i.e. an extensive continuous solid network, no steady-state flow, and solid-like rheological properties (Raghavan et al.,2012).

On the other hand, during the self-assembly of LMW gelators secondary forces such as Van der Waals or hydrogen bonding produce entangled chain matrix: monomers are clustered into a non-covalently bonded network that retains organic solvent, and as the network grows, it exhibits gel-like physical properties (Hirst et al., 2008). Difference amongst LMW physical organogels is governed by the kinetic properties of aggregates, i.e. solid versus fluid networks.

Despite the numerous developments in gelling processes, the molecular structure of a potential gelator is difficult to predict, as well as the choice of preferentially gelling solvents (Mujawar et al., 2014). Therefore, the prediction of characteristic gelation parameters, such as gel point and gelation time, is very hard. Kinetic and statistical mathematical theories had moderate success in predicting gelation parameters, although a simple, accurate and widely applicable theory has not yet been developed.

Some properties of organogel are briefly presented in the next sub-paragraph.

5.2.1 Organogels properties

Viscoelasticity

Viscoelasticity is associated with materials having both viscous and elastic properties (Garg et al., 2011). The organogels seems to follow Maxwell model of viscoelasticity (Toshiyuki et al., 2003). As briefly discussed above, organogels are characterized by a three dimensional matrix formed during the physical interaction amongst the gelator molecules. At lower shear rates, organogels act like a solid and hence shows an elastic property. As the shear stress is increased, the physical interacting points amongst the structures start getting weakened until the shear stress is high enough to disrupt the interactions and organogels starts flowing. This behavior may be best explained with the plastic flow behavior (Garg et al., 2011).

To understand the flow property of organogels, rheological properties of the gelator solution in apolar solvents during the preparation of gel system have been studied (Sahoo et al., 2011).

In case of solid matrix, the gelators are dissolved in apolar solvents at higher temperature. When temperature decrease the viscosity of the solution growth

and this behavior can be attributed to the precipitation of organogelators and then the formation of organogels take place through physical interactions amongst the gelators.

In case of fluid matrix, it has been observed that, when a certain amount of water is added to the gelator solution in apolar solvents, there is a consequent exponential increase in the viscosity component which may be attributed to the formation of rigid structure due to the entanglement of the fluid-fiber structures.

To better understand the viscoelastic properties of organogels, the reader is reminded to chapter 7.

Thermoreversibility

When organogels are heated up above a critical temperature, their solid matrix-like structure is loose and they start flowing. This behavior has been attributed to the disruption in the physical interactions amongst the gelator molecules due to the increase in the thermal energy within organogels. However, if the heated organogels systems are cooled down, the physical interaction amongst the organogelators prevail and organogels revert to the more stable configurations.

Thermostability

Organogels are inherently thermostable in nature; their stability may be attributed to the ability of the gelators to undergo self-assembly, under suitable conditions, to form organogels. As the gelators undergo self-assembly, it results in the decrease in the total free energy of the system and organogels return to a low-energy thermostable system. Due to the inherent thermostability of organogels, they have been proposed as a delivery vehicle for bioactive agents and for cosmetic applications where a longer shelf-life is desirable (Chen et al., 2007).

Chirality effects

The presence of chirality in the LMW gelators have been found to affect the growth and the stability of the solid-fiber networks. Thermoreversibility of the gels characterized by self-assembled solid-fiber network has also been associated with the chirality. A good solid-fiber gelator has a chiral center whereas chirality does not have any effect on fluid-fiber gelators. The chiral centers within the gelators helps in the formation of a compact molecular packing, which provides a thermodynamic and kinetic stability to organogels system (Fages, 2005).

5.3 Poly(methyl methacrylate) network

Poly(methyl methacrylate) (PMMA) or poly (methyl 2-methylpropenoate) is the synthetic polymer of methyl methacrylate (MMA) (figure 5.2). It is commonly called acrylic glass or simply acrylic.

The material was developed in 1928 in several different laboratories, and was first brought to market in 1933 by the Rohm and Haas Company under the trademark Plexiglas™.

Due to its various range of applications and potential end-use environments, PMMA has been the subject of numerous nanocomposite studies focusing on the improvement of strength and durability (Coleman et al., 2006; Jin et al., 2001).

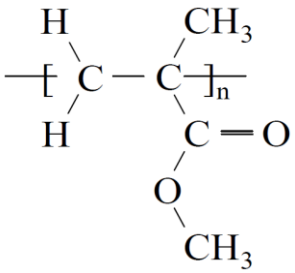

Figure 5.2. Poly (methyl methacrylate) repeat unit.

PMMA is a linear thermoplastic polymer, which is routinely produced by emulsion polymerization, solution polymerization, and bulk polymerization. Generally, radical initiation is used. PMMA can be obtained by free radical polymerization of vinyl monomers (MMA) (Fig. 5.3).

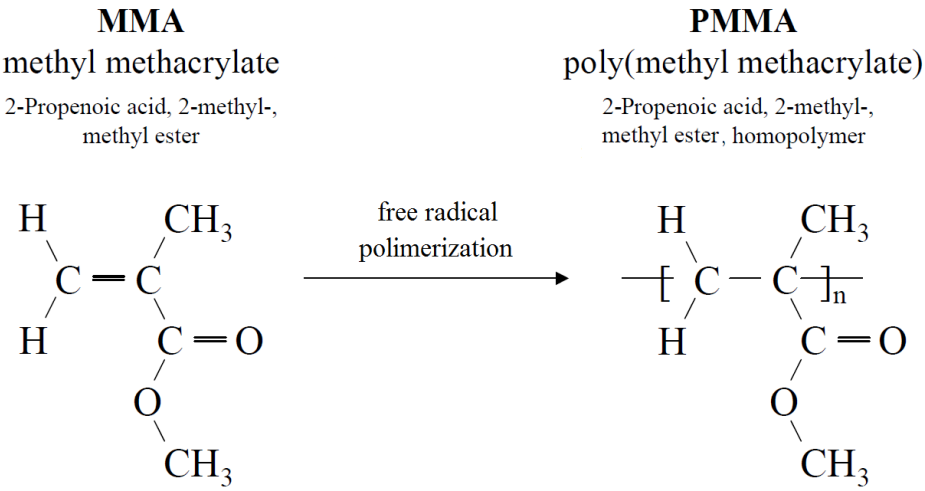

Figure 5.3. PMMA free radical polymerization.

Methyl methacrylate, in bulk liquid form, is polymerized under the influence of free-radical initiators to form solid PMMA. The presence of the pendant methyl (CH_3) groups prevents the polymer chains from packing closely in a crystalline fashion and from rotating freely around the carbon-carbon bonds. As a result, PMMA is a tough and rigid plastic and the polymer produced by radical polymerization (all commercial PMMA) is atactic and completely amorphous.

An important feature of this polymer is the perfect transmission of visible light, and, because it retains these properties over years of exposure to ultraviolet radiation and weather, it is an ideal substitute for glass.

PMMA is a member of a family of polymers called *acrylates*, or better known under the name *acrylics*.

Main PMMA properties are summarized as follow.

Physical properties

Physical properties	Values
Density	1,15-1,19 g/cm^3
Water absorption	0,3-2%
Moisture absorption at equilibrium	0,3-0,33%
Linear modulus shrinkage	0,003-0,0065 cm/cm
Melt flow	0,9-27 g/10 min

Table 5.1. PMMA physical properties.

PMMA has high mechanical strength, high Young's modulus and low elongation at break; in fact, it does not shatter on rupture. It is one of the hardest thermoplastics and is also highly scratch resistant. It exhibits low moisture (table 5.1) and water absorbing capacity, due to which products made have good dimensional stability. Both of these characteristics increase as the temperature rises. Its strength properties during injection molding differ significantly in longitudinal and transverse direction as a result of the orientation effect.

Mechanical properties

As in the case with other thermoplastics, the mechanical properties of PMMA vary as the temperature changes. This material tends to creep and it is not suitable for operation under multiple dynamic loads. Table 5.2 shows some of mechanical characteristics of PMMA.

Mechanical properties	Values
Hardness, Rockwell M	63-97
Tensile strenght	47-79 MPa
Tensile modulus	2.2-3.8 GPa
Tensile creep modulus, 1h	1800-2700 MPa

Table 5.2. PMMA mechanical properties.

Thermal properties

Thermal behavior is another important property of PMMA. The thermal stability of standard PMMA is only 65 °C. Heat-stabilized types can withstand temperatures of up to 100 °C. PMMA can withstand temperatures as low as -70 °C. Its resistance to temperature changes is very good.

PMMA is a combustible material, which continues burning even after the flame is removed; the products separated in the process of thermal destruction forming carbon dioxide, water, carbon monoxide and low-molecular-weight compounds, including formaldehyde (Zeng et al., 2002).

In table 5.3 the most important mechanical properties of PMMA are reported.

Thermal properties	Values
Coefficient of thermal expansion, linear 20 °C	60-130 µm/m °C
Specific heat capacity	1,46-1,47 J/g °C
Thermal conductivity	0,19-0,24 W/mK
Maximum service temperature, air	41-103 °C
Melting point	130 °C
Glass temperature	100-105 °C

Table 5.3. PMMA thermal properties.

Optical and electrical properties

PMMA exhibits very good optical properties; it transmits more visible light than glass (80-93% of visible light). Combined with its good degree of compatibility with human tissue, it can be used for replacement intraocular lenses or for contact lenses. Unlike glass, PMMA does not filter ultraviolet light. It transmits UV light down to 300 nm and allows infrared light of up to 2800 nm to pass.

Electrical properties

The low water absorption capacity of PMMA makes it very suitable for electrical engineering purposes. Its resistivity (10^{14}-10^{15} Ω cm) depends on the ambient temperature and relative humidity. Its dielectric properties are very good, and its dielectric constant (2.8-4), as well as the loss tangent, depends on the temperature, the relative humidity of air and the frequency.

Chemical and radiation resistance

Acrylics are unaffected by aqueous solutions of most laboratory chemicals, by detergents, cleaners, dilute inorganic acids, alkalis, and aliphatic hydrocarbons. However, acrylics are not recommended for use with chlorinated or aromatic hydrocarbons, esters, or ketones. It dissolves completely in chloroform, di- and tri-chlorethane, which is used for production of glues. The chemical resistance will vary with stress level, temperature, reagents and duration of exposure.

PMMA are physiologically harmless. Due to their low moisture absorption capacity they are not attacked by molds and enzymes.

PMMA is one of the polymers that is most resistant to direct sunshine exposure. Its strength characteristics exhibit small variations under the effect of UV-radiation, as well as in the presence of ozone. These properties of PMMA make it suitable for products intended for long open-air operation.

Due to its properties and easy processing, to the broad range of applications and potential end-use environments, PMMA has been the subject of numerous nanocomposite studies focusing on the improvement of strength and durability (Coleman et al., 2006; Marrs et al., 2006; Winey et al., 2007; Jin et al., 2001).
The suitability for a wide range of production and processing techniques, have made PMMA an excellent candidate for the aim of this work, also taking into account a previous doctoral research in this field (Pizzorusso, 2010). We have to remember that cleaning operations that involve solvents are very difficult to control, and are dangerous for both the conservator and the artifact. By loading the solvent into a gel, the rate of solvent evaporation is lowered and its penetration into the artistic substrate is controlled. In this way, covering layers are selectivity removed.

5.4 Solvents

In this paragraph, the main physical-chemical properties of solvents are briefly discussed, in order to introduce the application of liquid solvents as cleaning agents for works of art conservation.

Therefore, in sub-paragraphs 5.4.1 and 5.4.2 will reported the properties of the two solvents used for the synthesis of PMMA organogels as innovative cleaning tools, developed during this thesis and detailed in chapters 6 and 7.

5.4.1 Physical-chemical properties

The main properties that defined what type of compounds a solvent will be able to dissolve, and its miscibility with other solvents are polarity, dipole moment, polarizability and hydrogen bonding.

The rule ‘‘like dissolves like’’ is the base to choice the appropriate solvent for the cleaning of a surface; polar solvents dissolve polar compounds best and non-polar solvents dissolve non-polar compounds best (see paragraph 5.4.2). Strongly polar compounds or ionic compounds, dissolve only in very polar solvents such as water, while strongly non-polar compounds dissolve only in very non-polar organic solvents such as hexane. Indeed, water and hexane are not miscible with each other and will rapidly separate into two layers, even after being shaken.

Based on dielectric values, that must be greater than 15, is possible to discriminate protic and aprotic solvents. A protic solvent (i.e. water and alcohols) contains hydrogen atoms bound to either oxygen or nitrogen atoms, and can release H^+ ions upon dissociation. Instead, aprotic solvents (i.e. acetone or dichloromethane) cannot donate H^+ ions, and solvate positively charged species via their negative dipole.

For what concerns density (ρ), generally organic solvents possess a lower density than water and they will form an upper layer on top of the aqueous phase. In some cases, it is possible to refer to the specific gravity instead the density; specific gravity (*SG*, unitless value) is defined as the ratio between density of the solvent (ρ_{solv}) and density of water (ρ_{water}) at the same temperature. According to the SG value, a water-insoluble solvent will float (*SG*<1) or sink (*SG*>1) when mixed with water.

Another important property of solvents is the boiling point (*bp*), which is normally measured at 1 atm (1.013 bar), and it is defined at the pressure of 1 bar (0.987 atm).

The evaporation rate of a solvent depends on the *bp* value: small amounts of low-boiling solvents (*bp*<100 °C), such as diethyl ether or acetone, will evaporate quickly at room temperature, while high-boiling solvents (*bp*>100 °C), such as

water or dimethyl sulfoxide, need higher temperature, or the application of vacuum for fast evaporation.

In conservation applications such as cleaning, the choice of the solvent is ruled by its *bp*: volatile solvents (low *bp*) limit the penetration of dissolved materials through porous substrates. It must be noticed that the specific procedure to be adopted during a conservation treatment depends on the nature of the solvent and on its final use (Perrin and Armarego, 1988).

5.4.2 Solubilization process, polarity of solvents and Teas diagram

To better understand the thermodynamics involving in a cleaning process, it is important to describe the solubilization process using pure and mixed liquids.

In general, a solubilization occurs when the attractive forces between liquid solvent and substance prevail over the cohesive intermolecular forces of the substance, then the solubilization process takes place. Thermodynamically, the solubilization by a solvent (*S*) of the substance (*A*) occurs spontaneously when the variation of the Gibbs free energy of the process (ΔG_{solub}) is negative (Fratini and Carretti, 2013):

$$\Delta G_{solub} = G_{SA} - G_{SS} - G_{AA} < 0 \tag{5.1}$$

where G_{SA} is the Gibbs free energy of the solution, and G_{SS} and G_{AA} are the Gibbs free energies of the pure solvent and the pure solute, respectively. Solubilization process is influenced by three attractive forces, according to the theory of intermolecular interactions: hydrogen bonds, dipolar interactions and dispersion forces (Israelachvili, 2011).

According to the theory proposed by Hansen in 1966 (Hansen and Beerbower, 1971), the interaction forces between *A* and *S* molecules are additive, therefore the cohesive energy density δ_t^2 for a solvent is given as a function of the three partial solubility parameters:

$$\delta_t^2 = \delta_d^2 + \delta_p^2 + \delta_h^2 \tag{5.2}$$

where δ_d referred to dispersion forces, δ_p referred to dipolar interactions and δ_h referred to hydrogen bonds.

The Hansen parameters can be represented in terms of reduced solubility parameters, calculated as follow (Carretti and Dei, 2013):

$$f_d = \frac{100\delta_d}{\delta_d + \delta_p + \delta_h} \tag{5.3}$$

$$f_p = \frac{100\delta_p}{\delta_d + \delta_p + \delta_h} \tag{5.4}$$

$$f_h = \frac{100\delta_h}{\delta_d + \delta_p + \delta_h} \tag{5.5}$$

where f_d , f_p and f_h are the reduced solubility parameters due to hydrogen bonds, to polar forces, and to dispersion forces, respectively.

They are defined in such a way that:

$$f_d + f_p + f_h = 100 \tag{5.6}$$

In this way, each solvent can be univocally identified by a group of numerical parameters (see table 5.4), whose values take into account the relative strength of hydrogen bonding, polar and dispersion interactions among the solvent molecules (Horie, 1987).

The more similar are the singular reduced solubility parameters of two distinct substances (a solvent and a solute), the more mutually soluble they are.

Solvent	f_d	f_p	f_h
Methanol	30	22	48
Ethanol	36	18	46
n-Propanol	40	16	44
n-Butanol	43	15	42
Benzyl alcohol	48	16	36
Dimethylsulfoxide	41	36	23
Acetone	47	32	21
Ethyl acetate	51	18	31
Chloroform	67	12	21
Xylenes	83	5	12
Cyclohexane	96	1	3
Mineral spirits	90	4	6
n-Hexane	100	0	0
Water	18	28	54

Table 5.4. Reduced solubility for several solvents.

The reduced solubility parameters provide the possibility to report the Hansen parameters in a triangular diagram, named Teas chart (see figure 5.4). This diagram is a very useful tool in restoration practice, since in most cases a selective removal is desirable.

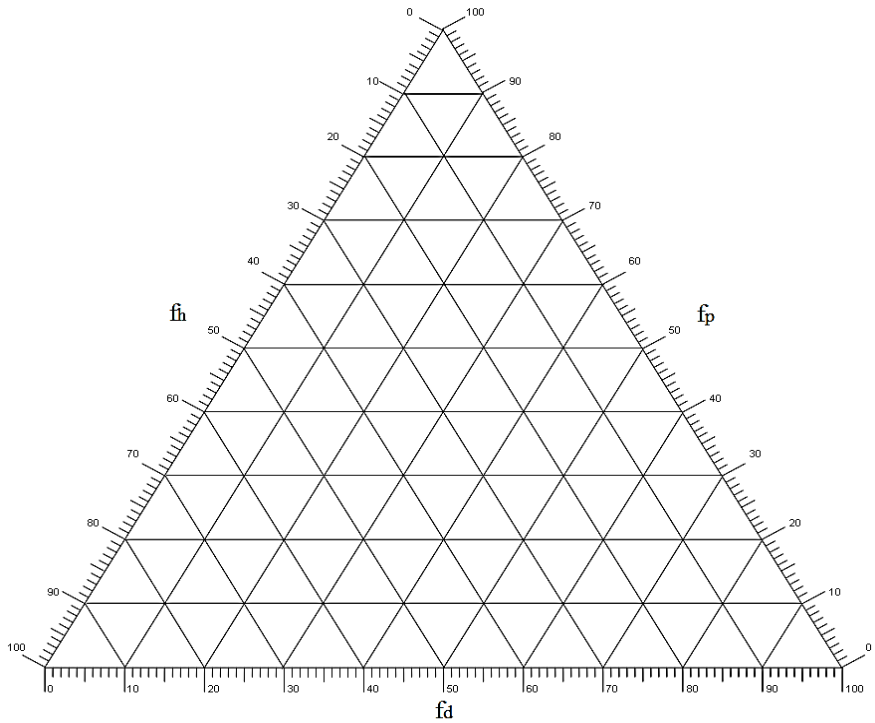

Figure 5.4. Teas chart in function of the three reduced parameters related to dispersion forces f_d, dipolar interactions f_p, and hydroge bonds f_h.

A selective removal, in this context, is intended as a choice of a solvent that has solubility parameters as similar to the substance to remove, while, at the same time, as different to the artifacts surface in order to avoid solubilization of materials to preserve.

Solvents are situated in the Teas diagram according to their solubility parameters. A cleaning system composed by the mixture of solvents has a different position in the diagram with regard to the position of the singular solvents. It gives the possibility to choose of the optimal cleaning tool, in terms of both cleaning efficiency and toxicity of the solvents used (Fratini and Carretti, 2013). The Teas diagram solubility/swelling of various solid substances (e.g. polymers) is given in the literature (Horie, C.V., 1987). Furthermore, it is possible to predict the solubility of a given substance using the Feller test (reader can refer to the literature on this subject).

5.4.3 Diethyl carbonate: a “green” solvent

Solvents are principal used in chemical processes to aid in mass and heat transfer, and to facilitate separations and purifications. They are also an important and often the primary component in cleaning agents, adhesives and coatings (paints, varnishes and stains). Solvents are frequently volatile organic compounds (*VOCs*) and are therefore a major environmental concern as they are able to form low level ozone and smog through free radical air oxidation processes (Lancaster, 2002). Moreover, they are often highly flammable and can cause adverse health effects including eye irritation, headaches and allergic skin reactions.

“Green Chemistry” can be defined as a chemical working process, utilizing raw materials, eliminating waste and avoiding the use of toxic and hazardous reagents and solvents (DeSimone, 2002). Twelve principles of “Green Chemistry” (Anastas and Warner, 1998), describing its main goals and explaining its definition in practice (Suresh and Sandhu, 2011). One of the principles of green chemistry refers to ‘*use safer solvents and auxiliaries*’ (Anastas and Warner, 1998; Clark and Macquarrie, 2002; Lancaster, 2002).

Over the last 15 years, new solvent alternatives started to attract attention and slowly began to replace conventional solvents (Shanab et al., 2013). They include water, ionic liquids, organic carbonates, carbon dioxide as well as bio solvents. These alternative solvents are characterized by a low toxicity, easiness to recycle, and inertness.

Organic carbonates represent an interesting class of organic solvents, which are known since the 1950s and they offer various advantages as solvents. (Reichardt, 2003).

As polar solvents (esters of carbonic acids) they offer a suitable liquid temperature range (e.g., for propylene carbonate, *mp*=-49 °C, *bp*= 243 °C)

(Anastas and Warner, 1998). They display a low (eco) toxicity, are completely biodegradable and also they are easily available in large amounts, and inexpensive.

Organic carbonates are primarily known as solvents for electrochemical purpose (Smart and al., 1999; Ding et al., 2001; Xu, 2004; Stephan, 2005) but are also widely used for extraction, pharmaceutical and medical applications. In recent years, organic carbonates were highlighted as possible alternatives to replace *VOCs*.

Six carbonates, which have been identified (figure 5.5) to be especially suitable as solvents, are identified and studied for their use in catalysis reactions (Schäffner et al., 2010). Transition information about the physicochemical properties should help to select the right organic carbonate as solvent in reactions and, especially, larger processes.

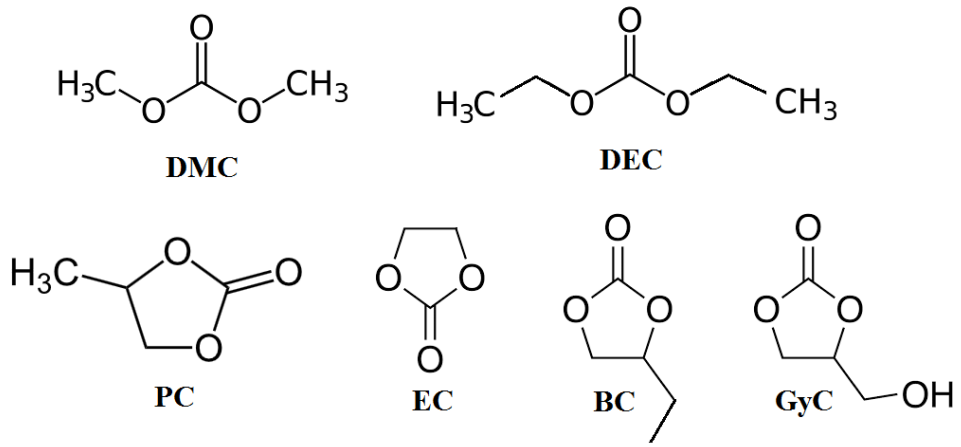

Figure 5.5. Organic carbonates representatives that have been used as solvent: dimethyl carbonate (DMC), diethyl carbonate (DEC), propylene carbonate (PC), ethylene carbonate (EC),butylene carbonate (BC), glycerol carbonate (GyC) (Schäffner et al., 2010).

Among organic carbonates, alkyl carbonates, attracted attention in various fields as very promising solvents. For example, Dimethyl carbonate (DMC) and diethyl carbonate (DEC), two typical alkyl carbonates, are the largely studied in the field

of fuel and chemical industries (Li et al., 2009; Rodrìguez et al., 2003; Luo et al., 2001; Comelli et al., 1996).

These solvents possess properties of nontoxicity and biodegradability and both of them have high oxygen content. Moreover, DEC is considered to be the option for meeting the oxygenated specifications on fuel and might serve as an additive for minimizing pollution (Dunn et al., 2002).

Diethyl carbonate (DEC), the second member of dialkyl carbonates, provides an interesting case study for understanding conformational preferences in molecules containing the ethoxy groups, such as esters. DEC is widely used (Labafzadeh et al., 2015; Zeng et al.,2015; Pacheco et al., 1997) as ethylating and carbonylating reagent in organic synthesis. Furthermore, it is employed as solvents of nitro cotton, cellulose ether, synthetic resin and natural resin in the textile printing and dyeing industry. It is used to prepare electrolyte in the capacitor and lithium battery. Diethyl carbonate is fundamental in the pharmaceutical industry, and it can also be used as fuel and lube additive, and finds application in the paint and plastic industry.

It is observed that mixing of different compounds offers improvement in properties such as volume, enthalpy and entropy of mixing, thereby reflecting the degree of the deviations from non-ideality. Information about the excess properties of liquid mixtures containing DEC and aromatic compounds (Gnanakumari et al., 2007), and their dependence on composition and temperature constitute are very important fundamental data owing to their applications in different fields.

Diethyl carbonate is listed as “green” solvent (Arockiam et al., 2009), and based on its physical-chemical properties (table 5.5), it was chosen during this work as potential cleaning agents for conservation of works of art. In particular, DEC

seems to be able to dissolving or swelling a wide range of natural and synthetic resins from water sensitive artifacts, such as paper artworks.

To justify the choice of diethyl carbonate as a potential cleaning solvent, here (table 5.5) are reported the principal properties of diethyl carbonate.

Properties	**Values**
Melting point (*mp*)	-74,3 °C (Ding, 2001)
Boiling point (*bp*)	126 °C (Lide, 1995; Smart, 1999)
Freezing point	-43 °C
Flash point	25 °C
Density (ρ)	0,975 g/cm^3 (Smart, 1999)
Viscosity (η)	0,753 cP (at 100 °C) (Yamamoto et al., 2006)
Enthalpy of fusion ($\Delta_{fus}H$)	9,24 kJ/mol (Ding, 2004)
Heat capacity (C_p)	1,0916 J/K (Ding, 2004)
Dielectric constant	2,82 (at 25 °C)
Liquid surface tension	0,0263 N/m (at 20 °C)
Liquid water interfacial tension	0,01286 N/m (at 20°C)
Vapor pressure	10,8 mm Hg (at 25 °C) (Daubert et al., 1989)
Molecular weight	118,13 g/mol

Table 5.5. Principal properties of diethyl carbonate.

It is important to specify that, during this work, DEC was used both for synthesis of polymeric network and as confined solvent in order to develop innovative PMMA organogels for the cleaning of water sensitive surfaces.

5.4.4 Methyl ethyl ketone

2-Butanone, well known as methyl ethyl ketone (MEK), is an organic solvent characterized by satisfactory boiling point, good solubility, volatility, and stability.

Chemically, methyl ethyl ketone is aliphatic ketone (figure 5.6) and the second link in the homologous series of aliphatic ketones; next to acetone, MEK is the most important commercially produced ketone.

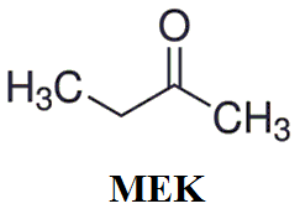

MEK

Figure 5.6. Methyl ethyl ketone.

It is widely used in various range of applications, for example as an extraction medium for fats, oils, paraffin waxes and resins (SRI, 2000). MEK is also employed in surface coatings, adhesives, printing inks, chemical intermediates, magnetic tapes and lube oil dewaxing agents (ATDSR, 1992). Therefore, this solvent has many natural sources (natural human metabolite, emitted by trees, plants, bacteria (Scriver et al., 2001; HSDB, 2001; ATSDR, 1992). On December 19, 2005, USEPA issued a final rule removing MEK from Section 112 (b) (1) of the Clean Air Act (USEPA, 2005); indeed, USEPA determined that ambient concentrations,

bioaccumulation or deposition of MEK may not reasonably be anticipated to cause adverse human health or environmental effects.

In table 5.6 the principal properties of methyl ethyl ketone are summarized.

Properties	**Values**
Melting point (*mp*)	-83,35 °C
Boiling point (*bp*)	79,64 °C
Freezing point	-86,96 °C
Flash point	-9 °C (Pohanish, 2012)
Density (ρ)	0,805 g/cm^3 (Lewis, 2007)
Viscosity (η)	0,40 cP (25 °C) (Lewis, 2007)
Enthalpy of fusion ($\Delta_{fus}H$)	8.44 kJ/mol
Heat capacity (C_p)	2,297 J/K
Dielectric constant	18,51 (at 20 °C)
Liquid surface tension	23,97 mN/m (at 25 °C) (Haynes, 2014-2015)
Vapor pressure	90,6 mm Hg (at 25 °C) (Alaire et al., 1995)
Molecular weight	72,11 g/mol

Table 5.6. Principal properties of methyl ethyl ketone.

MEK is a colourless liquid and its odor look like that of acetone. It is only partially miscible with water and it is completely miscible with most organic solvents. In

fact, it forms binary and ternary azeotropic mixtures in combination with water and several other organic solvents.

MEK is stable under normal conditions and in absence of air. It is unsaponifiable and does not form corrosive products under hydrolysis. It is heat and light stable. It only decomposes after prolonged exposure of UV.

It can be widely utilized in chemical synthesis. Its reactivity centers on the carbonyl group and its adjacent hydrogen atoms. Condensation, ammonolysis, halogenations and oxidation can be carried out under the proper conditions.

The use of methyl ethyl ketone for the removal of wax may seems a particular choice, considering that this solvent is out from the solubility area of waxes (see figure 5.7).

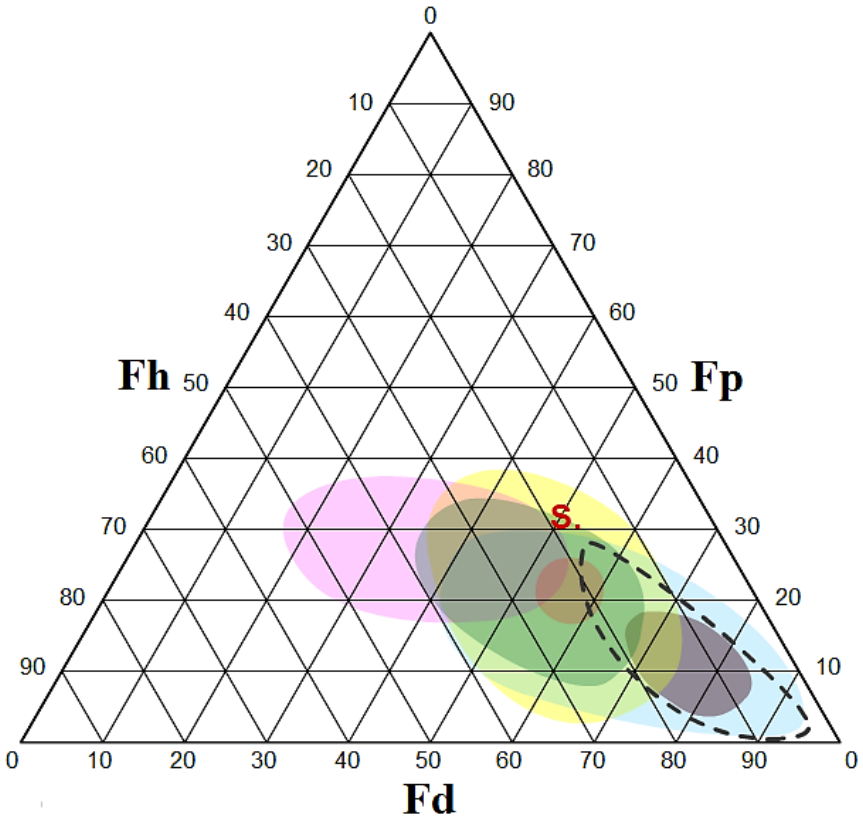

Figure 5.7. Teas chart (readapted from [http://www.icr.beniculturali.it/flash/progetti/TriSolv/TriSolv.html]). Solubility area of beeswax (dashed line) and MEK (reported as "S").

The Hansen solubility parameters for methyl ethyl ketone are: δ_D=16.0, δ_P=9.0 and δ_H=5.1 (Hansen, 2007).

However, it is known from literature that MEK is widely used industrial chemistry for solvent dewaxing process (Freund et al, 1982; Mohamed et al., 2008; As'Ad et al., 2015). Solvent dewaxing is a treatment method that employs recovery of microcrystalline or paraffin waxes from the heavy crude before it is processed.

In this context, preliminary tests on laboratory wax samples were performed in order to evaluate the efficiency of solubilization of methyl ethyl ketone.

As for DEC, in the present work a new PMMA organogel was synthetized and loaded with methyl ethyl ketone organic solvent. It was specifically designed for the selective removal of degraded waxy coatings from the surface of water sensitive surfaces, such as ancient inked paper.

References

Alarie, Y.; Nielsen, G.D.; Andonian-Haftvan, J.; Abraham, M.H. 1995. Physicochemical Properties of Nonreactive Volatile Organic Chemicals to Estimate RD50: Alternatives to Animal Studies. Toxicol. Appl. Pharmacol., 134, 92-99.

Anastas, P.T; Warner, J.C. 1998. Green Chemistry: Theory and Practice, Oxford University Press, New York.

Arockiam, P.; Poirier, V.; Fischmeister, C.; Bruneaua, C.; Dixneuf, P.H. 2009. Diethyl carbonate as a solvent for ruthenium catalysed C–H bond functionalization. Green Chem., 11, 1871-1875.

As'Ad, A.M.; Yeneneh, A.M.; Obanijesu, E.O. 2015. Solvent Dewaxing of Heavy Crude Oil with Methyl Ethyl Ketone. J. Pet. Environ. Biotechnol., 6, 213-217.

ATSDR (Agency for Toxic Substances and Disease Registry). Toxicological Profile for 2-Butanone. 1992. Available at http://www.atsdr.cdc.gov.

Berti, D.; Lo Nostro, P. 2013. Chapter 4. Cleaning I: Solvents and Solutions. In Nanoscience for the Conservation of Works of Art; Baglioni, P.; Chelazzi, D.; O'Brien, P. Eds.; Royal Society of Chemistry: Cambridge, pp. 252–279.

Carretti, E.; Dei, L. 2013. Chapter 5. Cleaning I: Applications. In Nanoscience for the Conservation of Works of Art; Baglioni, P.; Chelazzi, D.; O'Brien, P. Eds.; Royal Society of Chemistry: Cambridge, pp. 252–279.

Chen, Z.; Li, F; Yang H.; Yi, T.; Huang, C. A 2007. Thermostable and Long-Term-Stable Ionic-Liquid-Based Gel Electrolyte for Efficient Dye-Sensitized Solar Cells. Chem. Phys. Chem., 8, 1293-1297.

Clark, J.H.; Macquarrie, D.J. 2002. Handbook of Green Chemistry and Technology, Blackwell Science, London.

Coleman, J.N.; Khan, U.; Gun'ko, Y.K. 2006. Mechanical Reinforcement of Polymers Using Carbon Nanotubes. Advanced Materials, 18, 689-706.

Comelli, F.; Francesconi, R.; Ottani, S. 1996. Isothermal vapor–liquid equilibria of dimethyl carbonate + diethyl carbonate in the range (313.15–353.15)K. J. Chem. Eng. Data 41, 534–536.

Daubert, T.E.; Danner, R.P. 1989. Physical and Thermodynamic Properties of Pure Chemicals Data Compilation. Washington, D.C.: Taylor and Francis.

DeSimone, J.M. 2002. Practical Approaches to Green Solvents. Science, 297, 799-803.

Ding, M.S. 2004. Liquid-Solid Phase Equilibria and Thermodynamic Modeling for Binary Organic Carbonates. J. Chem. Eng. Dat. 49, 276-282.

Dunn, B.C.; Guenneau, C.; Hilton, S.A.; Pahnke, J.; Eyring, E.M. 2002. Production of diethyl carbonate from ethanol and carbon monoxide over a heterogeneous catalyst, Energy Fuels 16, 177–181.

Fages, F. 2005. Low Molecular Mass Gelators: Design, Self-Assembly, Function. Topics in Current Chemistry. Vol. 256, ed. Springer Berlin Heidelberg.

Feller, R. L.; Stolow, N.; Jones, E. H. 1985. On Picture Varnishes and Their Solvents; National Gallery of Art: Washington, DC.

Fratini, E.; Carretti, E. 2013. Chapter 10. Cleaning IV: Gels and Polymeric Dispersions. In Nanoscience for the Conservation of Works of Art; Baglioni, P.; Chelazzi, D.; O'Brien, P. Eds.; Royal Society of Chemistry: Cambridge, pp. 252–279.

Freund, M.; Csikòs, R.; Keszthelyi, S.; Mozès, G.Y. 1982. Paraffin Products. Properties, technologies, applications. Elsevier.

Garg, T.; Bilandi, A.; Kapoor, B.; Kumar, S.; Joshi, R. 2011. Organogels: Advanced and Novel Drug Delivery. System. Int. Res. J. Pharm., 2, 15-21.

Gnanakumari, P.; Venkatesu, P.; Mohan, K.R.; Rao, M.V.P.; Prasad, D.H.L. 2007.

Excess volumes and excess enthalpies of N-methyl-2-pyrrolidone with branched alcohols. Fluid Phase Equilib. 252, 137–142.

Hansen, C. M.; Beerbower, A. 1971. Solubility Parameters. In Kirk-Othmer Encyclopedia of Chemical Technology, Suppelment Volume; Standen, A., Ed.; Interscience: New York, NY, pp. 889–910.

Haynes, W.M. 2014-2015. Handbook of Chemistry and Physics. 95th Edition. CRC Press: Boca Raton, FL, pp. 6-183.

Horie, C.V. 1987. Materials for Conservation, Butterworths, London.

HSDB (Hazardous Substances Databank). 2001. Print-out for methyl ethyl ketone. Last Revision Date: 19-10-2015. Available at https://toxnet.nlm.nih.gov.

Israelachvili, J. N. 2011. Intermolecular and Surface Forces, 3rd ed.; Elsevier. Amsterdam.

Jin, Z.; Pramoda, K.P.; Guoqin, X.; Suat Hong, G. 2001. Dynamic mechanical behavior of melt-processed multi-walled carbon nanotube/poly(methyl methacrylate) composites. Chem. Phys. Lett. 337, 43-47.

Labafzadeh, S.R.; Helminen, K.J.; Kilpeläinen, I.; King, A.W.T. 2015. Synthesis of Cellulose Methylcarbonate in Ionic Liquids using Dimethylcarbonate. Chemsuschem 8, 77–81.

Lancaster, M. 2002. Green Chemistry: An Introductory Text, Royal Society of Chemistry, Cambridge, UK.

Lewis, R.J. Sr. 2007. Hawley's Condensed Chemical Dictionary, 15th Edition. John Wiley & Sons, Inc. New York, NY, pp. 829.

Li, D.; Fang, W.; Xing, Y.; Guo, Y.; Lin, R. 2009. Effects of dimethyl or diethyl carbonate as an additive on volatility and flash point of an aviation fuel. J. Hazard. Mater. 161, 1193–1201.

Lide, D.R. 1995. Handbook of Organic Solvents, CRC Press: Boca Raton, FL.

Liu, Q.; Hedberg, E.L.; Liu, Z.; Bahulekar, R.; Meszlenyi, R.K.; Mikos, A.G. 2000. Preparation of macroporous poly (2-hydroxyethyl methacrylate) hydrogels by enhanced phase separation. Biomat. 21, 2163–2169.

Luo, H.P.; Zhou, J.H.; Xiao, W.D.; Zhu, K.H. 2001. Isobaric vapor–liquid equilibria of binary mixtures containing dimethyl carbonate under atmospheric pressure, J. Chem. Eng. Data 46, 842–845.

Marrs, B.; Andrews R.; Rantell T.; Pienkowski D. 2006. Augmentation of acrylic bone cement with multiwall carbon nanotubes. J. Biomed. Mater. Res. A 77, 269-276.

Mohamed, N.H.; Zaky, M.T.; Farag, A.S.; Fahmy, A.F.M. 2008. Separation of Paraffin Wax Using Solvent Fractionation. Petrol. Sci. Technol. 26, 562–574.

Mujawar, N.K; Ghatage S.L.; Yeligar, V.C. 2014. Organogel: factors and its importance. Int. J. Biol. Chem. Sci. 4,758-773.

Murdan, S. 2005. Organogels in drug delivery. Expert Opin. Drug Deliv. 2, 489-505.

Pacheco, M.A.; Marshall, C.L. 1997. Review of Dimethyl Carbonate (DMC) Manufacture and Its Characteristics as a Fuel Additive. Energy Fuels 11, 2-29.

Perrin, D.D.; Armarego, W.L.F. 1988. Purification of Laboratory Chemicals, Pergamon Press, Oxford, 3rd ed.

Pohanish, R.P. 2012. Sittig's Handbook of Toxic and Hazardous Chemical Carcinogens, 6th Edition, Waltham, MA, pp. 1802.

Raghavan, S.R.; Douglas, J.F. 2012. The conundrum of gel formation by molecular nanofibers, wormlike micelles, and filamentous proteins: gelation without cross-links?. Soft Matter. 8, 8539-8546.

Reichardt, C. 2003. Solvents and Solvent Effects in Organic Chemistry, 3rd ed.;

Wiley-VCH: Weinheim.

Rodrìguez, A.; Canosa, J.; Tojo, J. 2003. Physical properties of the binary mixtures (diethyl carbonate + hexane, heptane, octane and cyclohexane) from T = 293.15K to T = 313.15K, J. Chem. Thermodyn. 35, 1321–1333.

Sahoo, S.; Kumar, N.; Bhattacharya, C.; Sagiri, S.S.; Jain, K.; Pal, K.; Ray, S.S.; Nayak, B. 2011. Paper on Organogels: Properties and Application. Des. Monomers Polym. 14, 95-108.

Schäffner, B; Schäffner, F.; Verevkin, S.P.; Börner, A. 2010. Organic Carbonates as Solvents in Synthesis and Catalysis. Chem. Rev. 110, 4554–4581.

Scriver, C.R.; Beaud, A.L. 2001. Part 9, Organic Acids, pp. 2146-2174; part 94, Disorders of Propionate and Methylmalone Metabolism, pp. 2179. In Metabolic and Molecular Basis of Inherited Disease, 8th edition. McGraw Hill Publishers, New York, NY, USA.

Shanab, K.; Neudorfer, C.; Schirmer, E.; Spreitze, H. 2013. Green Solvents in Organic Synthesis: An Overview. Curr. Org. Chem. 17, 1179-1187.

Smart, M.C.; Ratnakumar, B.V.; Surampudi, S. 1999. Electrolytes for Low-Temperature Lithium Batteries Based on Ternary Mixtures of Aliphatic Carbonates. J. Electrochem. Soc. 146, 486-492.

SRI International. 2000. Chemicals Economic Handbook. SRI Consulting, Menlo Park, CA, USA.

Sandhu, S.; Sandhu, J.S. 2011. Recent advances in ionic liquids: green unconventional solvents of this century. Part 1. Green Chem. Lett. Rev. 4, 289- 310.

Teas, J. P. 1968. Graphic Analysis of Resin Solubilities. J. Paint Technol. 40, 19–25.

Toshiyuki, S.; Daisuke O.; Kenji H. 2003. Viscoelastic Behavior of Organogels. Riron Oyo Rikigaku Koenkai Koen Ronbunshu 52, 477-478.

USEPA. 2005. Integrated Risk Information System (IRIS): Glossary of IRIS Terms.

Van de Witte; P., Dijkstra; P., Van den Berg, J.; Feijen, J. 1996. Phase separation processes in polymer solutions in relation to membrane formation. J. Membr. Sci. 117, 1–31.

Winey, K.I.; Vaia, R.A. 2007. Polymer Nanocomposites. MRS Bulletin 32, 314-322. Cambridge Univ. Press.

Xu, K. 2004. Nonaqueous liquid electrolytes for lithium-based rechargeable batteries. Chem. Rev. 104, 4303–4418.

Yamamoto, H.; Nishiyama, M.; Imagawa, H.; Nishizawa, M. 2006. $Hg(OTf)_2$-Catalyzed cyclization of alkynyl tert-butylcarbonate leading to cyclic enol carbonate. Tetrahedron Lett. 47, 8369-8373.

Zeng, Z.; Liang, W.I.; Chu, Y.; Zheng, H. 2015. In situ TEM study of the Li-Au reaction in an electrochemical liquid cell. Faraday Discuss.176, 95-107.

Zeng, W.R.; Li, S.F.; Chow, W.K. 2002. Preliminary Studies on Burning Behavior of Poly (methyl methacrylate) (PMMA). Journal of Fire Sciences. 20, 297–317.

PART III

Experimental

CHAPTER 6

Organogels synthesis

6.1 Introduction

The present chapter illustrates the preparation procedures and the materials used for the synthesis of poly(methyl methacrylate) organogels.

The basic idea is to develop new chemical gels containing organic solvent with specific key features, such as improved mechanical properties to ensure ease of handling and a completely residue-free treatment, and high retentiveness in order to provide a highly controlled cleaning process even on sensitive substrates. The preparation of chemical organogels based on the cross-linking of a monomer, methyl methacrylate (MMA), and a cross-linker, usually a divinyl-group molecule, in solvent solution was adapted for the cleaning of cellulosic-based artifacts.

In particular, two different organogels were developed with respect to final cleaning purposes. PMMA-DEC organogels are designed for the removal of Pressure Sensitive Tapes (PSTs) from water/solvent sensitive paper surfaces; on the other hand, PMMA-MEK organogel systems, developed in previous works (Pizzorusso, 2010; Baglioni et al., 2015), are optimized and specifically designed for the selective removal of wax contaminants from the surface of ancient paper.

6.2 Preparation of organogels

Here the preparation of PMMA organogels is presented. The chemical reaction that lead to the formation of the gel network is a radical polymerization of a monomer and a cross-linker in solution. The monomer, MMA, was

solubilized in pure organic solvents. The cross-linker used is ethylene-glycol-dimethacrylate (EGDMA).

In order to develop gel systems with the desired characteristic, the following parameters were tuned systematically: amount of cross-linker, different type of solvents, monomer-solvent phase ratio.

Organogels formulations were synthesized in two types of molds to obtain organogels with different final shapes: cylinders (2.5 × 2.5 × 1 cm^3) were used to carry out the gel characterization, while flat organogel sheets (3-4 mm thick) were deemed optimal for rheological characterization and for cleaning tests. The molds were PTFE cylinders with an inner diameter of 2.5 cm resistant to chemicals and high temperatures, and a glass caster (figure 6.1).

Figure 6.1. Representation of the constructed mold for casting organogel films: (1) glass plates; (2) glass thickener.

6.2.1 Materials

Table 6.1 shows a list of the chemicals used for the preparation of PMMA organogels. All chemicals were used as received.

Chemicals	Company	Purity	Linear formula	av. Mw (g/mol)
Methyl methacrylate (MMA)	Sigma-Aldrich	≥ 99%	$C_5H_8O_2$	100,12
Ethylene glycol dimethylacrylate (EGDMA)	Sigma-Aldrich	≥ 98%	$C_{10}H_{14}O_4$	198,22
2, 2'-azobis(isobutyronitrile) (AIBN)	Fluka	>98%	$C_8H_{12}N_4$	164,21
Diethyl carbonate (DEC)	Sigma-Aldrich	≥ 99%	$(C_2H_5O)_2CO$	118,13
Methyl ethyl ketone (MEK)	Sigma-Aldrich	≥ 99%	$C_2H_5COCH_3$	72,11

Table 6.1. Chemicals used for organogels preparation

Crosslinking of MMA in a polymerization reaction is done in the presence of a crosslinking agent. The most commonly used is ethyleneglycol dimethacrylate (EGDMA) and the crosslinking with MMA has been reported for a long time (Lazzari and Storti, 2014). Chemical structure of EGDMA is reported in figure 6.2. An extensively used thermal initiator is 2,2'-azobis(isobutyronitrile) (AIBN) (Herrn, 1983; Zhu et al., 1990; Donghee et al., 2009) which has an higher decomposition rate and it activates at low temperature forming a molecule of nitrogen gas and two 2-cyanoprop-2-yl radicals (figure 6.3).

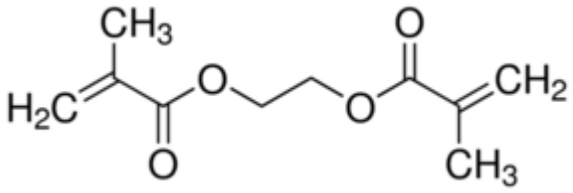

Figure 6.2. Chemical structure of crosslinking agent EGDMA.

6.2.2 Preparation procedure

The organogels were obtained by a free radical polymerization of MMA monomer and cross-linker EGDMA in solution. MMA was solubilized both in pure DEC and MEK and, to initiate the radical reaction, the initiator AIBN was added in the right proportion. The decomposition of the radical starter is induced by temperature (figure 6.3).

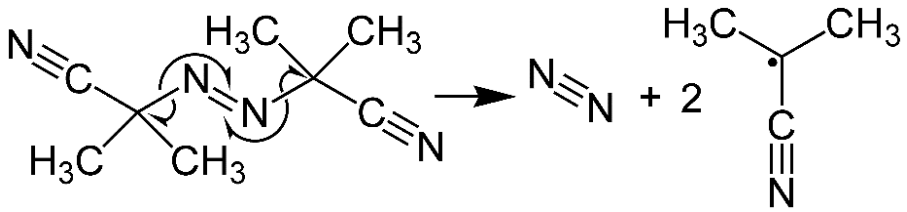

Figure 6.3. AIBN: formation of radical.

Fifteen synthesis trials were needed to develop gel systems with the desired characteristics for cleaning purpose, i.e. mechanical strength, adhesiveness, optical transparency and suitable solvent release.

Three synthesis series were performed tuning the monomer/solvent phase ratio, and consequently the quantity of cross linker (table 6.2). Moreover, the AIBN amount was adjusted to have the right quantity of radicals during the initiation phase of polymerization reaction, in order to contribute to a complete polymerization of the activated monomers. In fact, lower initiator concentrations means slower polymerization rates. If polymerization rate is

slow, oxygen may inhibits polymerization of monomers, resulting in gels that are mechanically weak. However, too much initiator could give rise to shorter average polymer chains and oligomers, which may produce turbid gels with low elasticity or, in limit cases, gel solutions that does not seem to have been polymerized.

Series	MMA/solvent % (w/w)	EGDMA % (w/w, respect to monomer)
Ist series	20/80%	from 1 to 3%
IInd series	30/70%	from 1 to 3%
IIIrd series	40/60%	from 1 to 3%

Table 6.2. Percentages (w/w) of monomer/solvent phase ratio and cross-linker used for synthesis trials.

As reported before, PMMA organogels preparation was performed in two types of molds to obtain organogels with different final shapes. The containers, i.e. PTFE cylinders and a glass caster, were sealed and placed into an oven at 65 °C for 6 hours.

In order to remove any unreacted monomer the gels were then washed by immersion into plastic vials (30 ml) filled with the corresponding solvent (DEC and MEK). The washing solvent was discarded and renewed daily. After seven washing cycles, the organogels were finally equilibrated through immersion in the respective solvents, before use.

6.3 Composition of the selected organogels

Here, only the systems that were considered more promising for cleaning application are reported and, therefore, these systems were selected for the physico-chemical and mechanical characterization.

These systems were chosen among a series of different synthesis: in order to obtain organogels with specific behaviors for the cleaning of paper surfaces, the quantity of cross-linker was systematically increased from 1 to 3 % with respect to the quantity of monomer and the monomer/solvent phase ratio, kept constant at 30/70 % (w/w).

The preparation of organogels with different solvent phases represents a powerful characteristic for cleaning purposes. In fact, as discussed in a previous chapter (chapter 5) these systems are specifically tailored for the removal of PST layers and waxes from paper surfaces. The percentages (w/w) of MMA and EGDMA used for the preparation of the selected organogels are presented in table 6.3. The gels are labeled as PMMA-DEC and PMMA-MEK, where DEC (diethyl carbonate) and MEK (methyl ethyl ketone) are the solvents used for the synthesis, respectively.

Gel	MMA % (w/w)	EGDMA % (w/w, respect to monomer)
PMMA-DEC.2	30%	2%
PMMA-DEC.3	30%	3%
PMMA-MEK.2	30%	2%
PMMA-MEK.3	30%	3%

Table 6.3. Percentages (w/w) of monomer and cross-linker used for synthesis of the selected systems.

6.3.1 General observations

After the synthesis, PMMA gels seem to have similar mechanical and macroscopic characteristics. PMMA-DEC and PMMA-MEK systems are perfectly transparent (figure 6.4), and if left inside the corresponding solvent tend to adsorb more liquid and to significantly swell. They are elastic and hard, giving to the systems a good mechanical stability; in some cases, the upper surface of the gel is sticky, may be, due to a not completed reaction, but this behavior tends to decrease after some washings.

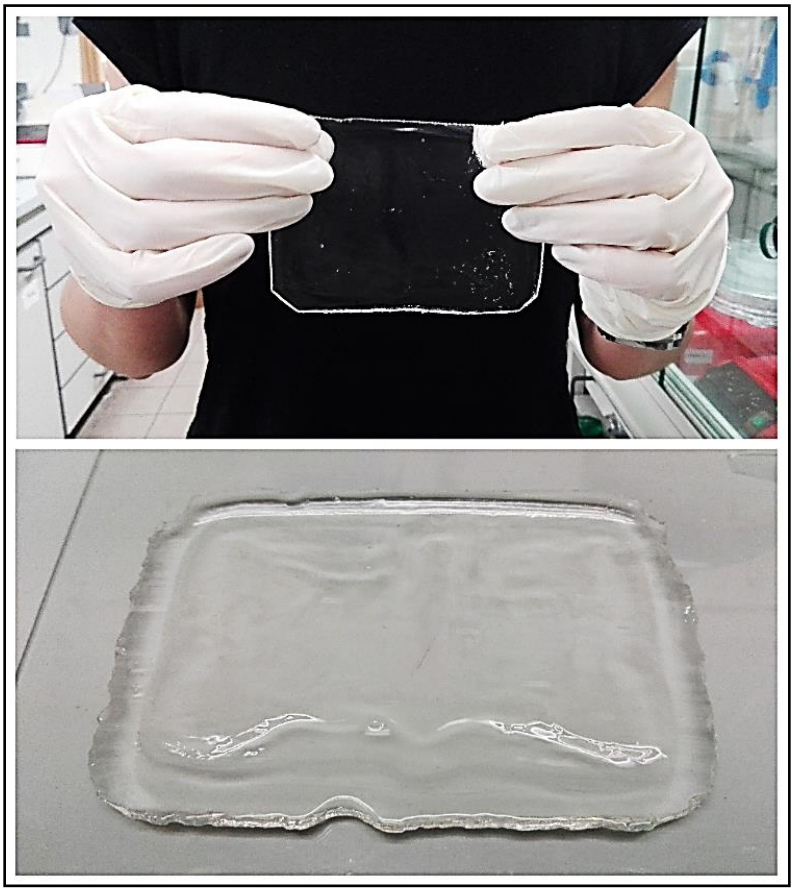

Figure 6.4. PMMA organogel films: PMMA-DEC (on the top); PMMA-MEK (on the bottom).

References

Baglioni, P.; Bonelli, N.; Chelazzi, D.; Chevalier, A.; Dei, L.; Domingues, J.; Fratini, E.; Giorgi, R.; Martin, M. 2005. Organogel formulations for the cleaning of easel paintings. App. Phys. A 121, 857-868.

Donghee, K.; Do Yang, L.; Kangseok, L.; Soonja, C. 2009. Effect of Crosslinking Agents on the Morphology of Polymer Particles Produced by One-Step Seeded Polymerization. Macromol. Res. 17, 250-258.

Hatada, K.; Kitayama, T.; Masuda, E. 1986. Studies on the Radical Polymerization of Methyl Methacrylate in Bulk and in Benzene Using Totally Deuterated Monomer Technique. Polym. J. 18 (5), 395-402.

Herrn, H.J. 1983. Free-Radical Polymerization Kinetics of Methyl Methacrylate at very High Conversions. Makromol. Chem. 184, 2563-2579.

Lazzari, S.; Storti, G. 2014. Modeling Multiradicals in Crosslinking MMA/EGDMA Bulk Copolymerization. Macromol. Theory Simul. 23, 15–35.

Pizzorusso, G. 2010. Synthesis and Characterization of Systems for the Micro-Confinement of Detergents for the Cleaning of Canvas Paintings. PhD thesis on Science for the Conservation of Cultural Heritage, University of Florence: Florence.

Zhu, s.; Tian, Y.; Hamielec, A.E. 1990. Radical concentrations in free radical copolymerization of MMA/EGDMA. Polym. 31, 154-159.

CHAPTER 7

Organogel characterization: methods and instrumental conditions

7.1 Introduction

In this chapter are described investigations over the physico-chemical characteristics of the selected polymeric formulations, which have shown the most promising applicative characteristics during preliminary cleaning trials.

Furthermore, samples composition and instrumental conditions are here reported.

The analysis of appositely prepared formulations, with poly(methyl methacrylate) as basic polymer, and two different organic solvents as solubilizing, porogenous and cleaning agents (diethyl carbonate and methyl ethyl ketone) were carried out through different methodologies.

The synthesis was carried out in two types of molds to obtain organogels with different final shapes: cylinders (2.5 × 2.5 × 1 cm^3) were used only to carry out the gel characterization, while flat organogel sheets (2-3 mm thick) were deemed optimal for the cleaning tests and for the mechanical properties evaluation. The molds were PTFE cylinders with an inner diameter of 2.5 cm resistant to chemicals and high temperatures, and a specifically designed glass caster.

The discussion over the obtained results will be reported in the chapter 8.

7.2 Reaction yield

Reaction yield quantifies the amount of product obtained in a chemical reaction. The quantification of percentage yield is an important information for a better understanding of the studied systems. For example, the weight ratio between the reacted monomers and the liquid phase inside gel, affects the mechanical and physico-chemical properties of the systems. The percentage yield can be defined as follows:

$$\text{yield (\%)} = \frac{\text{amount of obtained polymer}}{\text{amount of monomers}} \text{ x } 100 \qquad (7.1)$$

The 'amount of monomers' is the weight in grams used for the preparation of the gel and the 'amount of obtained polymer' after the reaction is calculated by weighing the oven-dried gel. Before the dehydration, gels were washed several times, in order to remove all the unreacted monomers.

7.3 Determination of monomer residues (ATR-FTIR)

After the synthesis, the PMMA organogels may still contain unreacted monomers and, for this reason, it is necessary to "wash" the gels in the same solvent used for the synthesis. Therefore, organogels were washed with 10 ml of the relative solvent, which was discarded and renewed daily; in this way, the molecules of monomer still present could migrate in the surrounding liquid phase. To obtain gels free of unreacted monomer, washing cycles were required after each synthesis.

Information about the presence of unreacted monomer still contained inside the gels was checked with Attenuated Total Reflectance Fourier Transform Infrared

Spectroscopy (ATR-FTIR). After each washing cycle (see above), ATR measures were made on this liquid, called 'Exchange solvent', daily for 7 days.
A Thermo Nicolet Nexus 870 FTIR spectrometer equipped with a Golden Gate diamond ATR with 128 scans and 4 cm^{-1} of optical resolution, in the 4000-650 cm^{-1} range, was used.

7.4 Solvent content and free solvent

The investigation on solvent content and free solvent content within organogels is of paramount importance to evaluate if a hydrogel has suitable characteristics for being used as cleaning systems.
In order to have information about the affinity of the polymer gel to the liquid phase, the equilibrium solvent content, Q, was determined gravimetrically and through calorimetric analysis. Q can be calculated as follows (Liu et al., 2000):

$$Q(\%) = \frac{W_i - W_d}{W_d} \times 100 \qquad (7.2)$$

were W_i is the weight of the completely swollen gel, and W_d is the weight of the dry sample.
The weight of the wet samples, W_d, was determined at two different times: 1) after preparation and 7 days of immersion in solvent; 2) on gels that were completely dry after preparation, and then let equilibrate with the solvent. This second measurement was carried out to verify if possible alterations of the porous structure (e.g. pore collapse) occurred during the drying and then affect the equilibrium solvent content. Accordingly, two different values of Q were obtained, the first being defined as Q_1 (before drying) and the second as Q_2 (after

re-loading with the solvent). The measurements were repeated three times for each PMMA system.

The calculation of the free solvent index (FSI) permits to estimate the quantity of solvent within organogels structure acting as bulk solvent, being thus available for the cleaning process. The general formula for the calculation of FSI is:

$$\mathrm{FSI}=\frac{\Delta \mathrm{H}_{exp}}{\mathrm{SC}\times\Delta \mathrm{H}_{theo}} \tag{7.3}$$

where $\Delta \mathrm{H}_{exp}$ (J/g) is the enthalpy of fusion of solvent determined experimentally for the given sample, $\Delta \mathrm{H}_{theo}$ (J/g) is the theoretical value for the enthalpy of fusion of bulk solvent, while SC is the solvent content, that corresponds to ESC for fully swollen organogels (see chapter 3, equation 3.2).

7.4.1 Thermal analysis (TGA and DSC)

Enthalpy of fusion of solvents, for the determination of the free solvent index (FSI), was calculated by integration of the peaks in thermograms obtained from Differential Scanning Calorimetry (DSC). Equilibrium swelled organogels samples (10-15 mg) were analyzed in Tzero™ aluminum hermetic pans using a Q2000 Calorimeter (TA INSTRUMENTS), which is equipped with an autosampler and a cooling device (Refrigerated Cooling System, RCS90 - TA INSTRUMENTS). The cooling system operates over the temperature range from -90 to 550 ˚C. Measurements were carried out at a constant nitrogen flow rate of 50 ml/min. Temperature range scan was from -90 to 25 °C with 0.5 °C/min rate.

The equilibrium solvent content before drying (Q_1) was also checked via Thermogravimetry (TGA). The instrument used was a SDT Q600 (TA INSTRUMENTS) with a temperature range from ambient temperature up to 1500

˚C. The balance sensitivity is 0.1 µg. Measurements were performed in a nitrogen atmosphere with a sample purge flow rate of 100 ml/min. After DSC measurements, the filled hermetic aluminum pans were pierced with a syringe needle to permit solvent evaporation and then used for the thermogravimetric analysis. The temperature scan used in the TGA experimental procedure was from 20 to 1500 ˚C, at constant heating rate of 10 ˚C/min.

FSI was calculated according to equation 7.3, by considering the theoretical value for the enthalpy of fusion of solvents.

7.5 Solvent release and solvent evaporation kinetics

The solvent release test is a simple experiment that gives a first hint about the porosity of the organogels and about their suitability as cleaning tools in cultural heritage conservation.

As already reminded, the goal of this project is the development of innovative gel systems able to release an amount of detergent fluid that should be sufficient for a good cleaning but not too much because of the water/solvent sensitive nature of cellulosic-based materials. Therefore, a medium propensity of release is necessary for a system with a good compromise between an effective cleaning power and an acceptable retention of solvent.

Evaporation kinetics were performed with the developed organogels to verify their ability to minimize the volatility and evaporation of the confined solvents. In fact, the capability of the gel of trapping the solvent inside its structure highlights the reduction of the solvent evaporation rate and the related health risk for restorers.

7.5.1 Solvent release

To assess the rate of solvent release of the PMMA formulations on porous substrates that mimic paper artifacts, the washed and fully swollen organogels were placed on a Whatman® sheet (diameter 55 mm, grade 1), and covered with a foil of Mylar® to prevent evaporation of the solvent. The quantity of released solvent was measured by weighing the Whatman® sheet over time, and then the residual solvent content of the gels was calculated accordingly.
Obviously, the limits of this test are quite evident because of the differences between a Whatman® paper (high purity, hardness, and chemical resistance) and a complex system like historical papers. Despite this, the solvent release test appears to be the easiest and fastest way to identify systems with the best application properties.

7.5.2 Solvent evaporation

In order to evaluate the evaporation kinetic of the designed solvents, both free and confined solvents were exposed at room temperature (25˚C) and RH 60 %. The loss of weight of swollen PMMA organogels was compared to that of petri dishes containing the same mass of free solvent. The size of the petri dishes (diameter = 10.9 cm) was selected to obtain a homogeneous film of free solvent (i.e., leaving no gaps) while maximizing the spreading of the solvent and the surface area exposed to air. Because we wanted to investigate the evaporation of solvents as separated from the influence of capillary suction, we chose to place the gels and free solvents on a non-porous surface. The aim was to simulate the spreading of solvents when they are used as non-confined in cleaning operations, as opposed to solvents confined in the PMMA organogels. The gels, on the petri dishes, were placed on the pan of an analytical balance.

The side glass doors of the balance enclosure were shut, while the top door was left open to allow air circulation as the weight loss was being recorded. Only normal air circulation was used (no ventilation/aspiration).
The evaporation kinetics were interrupted after one hour because, after this time, the differences between the gels and solvents became evident and because the times of application for a cleaning test are shorter (maximum 10-20 minutes). The measurements were repeated three times for each PMMA system.

7.6 Macroporosity and morphology (SEM)

Scanning Electron Microscopy (SEM) allows to obtain images of the samples at very high resolution and magnification in comparison to the conventional optical microscopy.
The electron gun produces an electron beam that is accelerated and focused by applying a potential difference. The beam passes through a system of electromagnetic lenses that manage the beam reducing the size up to the order of nm. When the primary electrons, accelerated along a column, affect the material, the electron-matter interaction produces backscattered electrons (BSE), secondary electrons (SE), Auger electrons and X-rays.
Secondary electrons are obtained by inelastic scattering phenomena between the electron beam and the material (valence electrons of the material). Their energy is lower than the energy value of the primary electron beam and the backscattered electrons (< 50 eV). They lose part of their energy on their way to the surface, being involved in more inelastic process and, therefore, only those closest to the surface of the material can actually escape from it and provide useful information. Secondary electrons come from the outer regions of the material (10-50 nm) giving maximum resolution topography. The number of SE

depends on different parameters and factors, mainly the atomic number Z of the sample and the energy of the incident beam.

Backscattered electrons are generated by the elastic scattering interactions between the electrons of the primary beam and the atoms of the material, whose energy is therefore close to that of the incident beam (> 50 eV). BSE come from a depth of the order of about 0.5-1 μm, therefore, they are not characterized by high topographical resolution. The BSE signal provides information on the local chemical composition of the material according to the backscatter coefficient:

$$\eta = \frac{n_{BS}}{n_B} \tag{7.4}$$

where n_B is the number of incident electrons on the sample and n_{BS} is the number of backscattered electrons. By increasing atomic number, the number of BSE increases, so the morphology of the surface can be related to its local chemical composition.

Two different detectors reveal the produced electrons and discriminate BSE and SE signals. The composition of the two information (signal from the detector and the local coordinates of the primary beam) allows to reconstruct a 3-D image. Each XY coordinates explored by the primary electron beam is associated to a z-value, directly connected with the amplitude of the signal revealed by the detector used and a black and white image is finally visible on the screen.

The scanning is performed by means of two pairs of electromagnetic coils placed internally to the objective lens, which move the electron beam on Cartesian coordinates X and Y of the sample surface via the signal electric sent.

Since SEM investigations must be done in a high vacuum conditions, the analysis were performed over dry gels: organogels were subject to a drying process, to

obtain xerogels whose porous structure is as close as possible to that of swollen organogels. The drying procedure is describe in the next chapter (chapter 8, section 8.6).

The images were acquired with a FEG-SEM ΣIGMA (Carl Zeiss, Germany) using an acceleration potential of 15 kV and a working distance of 4.8 mm (PMMA-DEC) and 3.7 mm (PMMA-MEK). A gold-metallization of xerogels was performed with an Agar Scientific Auto Sputter Coater.

7.7 Mesoporosity and nanoscale structure (SAXS)

The mesoporosity and the nanoscale structure of the gel systems were studied with scattering approach. This technique covers the entire size range of interest and is capable of measuring the structure dimensions, as well as to give detailed information on their interaction in a medium. In this experiment the intensity of the scattered radiation is measured as a function of the scattered angle, q. The scattering vector intensity, q, is related to the scattering angle and wavelength (Richardson, 2005):

$$q = \frac{4\pi \sin \theta/2}{\lambda} \tag{7.5}$$

The distances obtained from an experiment have a relation with the scattering vector intensity, that is distance ≈ 2π/q. Thus, larger scale structures (e.g. 100 Å or 10 nm) are related to smaller q. In order to achieve small q, small scattering angle and large wavelengths are necessary (e.g. small angle X-ray and neutron scattering techniques). In Small-Angle Scattering (SAS), distances in the range 1nm-1μm can be measured. X-rays radiation induces scattering from the

difference between electron densities, while neutron radiation is scattered by interaction with the nuclei, so they are independent of the atomic number.
The basics of a scattering experiment are evidenced in figure 7.1.

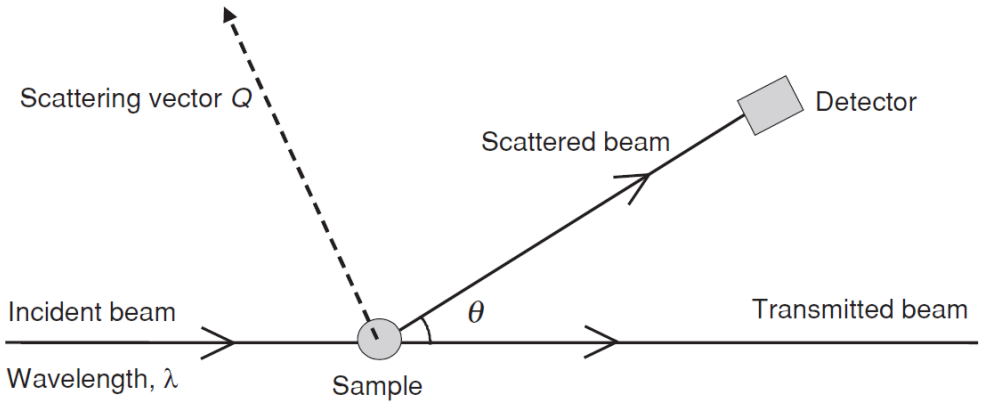

Figure 7.1. Schematic representation of a scattering experiment (Richardson, 2005).

Scattering techniques are non-destructive, since they do not need any sample preparation, such as out-gassing pre-treatment (needed in the case of Electron Microscopy) that can irreversibly damage the internal structure of swollen gels.
The average mesh and inhomogeneity sizes can be retrieved by using appropriate fitting models for scattering curves. In general, in a polymer network, the scattering intensity distribution, I(q), can be defined according to the Debye-Bueche approach (Fratini and Carretti, 2013) as:

$$I(q)=I_{Lorentz}(q) + I_{excess}(q)+bkg \qquad (7.6)$$

where we can assume that the scattering arises from two main contributions and a flat background, bkg.
The first contribution, $I_{Lorentz}(q)$, is a Lorentzian term (Ornstein–Zernike function), accounting for the scattering associated of a tridimensional network

where the correlation length ξ is the average distance between polymer chains. It can be expressed as follows:

$$I_{Lorentz}(q) = \frac{I_{Lorentz}(0)}{1+q^2\xi^2} \quad (7.7)$$

where is $I_{Lorentz}(0)$ is the Lorentzian intensity at q = 0 and ξ is the average mesh dimension of the network. If the correlation length among the inhomogeneous regions is larger than the correlation length of the cross-links ($a>\xi$), an "excess" structure factor that takes into account of the scattering excess may be considered. This second contribution, $I_{excess}(q)$, is a Debye-Bueche function (Debye and Bueche, 1949) that concerns the scattering at low q produced by inhomogeneities, as for example, solid-like polymer domains.

$$I_{excess}(q) = \frac{I_{excess}(0)}{(1+a^2q^2)^2} \quad (7.8)$$

where $I_{excess}(0)$ is the excess intensity at q=0 and a is the average dimension of the inhomogeneity domains accessible by the SAS experiment.

7.7.1 Mesh size and inhomogeneities

The network mesh size ξ is defined by the distance between two consecutive cross-linking points, which depends on the swelling degree of the polymer network (figure 7.2). Since there is a distribution of distances in a polymeric network, due to the random nature of the gelation process, the average mesh size values are average accounting for a 3D network system. Average mesh size

is the same as the measure of the average porosity in the nanometer scale (Fratini and Carretti, 2013).

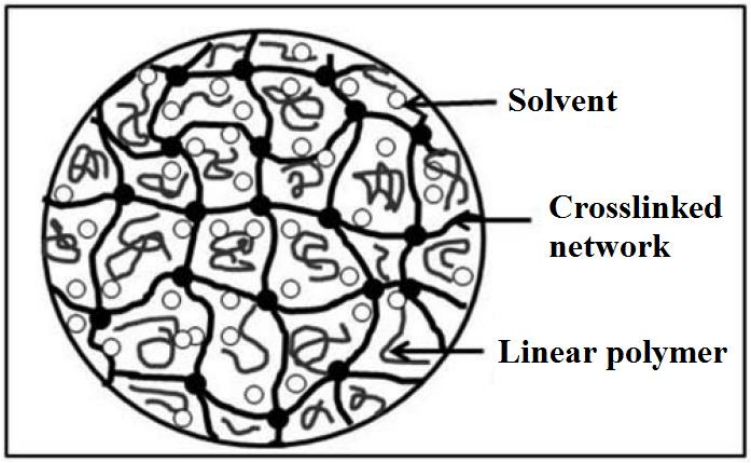

Figure 7.2. Schematic representation of the cross-linked structure of an organogel (Readapted from Benmouna et al., 2016).

Inhomogeneities in polymer gels are non-relaxing frozen polymer concentrations, which is dependent on the crosslinking density. The increase of inhomogeneities domains can lead to gel turbidity and can cause inhomogeneous responses in swelling and shrinking, as well as in rheological properties. According to Ikkai (Ikkai and Shibayama, 2005) there are three types of inhomogeneities in polymer gels, as illustrated in figure 7.3.

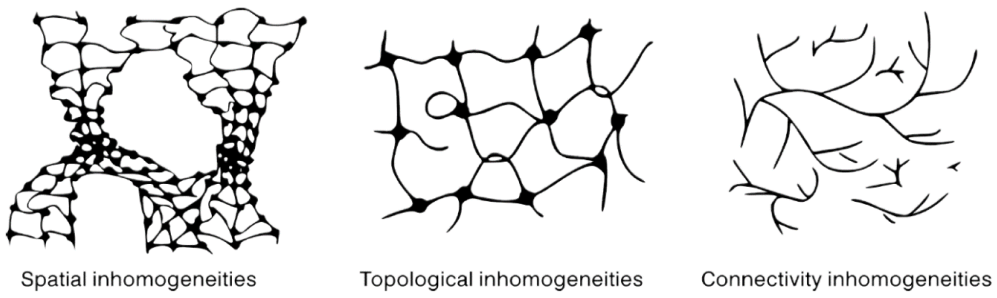

Figure 7.3. Types of inhomogeneities in gels (Ikkai and Shibayama, 2005).

The spatial inhomogeneities represent non-uniform spatial distributions of crosslinks. Topological inhomogeneities concern the defects on the topology of the polymer network (e.g. loops, trapped entanglements, dangling chains). The connectivity inhomogeneities are in relationship with the sizes and spatial distributions of clusters, which are predominant at the percolation threshold. Spatial inhomogeneities and mesh sizes can be examined through small-angle X-ray scattering techniques (SAXS).

Small-Angle X-ray scattering (SAXS) measurements were performed using a HECUS S3-Micro (Kratky-type camera) equipped with a position-sensitive detector (OED 50 M) containing 1024 channels of width 54 µm. Cu Kα radiation of wavelength λ= 1.542 Å was provided by a GeniX X-ray generator (Xenocs, Grenoble) working with a microfocus sealed-tube operating at a power of 50 W. The volume between the sample and the detector was kept under vacuum during the measurements to minimize scattering from the air. Scattering curves were obtained in the q-range between 0.01 and 0.55 $Å^{-1}$. Gel samples were placed into a 1 mm demountable cell with Kapton films as windows. The temperature was set to 25 ˚C and was controlled by a Peltier element, with an accuracy of ±0.1 ˚C. Scattering curves were corrected for the empty cell contribution and for the scattering of the Kapton films, considering the relative transmission factors.

7.8 Mechanical analysis: rheology of viscoelastic materials

Gels are viscoelastic materials from a mechanical point of view, which means that they possess contemporary mechanical behaviors typical of liquids and solids. As briefly discussed before (see chapter 3, section 3.3.2), the elastic fraction always prevails over the viscous behavior in gels.

Rheology is the science of material's flow behavior and deformation, which is directly in relation with the inner structure of the material.

When a material is subject to outside forces (figure 7.4), it will yield a stress/strain response.

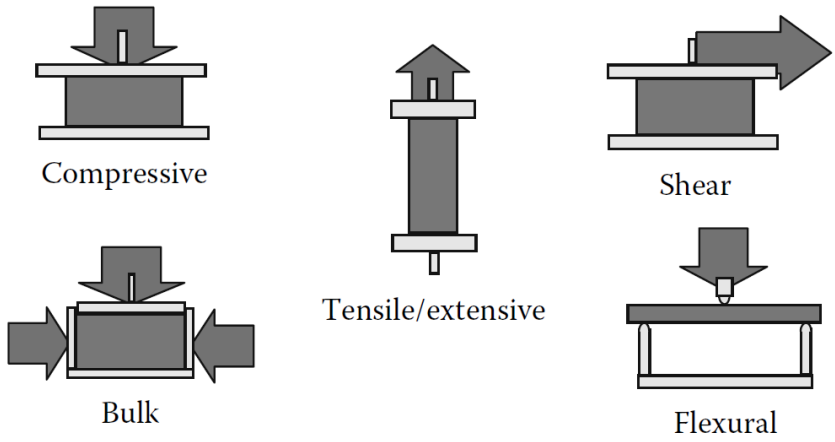

Figure 7.4. Examples of deformation modes. Geometric arrangements or methods of applying stress are shown (Menard, 2008).

In order to explain this phenomenon, the simple example of a shear stress on a cube is schematized in figure 7.5.

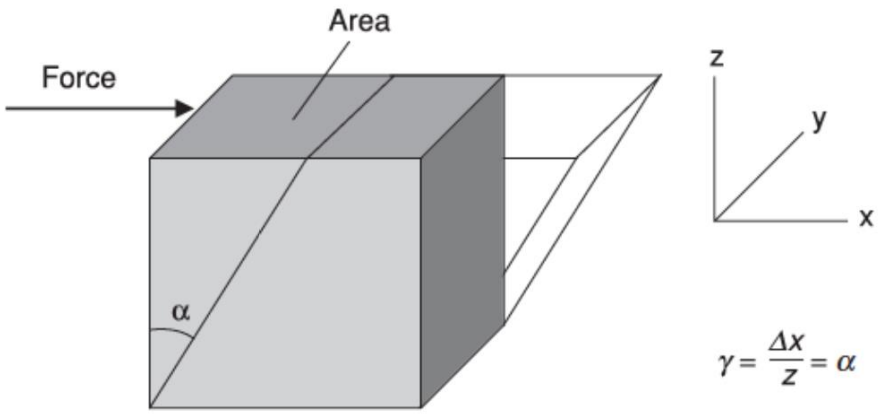

Figure 7.5. The shear stress and shear strain on a cube (Hughes, 2005).

The force is applied to the upper plane of the cube while the base is hold firmly; the resulting deformation shows a displacement with an angle α. The relation between the applied force and the deformation is due to the physical properties of the material.

The deformation is called *shear strain* γ, which is independent of the size of the material (dimensionless unit). The applied force is better explained by the *shear stress* σ, which is the force divided by the upper area of the cube, expressed in Pa or $N \cdot m^{-2}$. The *shear modulus G*, is now obtained (Hughes, 2005):

$$G = \frac{\sigma}{\gamma} \tag{7.9}$$

The viscoelasticity features of the system define the distinction between liquid-like and solid-like character of a gel. With enforcing a constant strain, the size of the stress is determined by the shear modulus (see equation 7.9).

When the molecules are forced to a higher energy state, they rearrange in the material to return to the initial energy state; some of the stored energy is dissipated by viscous flow and some stress is reduced. The time for the relaxation is determined by the balance of elastic and viscous processes (Goodwin et al., 2000; Hughes, 2005):

$$\tau = \frac{\eta}{G} \tag{7.10}$$

where η is the viscosity of the material. The ratio of the relaxation time t to the experimental observation is defined by the Deborah number:

$$De = \frac{\tau}{t} \tag{7.11}$$

Deborah number reflects the tendency of the material to appear either more viscous or more elastic. Therefore, the classification of the gels behavior can be:

- *De* $\gg$ 1: solid-like;
- *De* $\sim$ 1: viscoelastic;
- *De* $\ll$ 1: liquid-like.

Therefore, if observational times are rather small (in the order of seconds) and if $t \approx \tau$ the material displays both elastic and viscous characteristic and is named viscoelastic.

In the linear viscoelasticity region (LVE) each applied stress yields a proportional strain, that is, a straight line is observed if the force applied is plotted in function of the deformation. Over a critical limit, the force applied causes irreversible modifications on the material and may eventually break with further increasing stress. The rheological behavior of materials in the LVE region can be represented by combinations of Hookean springs and Newtonian dashpots. A Hookean spring obeys Hooke's law: the stress is linearly related to the displacement. An ideal Hookean solid has therefore an infinite elasticity, which is represented by G, accounting for the spring response (see equation 7.9). The dashpot is represented by a filled cup of Newtonian fluid with η viscosity, and a piston over the fluid. Therefore, the constant of proportionality is the shear viscosity (Goodwin and Hughes, 2000):

$$\sigma = \eta \dot{\gamma} \qquad (7.12)$$

Viscoelastic materials are represented by the combination of these two models and they can be visualized in series or in parallel. In the Maxwell model, the spring and the dashpot are placed in series, while when in parallel they are represented by the Kelvin-Voigt model (figure 7.6).

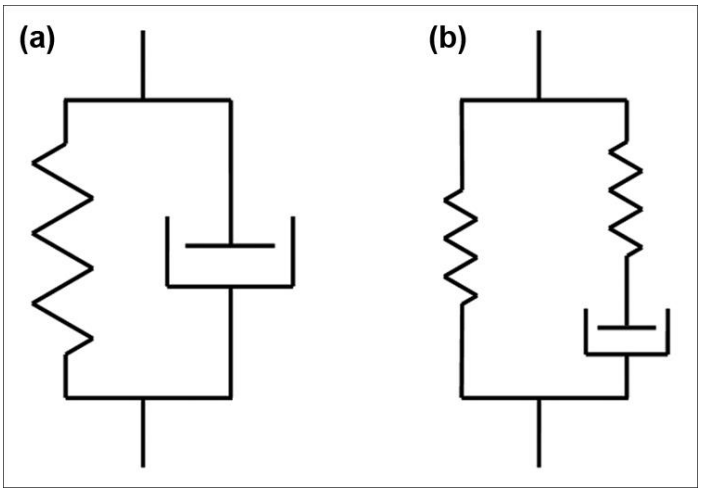

Figure 7.6. The Maxwell (a) and Kelvin-Voigt (b) models (Major, M.J. et al., 2012). The spring is related to materials elasticity, while the dashpot represents the ability of the material to flow.

The deformation of a sample when subject to a dynamic force is related to both polymer elastic (spring-like) and viscous (dashpot-like) behaviors. Dynamic mechanical analysis (DMA) is based on the application of a stress force to a sample and the observation of the materials response to that force. When a material is loaded with a constant force and a sinusoidal oscillating stress or strain is applied, it will deform sinusoidally, which offers detailed information on materials characteristics, if this test is carried out within its linear viscoelastic region. The sinusoidally oscillating strain (Menard, 1999; Rao, 2014) can be expressed by:

$$\gamma(\mathrm{t})=\gamma_0 \sin\omega t \tag{7.13}$$

where γ is the strain at time t, γ_0 is the strain amplitude and ω is the oscillation or angular frequency. The strain rate, $\dot{\gamma}(t)$, becomes:

$$\mathrm{d}\gamma/\mathrm{d}t = \dot{\gamma}(t) = \omega\gamma_0 \cos\omega t \tag{7.14}$$

The applied strain generates two stress moduli represented by an elastic component, also named in-phase stress (strain in line with stress) and by a viscous component, also called out-of-phase stress (δ=π/2), which sum express the generated total stress (σ_0):

$$\sigma_0 = G'\,\gamma_0\,\sin(\omega t) + G''\gamma_0\,\cos(\omega t) \tag{7.15}$$

In a viscoelastic material, the generated stress shows a difference between the applied strain, showed by a phase lag of δ radians. Therefore, the viscoelastic stress response, σ(t), of the materials to the applied strain over time in the linear viscoelastic region is as follows:

$$\sigma(t) = \sigma_0\,\sin(\omega t + \delta) \tag{7.16}$$

By combining the previous equations, it is possible to obtain:

$$G' = \left[\frac{\sigma_0}{\gamma_0}\right]\cos\,\delta \tag{7.17}$$

$$G'' = \left[\frac{\sigma_0}{\gamma_0}\right]\sin\,\delta \tag{7.18}$$

where *G'*(Pa) is the storage modulus associated with the elastic response of the material, and *G''*(Pa) is the loss modulus, associated to the energy loss in internal motion. Therefore (see figure 7.7), for an ideal elastic solid, *G''* is zero and the stress and the strain will be in phase, while for an ideal liquid, there is not any elastic component, so *G'* is zero and the stress and the strain will be out of phase by 90°. The vector sum of these two moduli provides with the complex shear modulus (Menard, 1999):

$$G^* = G' + iG'' = \sqrt{G'^2 + G''^2} \tag{7.19}$$

If *G'>>G''* the material behaves more like a solid, i.e. the deformations are essentially elastic or recoverable. If *G''>>G'* then the energy used to deform the material is dissipated by the viscosity of the system, so the material behaves more like a liquid. The viscoelastic moduli determined over a range of frequencies can indicate transition zones (e.g. sol-gel transition), which correspond to relaxation processes dependent on the structure of material (Menard, 1999).

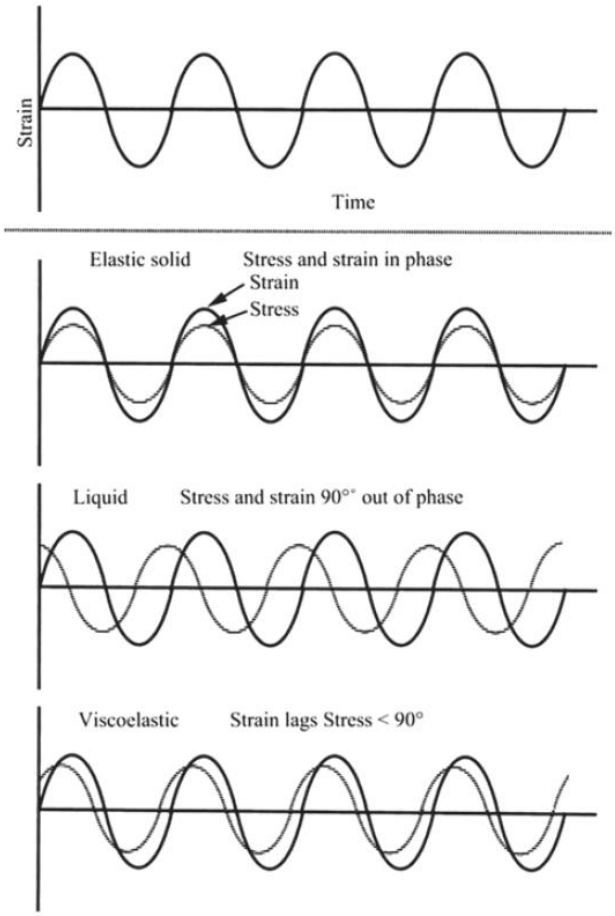

Figure 7.7. Stress and strain response of a Newtonian liquid, a viscoelastic liquid, and an elastic solid (Rao, 2014).

The tangent of the phase angle (δ), also called *damping factor*, can define how efficiently the material loses energy to molecular rearrangements and internal friction. In other words, it is the ratio of the energy dissipated to that stored per cycle of deformation (Rao, 2014), therefore:

$$\tan \delta = G''/G' \tag{7.20}$$

Since there is an extensive literature among numerous scientific and technologic areas on this subject, the viscoelastic parameters are usually expressed in various ways. The parameters used in this thesis are the ones related to the shear deformation, and are summarized in table 7.1.

Parameters	**Shear deformation**
Oscillating strain	γ(t)
Stress-relaxation modulus	*G*(t)
Storage modulus	*G'*
Loss modulus	*G''*

Table 7.1. Summary of viscoelastic parameters from shear deformation.

Polymer solutions can be classified according to their rheological behavior in oscillatory measurements, i.e. according to the frequency dependence of storage and loss shear moduli (Nishinari, 2009):

- *Strong gels*

G' is far larger than *G''* and both moduli are independent of frequency (e.g. agar gels).

- *Structured liquids*

Also called weak gels (even if they fail to fulfill the definition of a gel). *G'* is slightly larger than *G''* and both moduli are slightly dependent on frequency (e.g. xanthan gels).

- *Entangled polymer solutions*

G' is smaller than *G''* at lower frequencies but both moduli increase with increasing frequency and show a crossover. After the crossover *G'* is higher than *G''*.

- *Non-entangled polymer solutions*

G' is far smaller than *G''* at all the frequencies and both moduli are strongly dependent on the frequency.

The rheological measurements were carried out on a TA Instrument Hybrid Rheometer DISCOVERY HR-3, using a plate-plate geometry (Flat Plate 40mm diameter) and a Peltier for temperature control.

Swollen organogel samples were shaped with a circular diameter similar to plate-plate instrument's geometry.

In table 7.2 are listed the operating conditions adopted during the measurements:

		Amplitude Sweep	Frequency Sweep
PMMA-DEC	Axial Force (N)	5 N	5 N
	Temperature (°C)	25 °C	25 °C
	Frequency (Hz)	1 Hz	100 to 0.001 Hz
	Strain (%)	10^{-3} ÷ 80 %	0.1 %
PMMA-MEK	Axial Force (N)	7 N	7 N
	Temperature (°C)	25 °C	25 °C
	Frequency (Hz)	1 Hz	100 ÷ 0.01 Hz
	Strain (%)	10^{-2} ÷ 80 %	0.1 %

Table 7.2. Summary of parameters adopted for rheological measurements of PMMA-DEC and PMMA-MEK organogels.

The PMMA-DEC organogel samples were filled on the edges with silicon oil, to prevent the rapid evaporation of solvent and then the excessive stiffening of the polymeric film.

On the other hand, we encountered some problems during the measurements of PMMA-MEK samples: it was not possible to use the silicon oil and in this case, to avoid solvent evaporation, the edges of polymeric film were constantly loaded with MEK.

References

Benmouna, F.; Zemmour, S.; Benmouna, M. 2016. Structural Properties and Phase Behavior of Crosslinked Networks in Polymer Solutions. J. Macromol. Sci. Phy. 55, 319-329.

Debye, P.; Bueche, A. M. 1949. Scattering by an Inhomogeneous Solid. J. Appl. Phys. 20, 518–525.

Fratini, E.; Carretti, E. 2013. Chapter 10. Cleaning IV: Gels and Polymeric Dispersions. In Nanoscience for the Conservation of Works of Art; Baglioni, P.; Chelazzi, D.; O'Brien, P., Eds.; Royal Society of Chemistry: Cambridge; pp. 252–279.

Goodwin, W.; Hughes, R.W. 2000. Rheology for Chemists. An Introduction. Royal Society of Chemistry: Cambridge.

Hughes, R. 2005. Practical Rheology. In Colloid Science: Principles, Methods and Applications. Blackwell Publishing; pp. 201–227. Oxford, UK.

Ikkai, F.; Shibayama, M. 2005. Inhomogeneity Control in Polymer Gels. J. Polym. Sci. Polym. Phys. 43, 617–628.

Joy, D.C. 2006. Scanning Electron Microscopy. Materials Science and Technology. Wiley-VCH, Verlag GmbH & Co. KGaA.

Liu, Q.; Hedberg, E.L.; Liu, Z.; Bahulekar, R.; Meszlenyi, R.K.; Mikos, A.G. 2000. Preparation of macroporous poly(2-hydroxyethyl methacrylate) hydrogels by enhanced phase separation, Biomaterials 21, 2163-2169.

Major, M.J.; Kenney, L.P.J.; Twiste, M.; Howard, D., 2012. Stance phase mechanical characterization of transtibial prostheses distal to the socket. A review. J. Rehabil. Res. Dev. 49, 815-830.

Menard, K.P. 1999. Dynamic Mechanical Analysis: A Practical Introduction. CRC Press: Boca Raton, FL.

Nishinari, K. 2009. Some Thoughts on the Definition of a Gel. Progr. Colloid. Polym. Sci. 136, 87–94.

Rao, M.A. 2014. Chapter 3. Measurement of Flow and Viscoelastic Properties. In Rheology of Fluid, Semisolid, and Solid Foods; Springer US, pp. 63–160. Boston, MA.

Richardson, R. 2005. Scattering and Reflection Techniques. In Colloid Science: Principles, Methods and Applications. Blackwell Publishing, pp 228–254. Oxford, UK.

CHAPTER 8

Results and discussion

8.1 Introduction

In this chapter, the results of physico-chemical and mechanical characterization of the selected systems are discussed. Since the PMMA organogels were synthetized using two different solvents (DEC and MEK), every section reported the characterization for both PMMA-DEC and PMMA-MEK organogels.

Unfortunately, the presence of solvents has caused some problems during the characterization of the PMMA organogels. For example, the determination of the free solvent index parameter for PMMA-MEK systems was not possible due to the low freezing point of the used solvent (-86.96 °C), which is closer to the limit reached by our DSC apparatus (-90 °C. See chapter 7, section 7.4.1).

Moreover, some problems have been encountered during the lyophilization of gel samples obtaining xerogels: the macrostructure was completely destroyed and the resulting Scanning Electron Microscopy images are useless for any type of analysis or comparison.

8.2 Reaction yield

As reported in the section 7.2, it was calculated the reaction yield (in percentage) of the gel synthesis; the results are mean values over a set of three measures.

Gel	Reaction yield %
PMMA-DEC.2	88,8%
PMMA-DEC.3	97,9%
PMMA-MEK.2	82,9%
PMMA-MEK.3	85,6%

Table 8.1. Reaction yield (in percentage) of organogel systems.

The results highlight a very good yield for all formulations, especially for the PMMA-DEC.3 system, probably due to the good monomer/ cross-linker ratio. It must to be noticed that the percentage (w/w) of initiator added in the synthesis mixture is the same for all systems.

8.3 Determination of monomer residues

In the previous chapter, we stresses that, after synthesis, the PMMA organogels contain unreacted monomers, which can be removed trough washing cycles in the same solvent used during the preparation. To obtain a gel free of monomer residues, a series of washing cycles were necessary.

After each washing cycle, ATR measures were made on this liquid, called 'Exchange solvent', daily for 7 days.

Figure 8.1 shows the comparison between the ATR-FTIR spectra of MMA (only monomer), DEC (only solvent), and the exchange solvent (after 5 cycles).

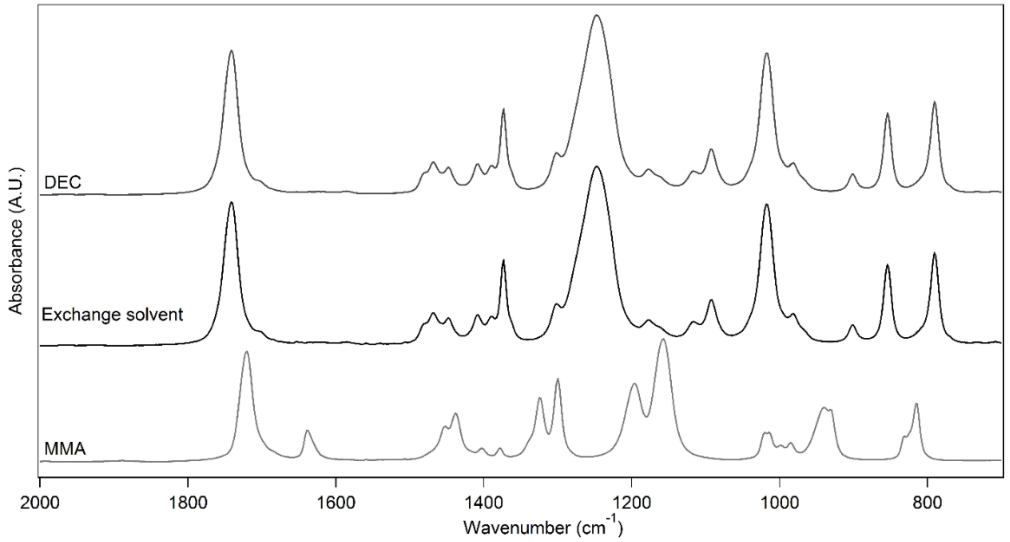

Figure 8.1. ATR-FTIR spectrum of DEC that was let to exchange with a PMMA-DEC organogel (exchange solvent) after seven washing cycles, as compared to the spectra of DEC, and MMA.

Already after two washing cycles (IR spectrum not reported here), most of the unreacted monomer is removed. Overall, five washing cycles were necessary to obtain a gel free of monomer, as shown by the disappearance of the MMA bands at 815 (ν_s C-O-C) and 830 cm^{-1} (CH_2 rocking), which were highlighted as they do not overlap with any band of DEC (figure 8.2).

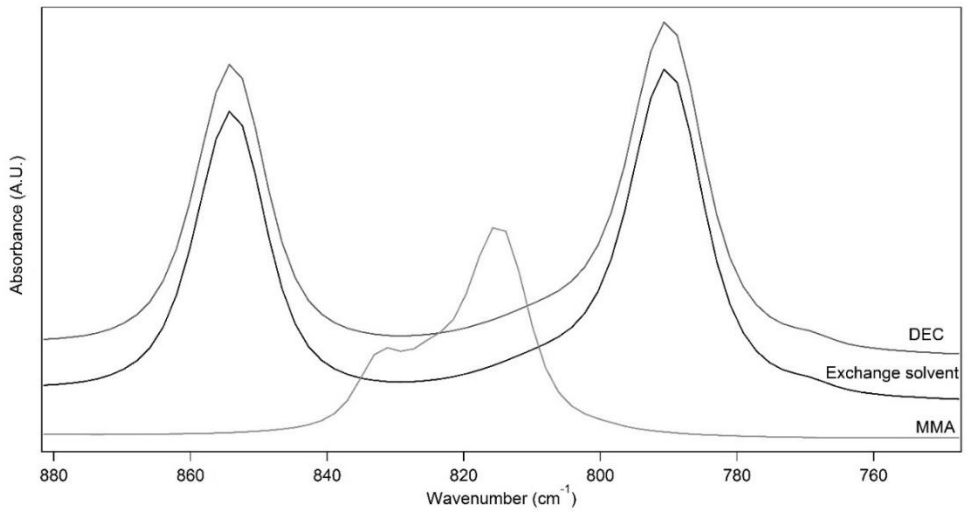

Figure 8.2. ATR-FTIR spectra: detail of the 880-700 cm^{-1} region.

Regarding PMMA-MEK systems, monomer-free gels are obtained after seven washing cycles. In fact, the upper surface of the gels was sticky after the synthesis process, probably due to a not complete reaction. This behavior is in agreement with the reaction yield values obtained for PMMA-MEK organogels. Figure 8.3 presents the comparison between ATR-FTIR spectra of pure MMA, pure MEK solvent and exchange solvent after 7 washing cycles.

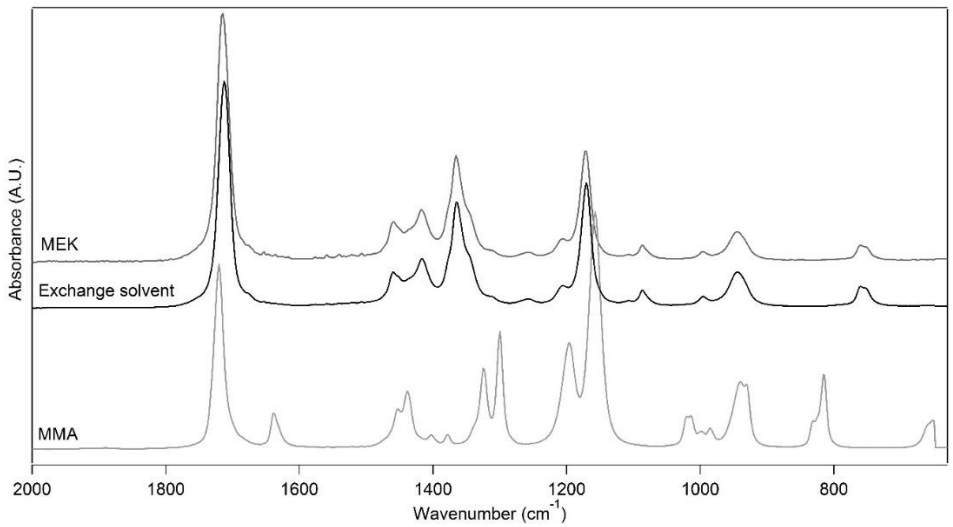

Figure 8.3. ATR-FTIR spectrum of MEK that was let to exchange with a PMMA-MEK organogel (exchange solvent) after seven washing cycles, as compared to the spectra of MEK, and MMA.

Differently from PMMA-DEC, in this case a series of ATR-FTIR analysis were performed to ensure the removal of unreacted monomer. In fact, the absorption band of MMA at 1720 cm^{-1} is nearby to MEK peak at 1716 cm^{-1}. Figure 8.4 shows the area between 1800 and 1600 cm^{-1}, where is not observable the overlap of above mentioned bands.

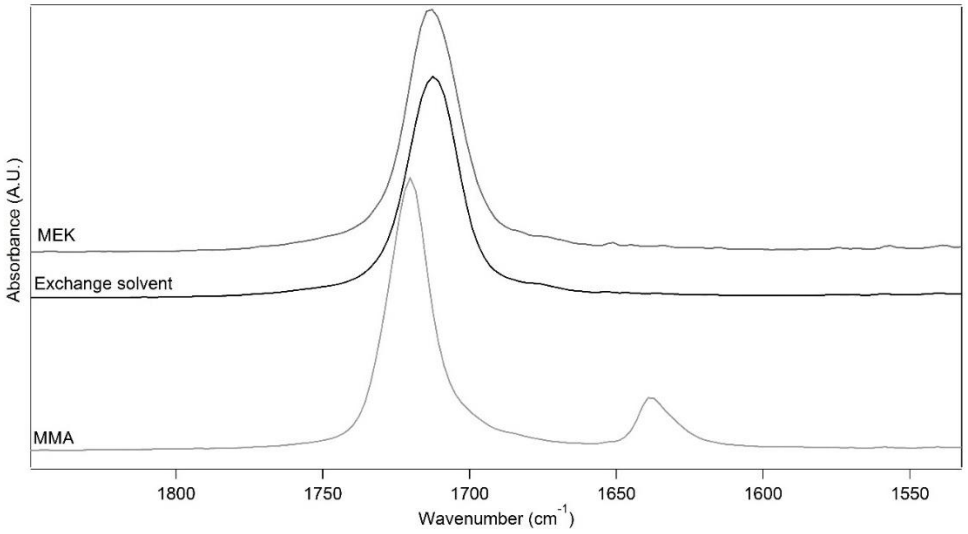

Figure 8.4. ATR-FTIR spectra: detail of the 1800-1600 cm^{-1} region.

8.4 Determination of solvent content and free solvent index

The values of equilibrium solvent content (Q), for the examined PMMA-DEC and PMMA-MEK organogels, were obtained through gravimetrical measurements (see chapter 7, equation 7.2). The obtained results were compared with equilibrium solvent content (ESC) values checked via Thermogravimetry (TGA). The results are listed in table 8.2.

Gel	Preparation solvent % (w/w)	Q_1 % (±0,1)	Q_2 % (±0,1)	ESC % (TGA)
PMMA-DEC.2	70%	85,2%	84,7%	84,1%
PMMA-DEC.3	70%	83,3%	82,9%	74,7%
PMMA-MEK.2	70%	84,7%	84,6%	85,7%
PMMA-MEK.3	70%	84,4%	84,3%	84,7%

Table 8.2. Equilibrium solvent content of PMMA-DEC organogels.

The value Q_1 is solvent content of the organogels that were equilibrated 7 days with DEC and MEK right after the synthesis and Q_2 the solvent content for the gels dried after the synthesis and then re-loaded with solvents. For all the PMMA formulations, the equilibrium solvent content is higher than the percentage of solvent used during the synthesis ("Preparation solvent"), which confirms that both DEC and MEK have a high affinity for the PMMA polymeric network. Overall, Q_1, Q_2 and ESC of the PMMA-DEC.3 and PMMA-MEK.3 gels are lower than that of the other formulations, which is in agreement with the highest amount of cross-linker used in preparation mixture. In principle, in the case of dried and re-solvated gels a partial collapse of the porous structure could be expected during the drying process, leading to lower values of Q_2 as compared to Q_1. However, the difference between Q_1 and Q_2 is almost irrelevant. The ESC values obtained through TGA for all the PMMA formulations are in good agreement with the values obtained gravimetrically, while for the PMMA-DEC.3 the solvent content is lower.

There are few reports on the coagulation of a solvent bound in the gel. Higuchi et al. (Higuchi et al., 1985) and Cha et al. (Cha et al., 1993) investigated the melting behavior of water in a polyvinyl alcohol (PVA) swollen gel and showed the existence of free and freezable bound water. The coagulation dimension of a solvent is closely related to the decrease in melting temperature.

Recently, the melting behavior of a solvent in a non-hydrogel, Isotactic polypropylene (iPP)/o-dichlorobenzene, was reported (Nakaoki and Harada, 2005; 2006). It was confirmed that there are two melting peaks for o-dichlorobenzene in the gel: one is a sharp melting peak at the same temperature as that of pure solvent and the other is a broad peak detected at a lower temperature than that of the pure o-dichlorobenzene. The respective melting

peaks were assumed to be free and freezable bound solvents. The solvent molecules can be located only in the non-crystalline region.

In this context, it is accepted that within a solvent-swollen polymer the states of solvent should be divided into two categories: free solvent, characterized by thermal phase transitions similar to that of bulk solvent and freezable bound solvent, whose phase transitions is expected to be shifted in respect to bulk solvent.

Then, PMMA-DEC systems were investigated with Differential Scanning Calorimetry (DSC) to determine free solvent index (FSI). Figure 8.5 shows DSC thermogram of PMMA-DEC.3 sample, in the range of melting temperature of free solvent.

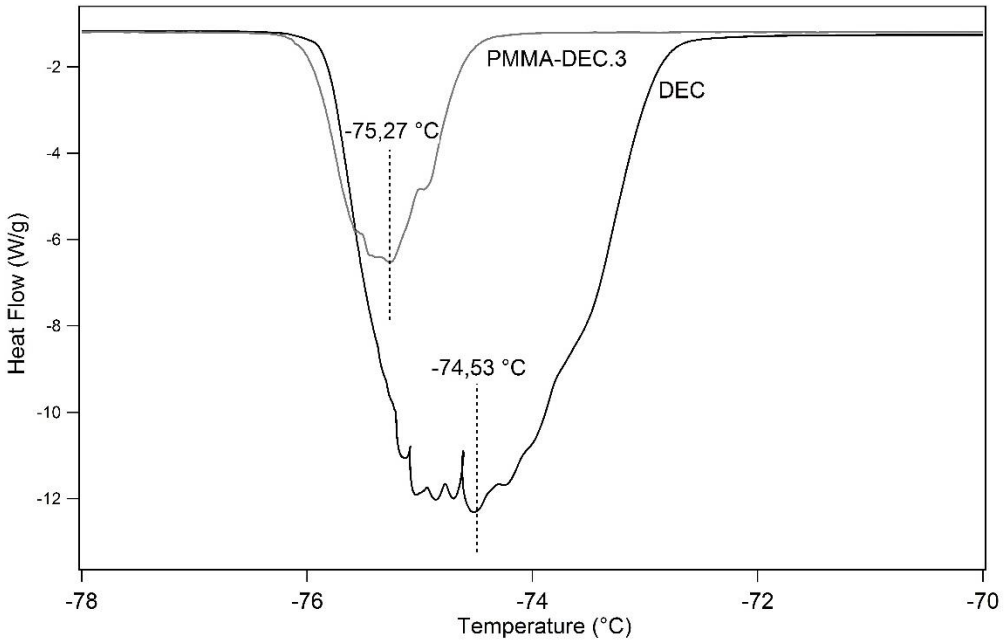

Figure 8.5. DSC thermogram of the fully swollen PMMA-DEC.3 system.

According to Ding et al. (Ding et al., 2001; Ding, 2003), the melting temperature (T_m) of DEC (-74.53 °C) obtained during calorimetric measurements, is more than 30 degrees lower than currently accepted value of -43 °C (Handbook of

Chemistry and Physics, 2015). As expected the T_m of PMMA-DEC system is lower than the free solvent; the thermal transition is related to the melting of free solvent contained inside organogel. This behavior indicates that the presence of PMMA induces a change in the state of solvent within gel.

Integration of the thermograms yields the enthalpy of fusion of the solvent contained within the organogels, which allows to calculate the free solvent index (FSI), as reported in chapter 7 (section 7.4), considering that the ΔH_{theo} (J/g) is the theoretical value of the specific enthalpy of fusion of diethyl carbonate at -74,3°C (Ding, 2003). Free solvent index is an important parameter that gives the fraction of free solvent over the total amount of solvent.

Table 8.3 summarizes equilibrium solvent content and free solvent index for investigated samples.

Gel	ESC % (TGA)	FSI (DSC)
PMMA-DEC.2	84,1%	0,28
PMMA-DEC.3	74,7%	0,21

Table 8.3 Equilibrium solvent content % (ESC) and free solvent index (FSI) of PMMA-DEC organogels.

The FSI values of the selected organogels are all quite similar to each other; this means that the same fraction of solvent inside gels is strongly bounded to the polymer network. A part of DEC, around 20-30 %, is free to move within the gel structure. Unfortunately, the lack of studies around poly(methyl methacrylate) organogels in literature has not allowed the comparison of our results.

Furthermore, the evaluation of freezable bound solvent index was not possible due to the low freezing point reached by the PMMA-DEC system, which is closer to the scanning limit of our DSC apparatus (-90 °C).

As reported in the introduction, the determination of the free solvent index and freezable bound solvent index parameters of PMMA-MEK systems was not possible, still due to the low freezing point of MEK (-86.96 °C), which is very closer to the limit reached by DSC device.

8.5 Solvent release and solvent evaporation kinetics

Figure 8.6 and 8.7 show the rate of solvent release of the PMMA-DEC and PMMA-MEK formulations on porous substrates that mimic paper artifacts.
The solvent content values at t=0 correspond to the percentage of liquid phase after 7 days of swelling the gels with solvent, i.e. the Q_1 values listed in table 8.2. The PMMA-DEC.3 gel exhibits a slower and more gradual release than PMMA-DEC.2, especially during the first 25 minutes (representative of typical application times of gels in cleaning interventions), as well as PMMA-MEK.3 in respect to PMMA.MEK.2 gel. The slower release kinetic of PMMA-DEC.3 and PMMA-MEK.3, hence their higher retentiveness as compared to the other formulations, is consistent with the higher percentage of cross-linker used for PMMA-DEC.2 and PMMA-MEK.2.

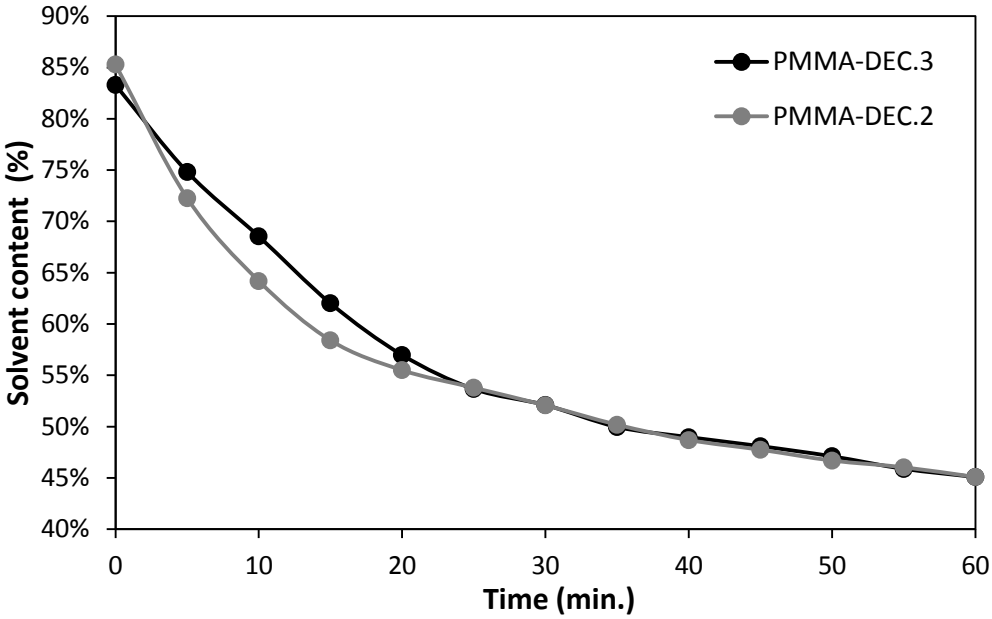

Figure 8.6. Solvent release kinetic curves of the PMMA-DEC.2-3 organogels, expressed as solvent content of the gels during the first hour of application on a model paper substrate.

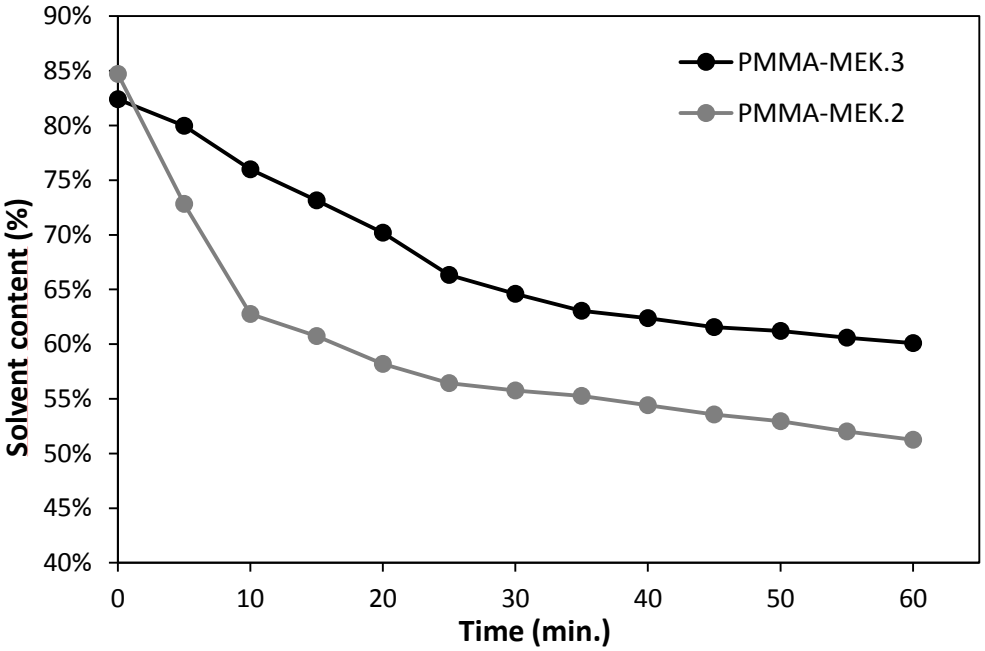

Figure 8.7. Solvent release kinetic curves of the PMMA-MEK.2-3 organogels, expressed as solvent content of the gels during the first hour of application on a model paper substrate.

Evaporation kinetics were performed to verify the ability of PMMA network to minimize the volatility and evaporation of the confined solvent. Figure 8.8 reports the comparison for the two studied PMMA-DEC organogels. Figure 8.9 shows the solvent release behavior of free MEK and solvent confined within PMMA-MEK systems.

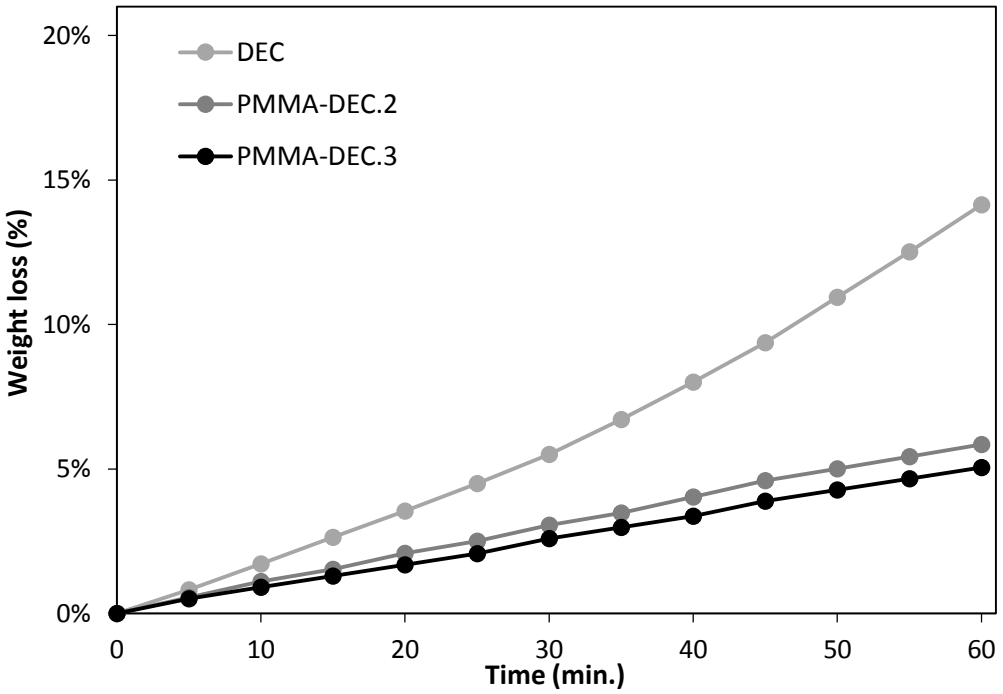

Figure 8.8. Weight loss through evaporation of free DEC (from petri dishes) as compared to that of DEC confined in the PMMA networks.

In all experiments, it is evident that solvent confined in the gels shows a drastic reduction of volatility due to the retention power of the polymer network. This feature has important applicative relevance because lower evaporation rates decrease the impact of solvents on operators during the cleaning intervention.

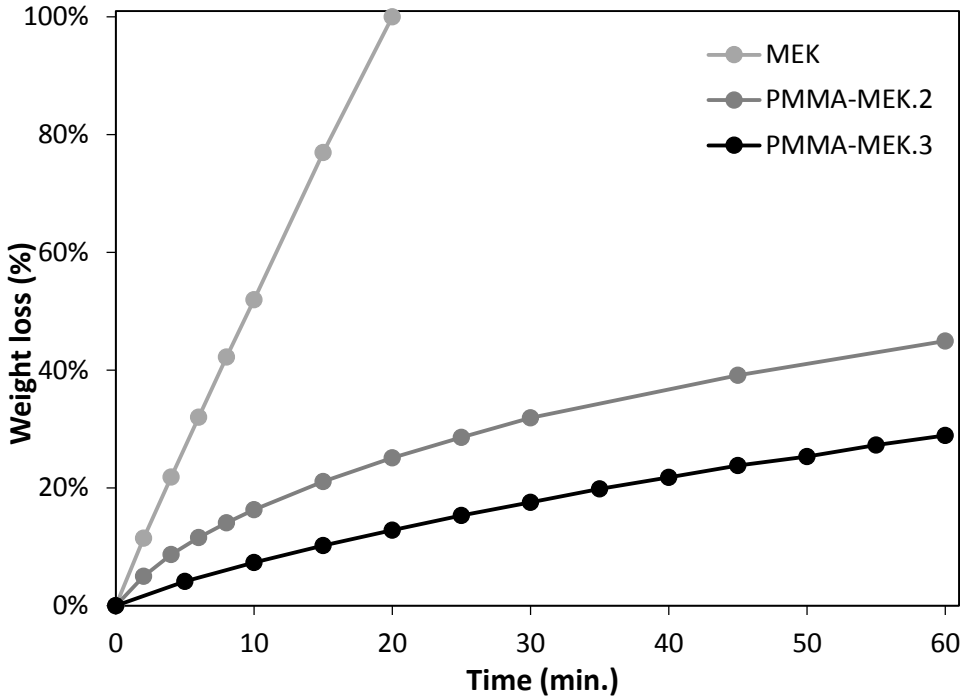

Figure 8.9. Weight loss through evaporation of free MEK (from petri dishes) as compared to that of MEK confined in the PMMA networks.

It must be noticed that the PMMA-DEC.3 and PMMA-MEK.3 organogels, which are characterized by a higher amount of cross-linker, show a decreased evaporation rate as compared to the less cross-linked systems.

These results are in good agreement with the purpose to increase the retentiveness of gels.

The evaporation kinetics were interrupted after an hour because, after this time, the differences between the gels and solvents became evident and because the times of application for a cleaning test are shorter (maximum 20-25 minutes).

In figure 8.10 are detailed the evaporation kinetics of PMMA-DEC and PMMA-MEK systems as compared to the correspondent free solvents, during the first 25 minutes.

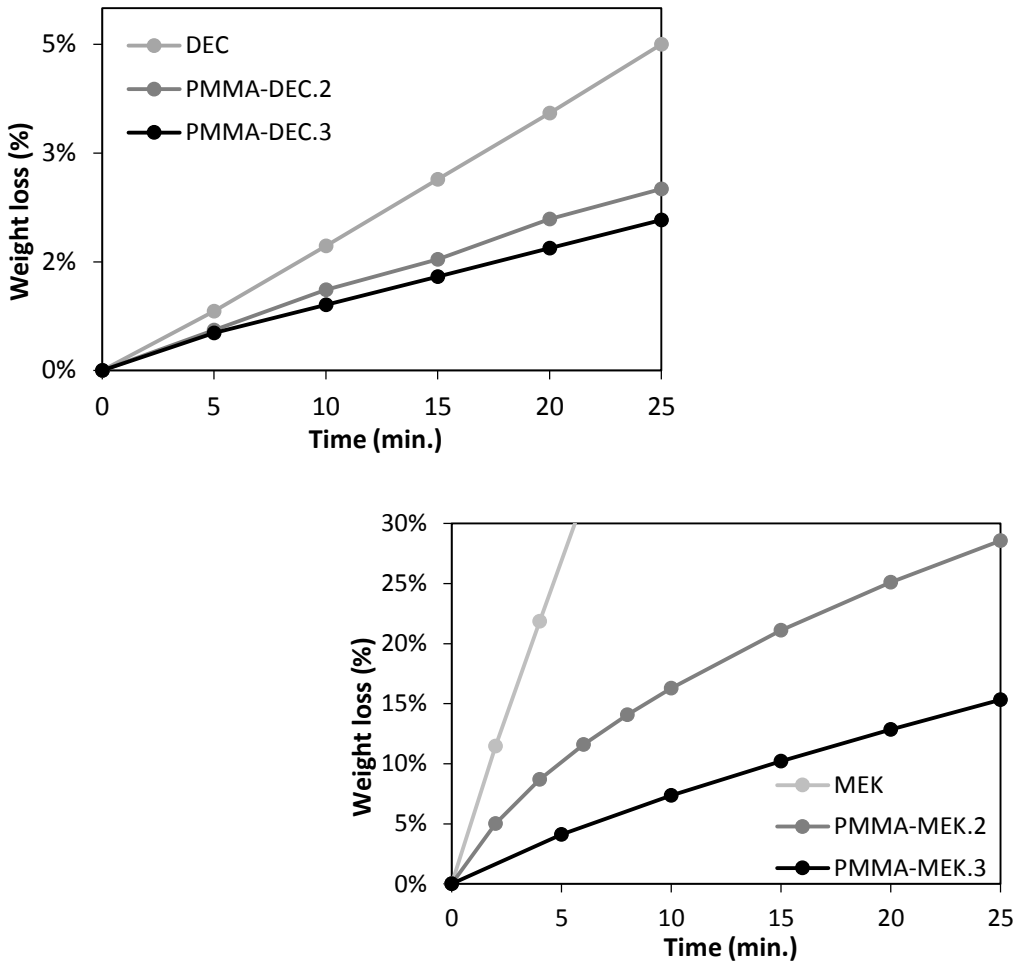

Figure 8.10. Detail of the weight loss during the first 25 minutes. The evaporation of free solvents (on the top DEC, on the bottom MEK) is compared to that of solvents confined in the PMMA networks.

8.6 Determination of macroporosity

The scanning electron microscopy (SEM) provides to examine the organogels porosity on a micrometer scale. The presence of solvents have caused some problems during the lyophilization of PMMA systems. In order to obtain the xerogels, the PMMA samples were dried under fume hood with ventilation (T≈25

°C, R.H.≈60%) for two weeks and then placed in oven (T≈35 °C) until obtain a constant weight.

The figures 8.11 and 8.12 show the SEM images obtained during the analysis for PMMA-DEC.3 and PMMA-MEK.3 samples.

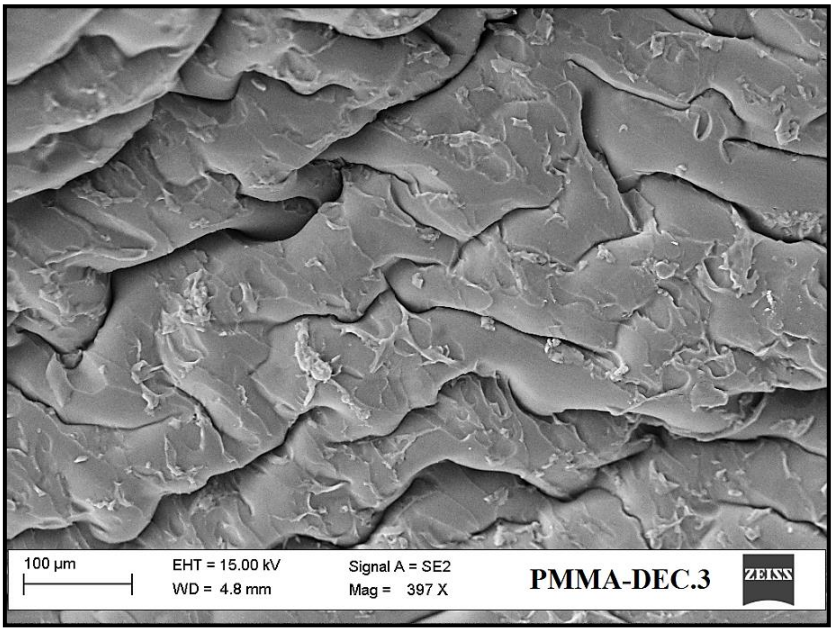

Figure 8.11. SEM image: PMMA-DEC.3 sample.

Unfortunately, the PMMA xerogels macrostructure was completely destroyed during the drying procedure and the resulting SEM images are useless for any type of analysis or comparison.

In fact, at the end of the drying process the xerogels appeared transparent. This means that during the evaporation of solvent, the structure of the gel collapsed and the macropores reduced in size increasing the light transmission.

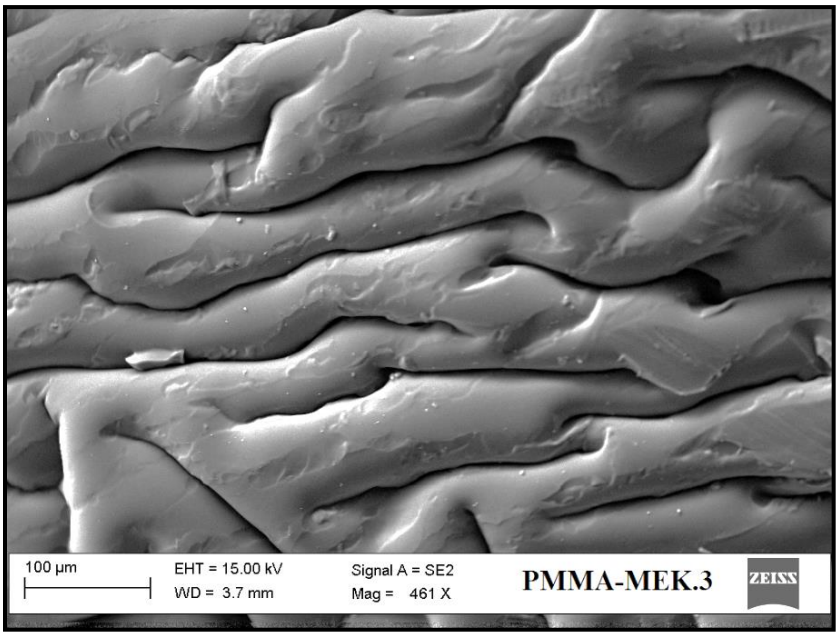

Figure 8.12. SEM image: PMMA-MEK.3 sample.

During the air drying process the gel structure is subjected to very large surface tension forces imposed on pores when there is a liquid/gas interface. As gel dries, the liquid/gas interface travels through the surface of the material inducing shrinkage and a general collapse of the network.

8.7 Determination of mesoporosity

The nano-scale structure of swollen PMMA organogels systems was studied through SAXS measurements, in particular to detail the mesh size, ξ, which identifies the polymer network texture and the size of inhomogeneities, a.

As reported in the literature (Panyukov and Rabin, 1996; Ikkai and Shibayama, 2005) less homogeneous structures are likely to form when the syntheses are conducted at higher polymer volume fractions (solvent-poor systems) and/or higher cross-linker concentration.

Best fitting curves for PMMA-DEC and PMMA-MEK organogels are reported as solid lines in figures 8.13 and 8.14, respectively.

Figure 8.13 shows the SAXS intensity distribution for samples PMMA-DEC.2 and PMMA-DEC.3. Fitting of the scattering curves was performed according to the Debye-Bueche model (Debye and Bueche, 1949; Fratini and Carretti, 2013).

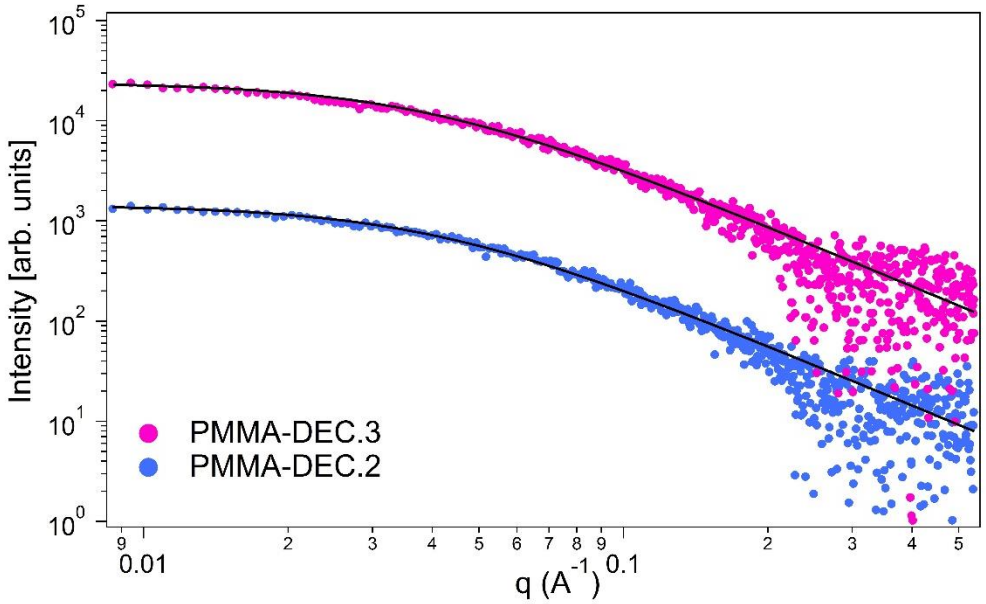

Figure 8.13. SAXS curve (dots) and Debye-Bueche fit (solid line) of the PMMA-DEC organogel systems.

The contribution $I_{excess}(q)$ in Debye-Bueche function (see chapter 7, equation 7.6), that concerns the scattering at low-q produced by inhomogeneities, was omitted since in the acquired SAXS profiles no intensity increase was observed in the low-q region. $I_{Lorentz}(q)$ is the scattering intensity at q = 0, dependent from the contrast between the polymer and the solvent and from the volume fraction of the polymer in the gel.

Table 8.4 lists the fitting parameters related to best fits shown in SAXS experiment.

	$I_{Lorentz}$ (0)	ξ (nm)	bkg
PMMA-DEC.2	7.36 ± 0.05	3.09 ± 0.01	0.20 ± 0.04
PMMA-DEC.3	6.34 ± 0.04	2.48 ± 0.02	0.15 ± 0.02

Table 8.4 SAXS fitting parameters of the PMMA-DEC organogels.

PMMA gels, the system which presents an higher mesh size is PMMA-DEC.2, according to its higher ESC value. In fact, it is known that solvent content affects ξ (Canal and Peppas, 1989).

The difference between the two formulations can be explained by the fact that greater quantities of absorbed solvent require a greater pores volume, thus also the mesopores become larger.

For what concerns the investigation of PMMA-MEK formulations, the scattering curves were interpreted using the Debye-Bueche model, as well as for PMMA-DEC systems, considering also the scattering at low-q values I_{excess} (q), which produced inhomogeneities, *a*.

The SAXS curves of the PMMA-MEK gels are shown in figure 8.14 and the results of the Debye-Bueche fitting are listed in table 8.5.

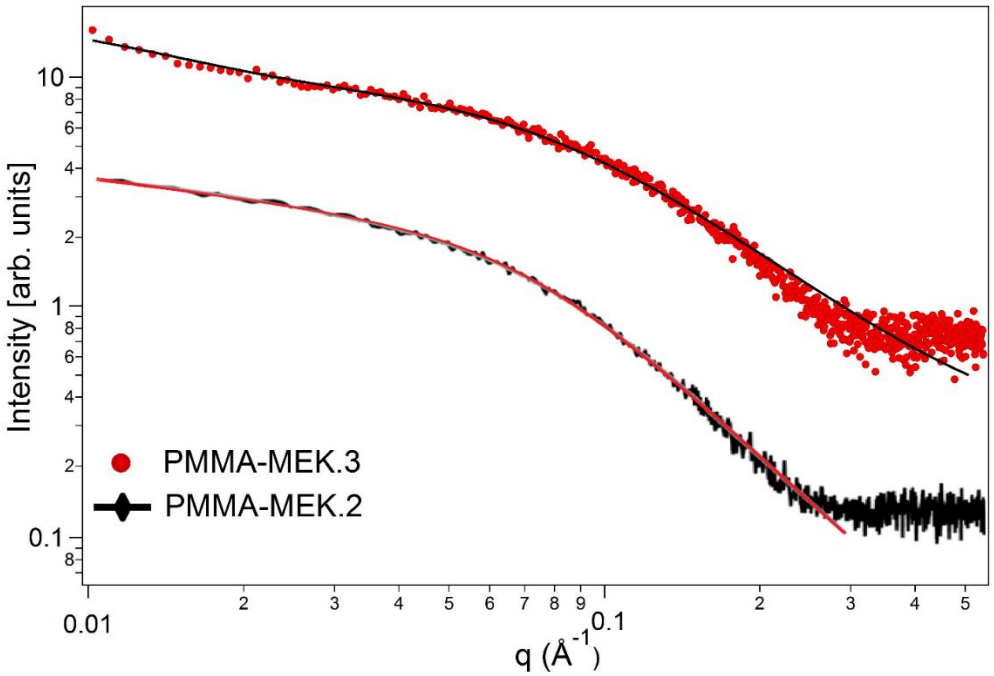

Figure 8.14. SAXS curve and Debye-Bueche fit (solid line) of the PMMA-MEK organogels.

	$I_{Lorentz}$ (0)	ξ (nm)	I_{excess} (q)	*a* (nm)	bkg
PMMA-MEK.2	47.10 ± 0.30	1.59 ± 0.01	18.10 ± 0.50	5.50 ± 0.20	0.40 ± 0.05
PMMA-MEK.3	9.26 ± 0.08	1.10 ± 0.10	9.58 ± 0.63	6.00 ± 0.30	0.23 ± 0.01

Table 8.5 SAXS fitting parameters of the PMMA-MEK organogels.

The size of gel inhomogeneities (*a*) is slightly higher for the PMMA-MEK.3 formulation as compared to PMMA-MEK.2. It must be noticed that a high concentration of cross-links in the gel network leads to greatly disordered structures (solid-like regions) (Ikkai, 2005; Panyukov,1996). Overall, the increased amount of cross-linker used in the synthesis of the PMMA-MEK.3 gel led to a decrease in the mesoporosity, which could contribute to its higher retentiveness, as feature required for applications on paper.

As well as PMMA-DEC systems, the solvent content of the polymeric network influences the mesh size ξ: the higher solvent content (see table 8.2) the higher mesh size.

8.8 Mechanical analysis

In order to investigate the dynamic mechanical properties of the selected formulations of PMMA organogels, amplitude sweep and frequency sweep tests were carried out on flat samples. The dependence of the complex moduli *G'* (storage modulus) and *G''* (loss modulus) on the frequency of the applied shear perturbation was investigated.

It must to be noticed that the rheological measurements performed on PMMA-MEK samples have given some problems because of high volatility of MEK. In fact, as reported in previous chapter, to avoid solvent evaporation, the edges of polymeric film were constantly loaded with MEK. These shrewdness resulted in anomalous response of gel to instrument's stimuli therefore, in order to obtain consistent results, the measurements were repeated several times.

In figures 8.15 and 8.16 is evidenced that all the investigated systems have a similar mechanical behavior: G' is always higher than the G'' and both moduli, in the LVE range, are independent from the angular frequency of the applied shear stress.

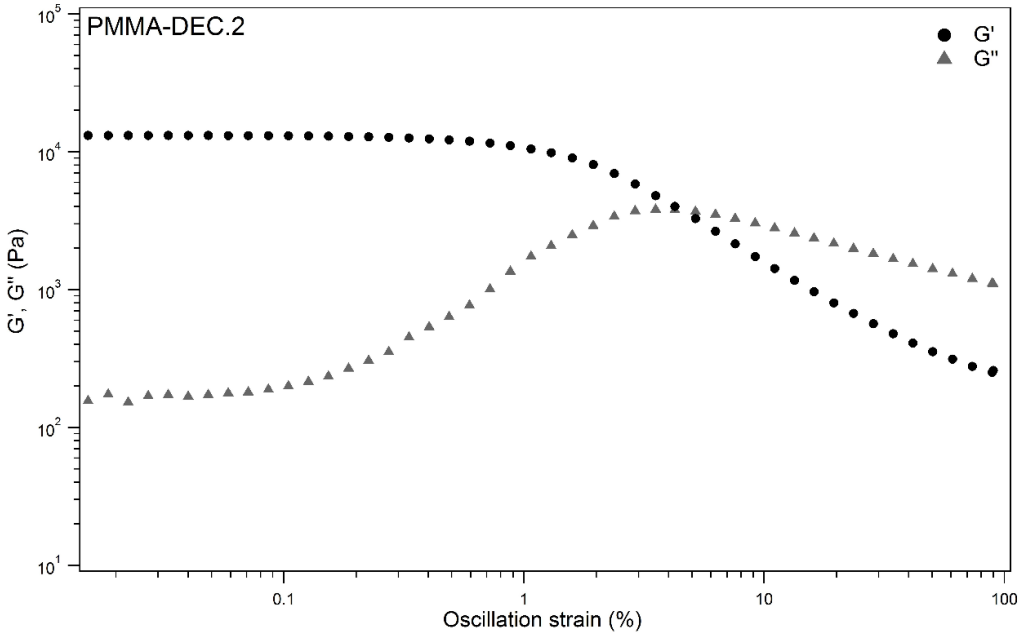

Figure 8.15. Amplitude sweep: log-log plot of storage G' (dot marks) and loss G'' (triangular marks) moduli of PMMA-DEC.2 organogel.

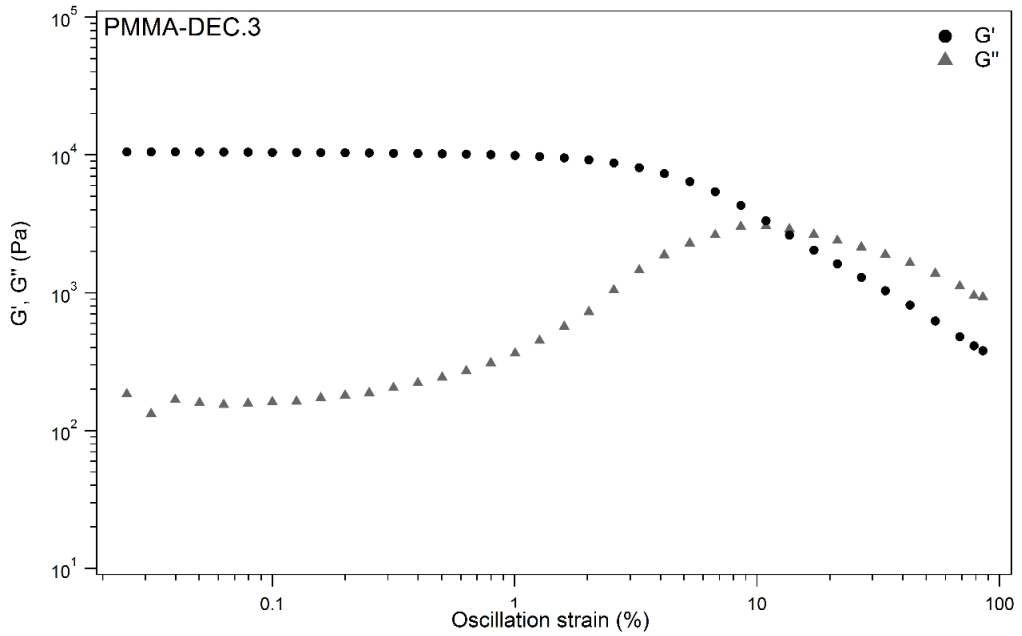

Figure 8.16. Amplitude sweep: log-log plot of storage G' (dot marks) and loss G'' (triangular marks) moduli of PMMA-DEC.3 organogel.

PMMA-MEK systems displayed the same behavior of PMMA-DEC networks, as shown in figures 8.17 and 8.18.

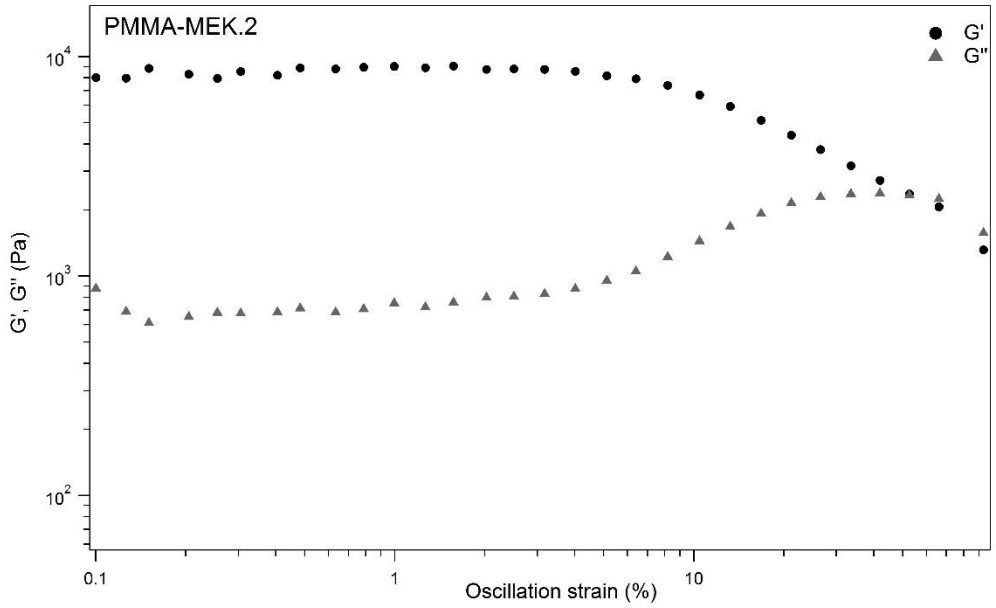

Figure 8.17. Amplitude sweep: log-log plot of storage G' (dot marks) and loss G'' (triangular marks) moduli of PMMA-MEK.2 organogel.

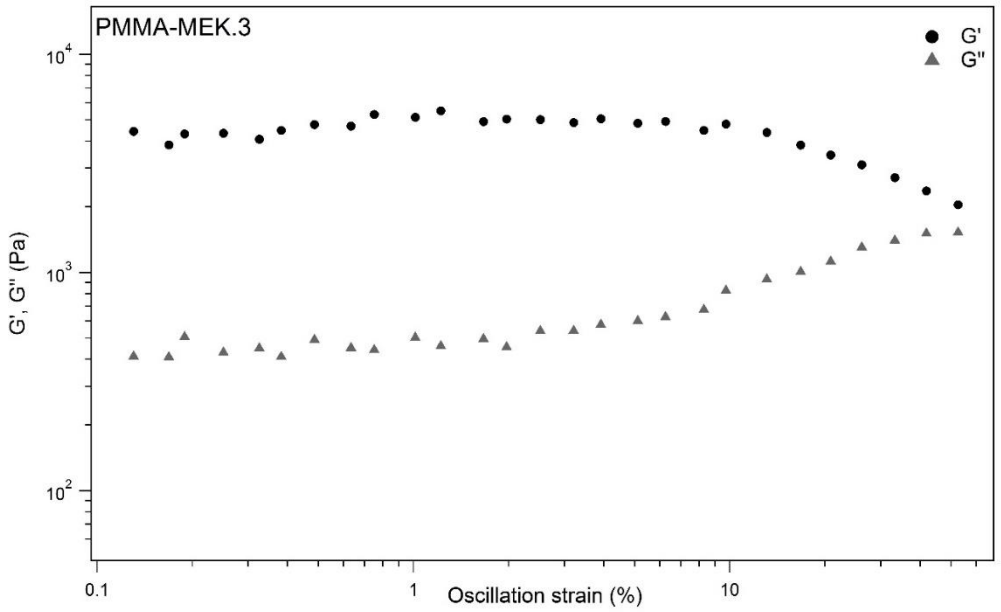

Figure 8.18. Amplitude sweep: log-log plot of storage G' (dot marks) and loss G'' (triangular marks) moduli of PMMA-MEK.3 organogel.

The viscoelastic behavior of our systems can be described by values of critical strain (γ_c), which has been calculated for all organogel formulations. PMMA-DEC.2 and PMMA-DEC.3 have γ_c = 1,4% and γ_c = 6% respectively, while PMMA-MEK.2 and PMMA-MEK.3 present γ_c = 7,8% and γ_c = 15,2%. These results are in agreement with the high concentration of cross-links in the PMMA-DEC.3 and PMMA-MEK.3 formulations.

Below these percentage of critical strain, the structure of polymeric network is intact and the material behaves solid-like; furthermore, G'>G" indicating that the material is highly structured. Increasing the strain above the γ_c, the structure collapses and the mechanical energy given to the material is dissipated, meaning that the material flows. The crossover point where G" becomes larger than G' is the moment where the applied mechanical force overtakes the molecular or inter particles forces and the material becomes progressively more fluid-like.

The results obtained during amplitude sweep analysis confirm a highly structured network of all organogels formulations. Figures 8.19 and 8.20 show the comparison of the oscillatory frequency-sweep measurements, acquired in the LVE range, for both organogel series: it can be noticed that all formulations produced gel-like systems.

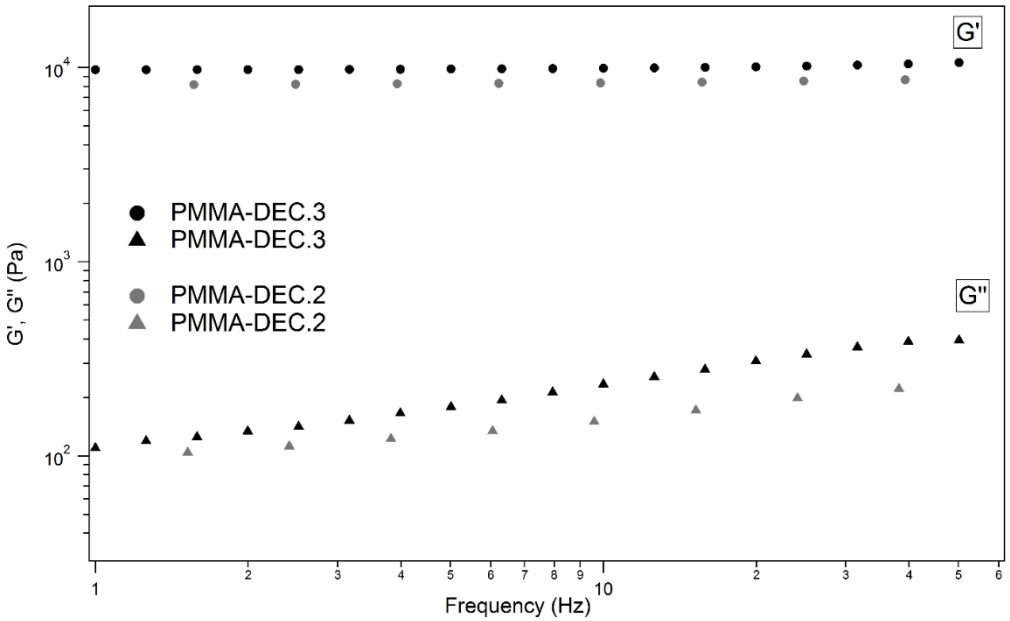

Figure 8.19. Frequency sweep: log-log plot of storage *G'* and loss *G"* moduli of PMMA-DEC systems.

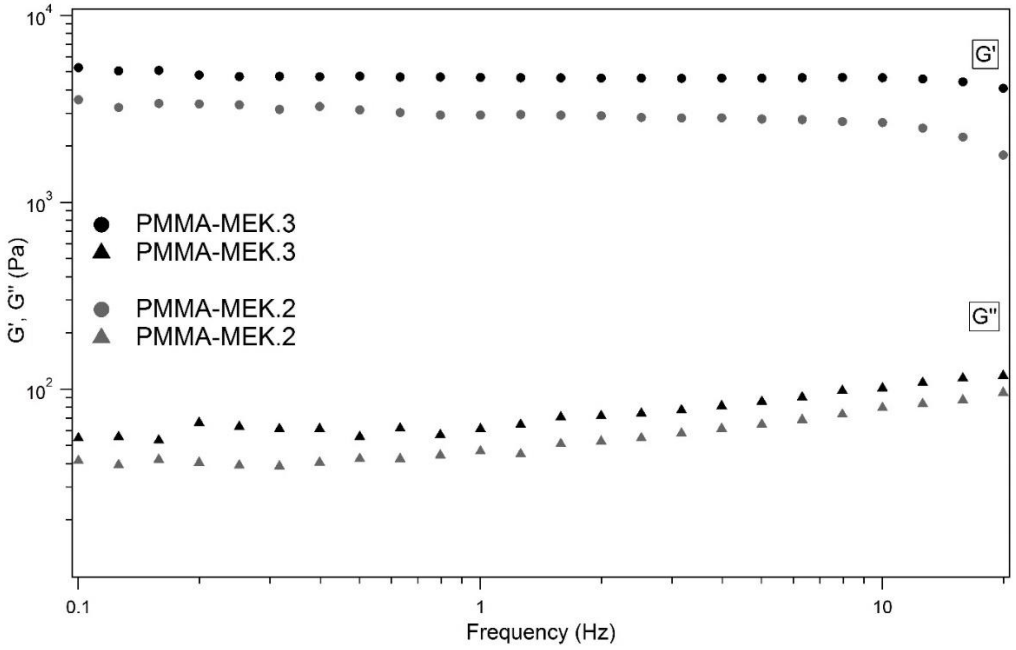

Figure 8.20. Frequency sweep: log-log plot of storage *G'* and loss *G"* moduli of PMMA-MEK systems.

Moreover, the values registered for tanδ = *G''*/*G'* (comparable for PMMA-DEC gels ≈ 0.02 and for PMMA-MEK ≈ 0.1) indicate that the PMMA systems are strong chemical organogels (figure 8.21).

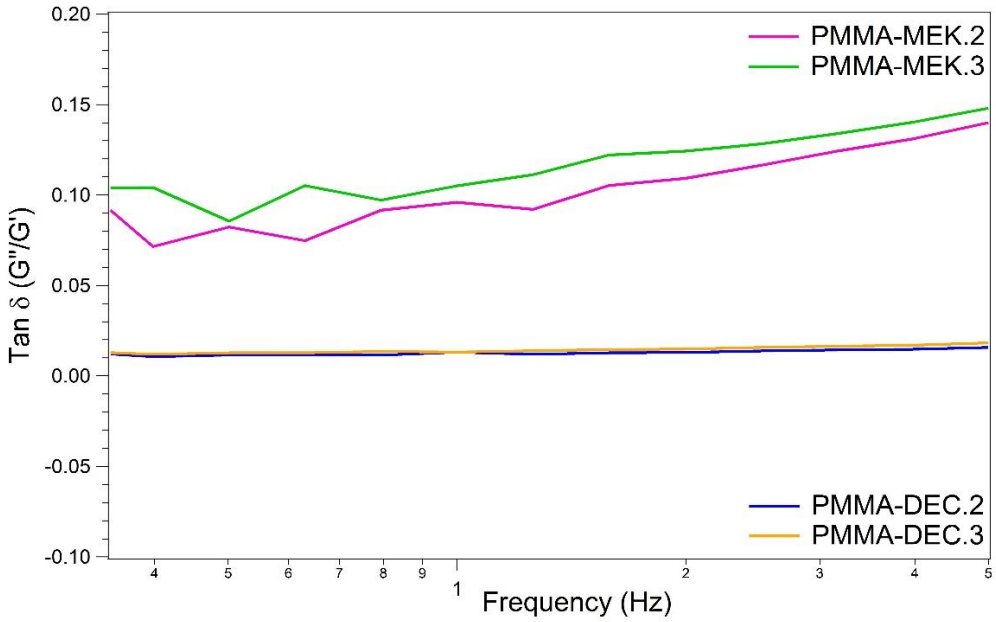

Figure 8.21. Tan δ plot of PMMA-MEK and PMMA-DEC systems.

For viscoelastic fluids a characteristic frequency dependence of the elastic and loss modulus that is $G' \propto \omega^1$ and $G'' \propto \omega^2$, is observed at low frequencies (Goodwin and Hughes, 2000). In this case the rheological behavior of the PMMA systems is characterized by an invariance of the G' modulus from the frequency ($G' \propto \omega^0$) and G' >> G'' over the explored frequency range, i.e. deformation in the linear viscoelastic range will be essentially elastic or recoverable. Thus, all the investigated PMMA-DEC systems show a gel-like behavior (Almdal et al., 1993), which means that they hold their shape, likewise to a solid.

References

Almdal, K.; Dyre, J.; Hvidt, S.; Kramer, O. 1993. Towards a Phenomenological Definition of the Term “Gel.” Polym. Gels Netw. 1, 5-17.

Canal, T.; Peppas, N.A. 1989. Correlation between mesh size and equilibrium degree of swelling of polymeric networks. J. Biomed. Mater. Res. 23, 1183-1193.

Cha, W.I.; Hyon, S.H., Ikada, Y. 1993. Microstructure of poly(vinyl alcohol) hydrogels investigated with differential scanning calorimetry. Macromol. Chem. 194, 2433–2441.

Debye P.; Bueche, A.M. 1949. Scattering by an Inhomogeneous Solid. J. Appl. Phys. 20, 518-525.

Ding, M.S.; Xu, K.; Zhang, S.; Jow, T.R. 2001. Liquid/Solid Phase Diagrams of Binary Carbonates for Lithium Batteries - Part II. J. Electrochem. Soc. 148, 299-304.

Ding, M.S. 2004. Liquid−Solid Phase Equilibria and Thermodynamic Modeling for Binary Organic Carbonates. J. Chem. Eng. Data 49, 276-282.

Fratini, E.; Carretti, E. 2013. Chapter 10. Cleaning IV: Gels and Polymeric Dispersions. In Nanoscience for the Conservation of Works of Art; Baglioni, P.; Chelazzi, D.; O’Brien, P., Eds.; Royal Society of Chemistry: Cambridge; pp. 252–279.

Goodwin, W.; Hughes, R.W. 2000. Rheology for Chemists. An Introduction; Royal Society of Chemistry. Cambridge.

Higuchi, A.; Iijima, T. 1985. DSC investigation of the states of water in poly(vinyl alcohol) membranes. Polym. 26, 1207.

Ikkai, F.; Shibayama, M. 2005. Inhomogeneity Control in Polymer Gels. J. Polym. Sci. Part B Polym. Phys. 43, 617–628.

Nakaoki, T.; Harada, S. 2006. Relationship between melting behavior of solvent and molecular morphology for isotactic polypropylene/o-dichlorobenzene gel. Curr. Trends Polym. Sci. 10, 47–54.

Nakaoki, T.; Harada, S. 2005. Melting behavior of bound solvent in isotactic polypropylene/o-dichlorobenzene gel. Polymer J. 37, 429–433.

Panyukov, S.; Rabin, Y. 1996. Statistical Physics of Polymer Gels. Phys. Rep. 269, 1–131.

PART IV

Cleaning of contemporary and historical paper artworks

CHAPTER 9
Cleaning of paper artworks

9.1 Introduction

Cleaning of cultural heritage artifacts is one of the most delicate operations in restoration practice because it is potentially invasive and aggressive for the original materials, as well as completely irreversible. Paper artworks, such as drawings and books, may be classified as water/solvent sensitive materials due to their chemical nature, i.e. cellulose-based, and for the presence of artistic media, e.g. inks, dyes and pigments.

As discussed in previous chapters, the list of unwanted materials to be removed from artifacts surface includes a wide group of substances: from deposits of pollutants and grime to aged adhesives and waxy coatings. The presence of unwanted substances on paper artifacts may cause a series of irreversible degradation processes and cleaning become a necessary intervention. In particular, the removal of pressure sensitive tapes (PSTs) and waxes from cellulose-based artifacts represent a challenge for paper conservator worldwide. Due to their nature, PSTs and waxy compounds establish strong interactions with the cellulosic fibers; the adhesive forces between these materials and the paper fibers are stronger than the cohesive ones among the fibers themselves. Traditional cleaning methods, e.g. dry mechanical action (Zervos and Alexopoulou, 2015) or removal by mixtures of organic solvents (Casoli et al., 2014), involve several drawbacks, especially when the treatment is carried out on naturally aged and degraded objects such as fragile and aged paper.

In this chapter the applications of innovative chemical organogels, PMMA-DEC and PMMA-MEK, for the removal of PSTs and waxes from water/solvent sensitive paper surface are presented.

These cleaning systems are previously tested on laboratory paper samples, which mimic the real paper artworks in order to choose the best performing organogel formulation.

The first part of the chapter is dedicated to a briefly description of the paper artworks and the assessment of conservation issues. The physical-chemical characterization of papers, PST and wax was performed through ATR-FTIR technique. A Thermo Nicolet Nexus 870 FTIR spectrometer equipped with a Golden Gate diamond ATR with 128 scans and 4 cm^{-1} of optical resolution, in the 4000-650 cm^{-1} range, was used.

In the second part of chapter, the cleaning treatments performed on the selected paper artworks through the application of innovative chemical organogels are described. Furthermore, the results will be discussed.

9.2 Contemporary paper artworks: Federico Fellini's drawings

The restoration of several drawings of Federico Fellini (property of Cineteca del Comune di Rimini) was performed in collaboration with Opificio delle Pietre Dure (Florence). These artworks are characterized by the presence of aged pressure sensitive tapes on paper surface, which often cover the artistic technique.

Here, the artwork entitled "*Anniversario. 14 Maggio 1957-14 Maggio 1987"* is briefly described (figure 9.1). Cleaning procedure, results and discussion will be reported in the second part of this chapter.

Figure 9.1. *Anniversario*. *14 Maggio 1957-14 Maggio 1987*.

The drawing was realized on a white paper sheet (industrial manufacturing), with dimensions of 22x28 cm. As visible in figure 9.1, the main technique is marker pen, with pen and pencil lines. The PST was applied in correspondence of red colorful strokes (figure 9.2), probably to mend rips of paper support.

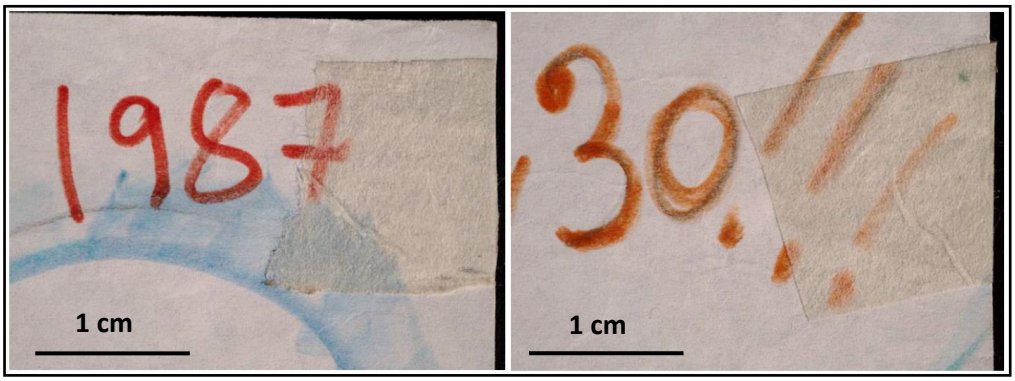

Figure 9.2. "*Anniversario*. *14 Maggio 1957-14 Maggio 1987"*. Detail of PST layers in correspondence of red marker.

Among traditional procedures for the removal of PSTs, the most used is the application of neat organic solvents. However, the lack of control in cleaning process, due to impossibility of monitoring penetration and spreading of the solvent within the treated matrix may cause several drawbacks, i.e. the risks for the treated artifact and the potential hazard to the health of the operators. To avoid undesired effects during a removal treatment, the PMMA-DEC organogel systems, developed as innovative cleaning tools, are tested for the first time for the removal of adhesives tapes from paper surface.

9.2.1 Characterization of paper and aged PSTs

ATR-FTIR measurements were performed at laboratory of Opificio delle Pietre Dure, while the obtained data were elaborate during this study. Figure 9.3 shows the comparison between IR spectrum of drawing's paper and standard Whatman® filter paper (grade 1).

Absorption band at 3691, 3647 and 2930 cm^{-1} and broad band at ~1000 cm^{-1} correspond to kaolin filler (IRUG database, URL: http://www.irug.org/jcamp-details?id=56), which is used to improves paper appearance and its strength (Bundy and Ishley, 1991).
The peaks at 2930 and 1793 cm^{-1} (ν OH and ν C=O, respectively) can be due to paper oxidation (Duràn et al., 2016; Lojewska et al, 2005).

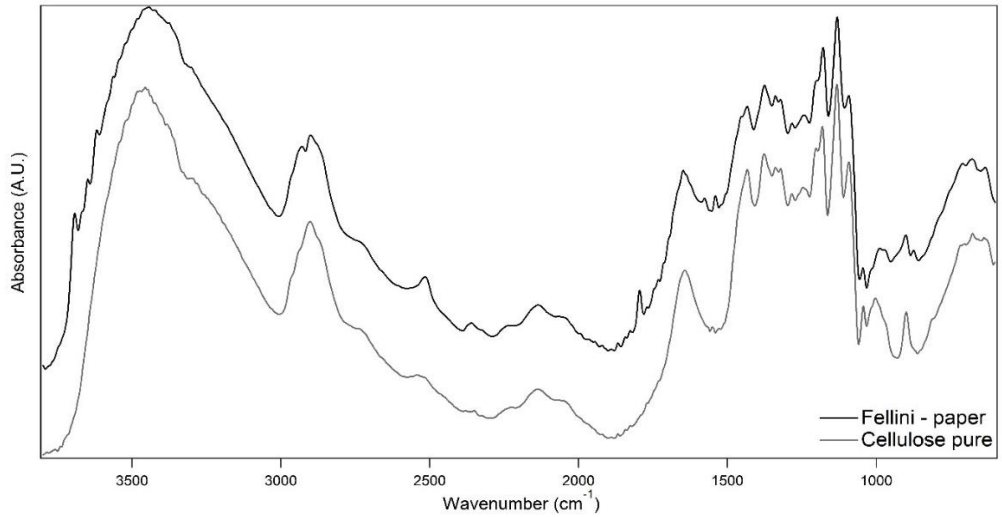

Figure 9.3. ATR-FTIR spectrum of Fellini's paper as compared to standard filter paper (pure cellulose).

In the same way, samples of pressure sensitive tape were studied in order to determine the nature of backing and adhesive.

In figure 9.4 is reported the comparison between PST spectra (backing and adhesive) and an acrylic adhesive reference; PST was directly sampled from drawing.

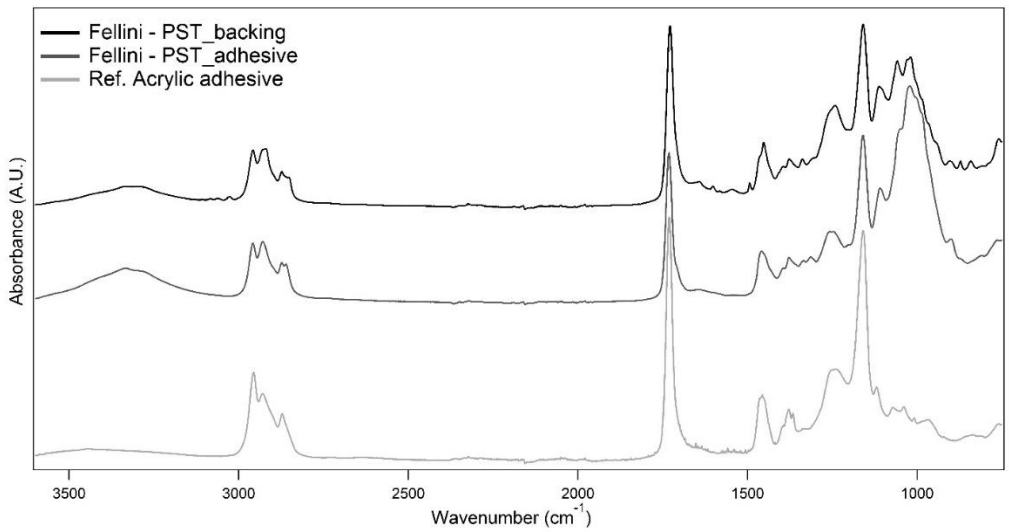

Figure 9.4. Comparison between ATR-FTIR spectra of PST backing, PST adhesive and acrylic adhesive reference.

The presence of acrylic compounds, both in adhesive and backing, is evidenced by the strong peaks at 1730 cm^{-1} (ν C=O) and 1158 cm^{-1} (δ CH). As discussed in chapter 2, acrylic pressure sensitive adhesives are typically random copolymers of a long side-chain acrylic (e.g. n-butyl acrylate or 2-ethylhexyl acrylate), and acrylic acid to improve adhesion and optimize elongational properties. (Creton, 2003).

For what concerns the backing, the absorption bands in the range 1100-800 cm^{-1}, which are also evident in adhesive spectrum, are typical of cellulose-derived materials.

The results suggest that pressure sensitive tape used in Fellini's drawing can be Masking Tape (Benedek and Feldstein, 2009).

9.3 Historical paper artworks: "*In officio et Missa solemni pro defunctis*" (1852 AD)

Beside Fellini's contemporary paper artworks, during this work we focused our attention also on historical papers. In particular, a printed book entitled "*In officio et Missa solemni pro defunctis*", of the mid-19th century, represent an interesting case study because of the abundance of waxy spots (figure 9.5) which cover the surface of the paper sheets.

This book coming from the historical archive of a Florentine Church (Chiesa di Sant'Ilario a Colombaia – Porta Romana, Florence) and its origin can justify the presence of wax over the sheets, probably due to dropping of wax from candles used as a light source during reading sessions.

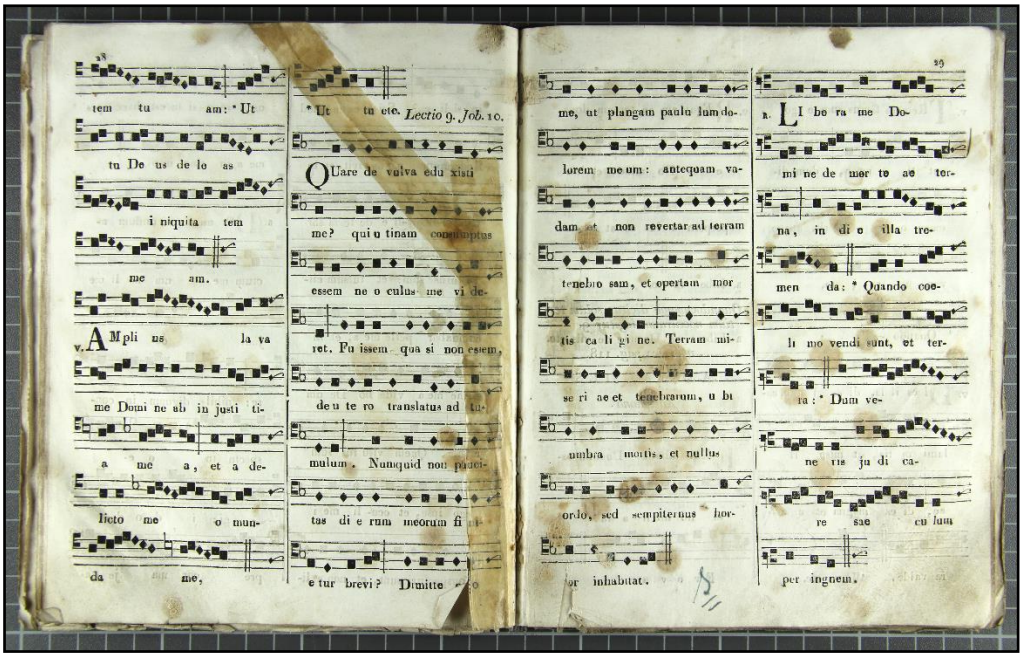

Figure 9.5. "*In officio et Missa solemni pro defunctis*" (1852 AD).

Wax is difficult to remove from objects and its presence severely limits an objects repeatability. Attempts at removing wax coatings involving, among traditional cleaning methods, the use of room temperature solvents, which were found to incompletely dissolve wax (Johnson, 1984; Moffett, 1996). Usually, dry cleaning is the easiest and fastest way adopted by restorers for the removal of waxy layers from paper surface. However, as reported in chapter 2, it can be potentially aggressive, uncontrolled and unselective, especially when it is carried out with traditional tools, i.e. brush, cotton swab, scalpel and hot iron.

Before the cleaning treatment of printed book, physical-chemical characterization of paper and wax was performed.

9.3.1 Characterization of paper and wax

ATR-FTIR analysis of paper (figure 9.6) shows the characteristic absorption bands of cellulose: 3332 cm^{-1} (ν OH), 1159 cm^{-1} (ν_a C-CO), 1108 cm^{-1} (ν C-O-C glycosidic),

1053 and 1027 cm^{-1} (ν C-OH I and II alcohol, respectively), 880 cm^{-1} (ν_s C-O-C) (Garside and Wyeth, 2003).

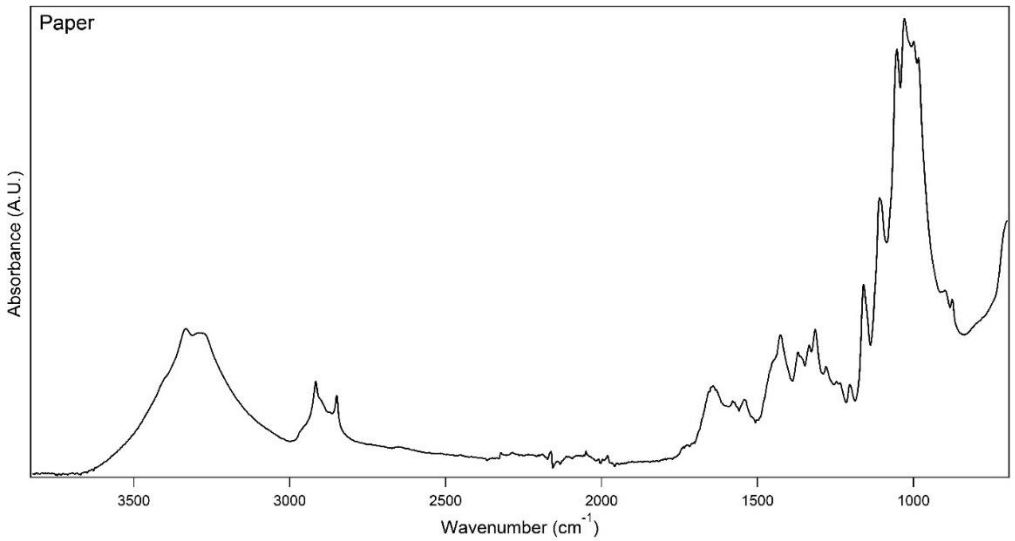

Figure 9.6. ATR-FTIR spectrum of printed book's paper.

Furthermore, the presence of peaks at 1577 and 1541 cm^{-1} are possibly due to calcium stearate (Gorassini et al., 2008; Librando et al., 2011), a wax used in paper production as a lubricant to provide good gloss, preventing dusting and fold cracking (Lower, 1990).
Despite the appearance, paper support has a good preservation that may be due to the hand made manufacturing.

In order to characterize the wax contaminant, some of the spots from different areas were sampled with a scalpel (figure 9.7). Analysis were performed through ATR-FTIR technique.

Figure 9.7. Sampling of wax.

The wax samples were analyzed by ATR-FTIR (figure 9.8) and the result was compared with the spectra of waxes used for the manufacturing of candles during the 19th century. In particular, we choose beeswax and paraffin wax as model samples (Guzialowska, 2013).

Beeswax was an excellent substance for candle and restricted in usage for churches and royal events, due to their great expense. On the other hand, the manufacture of candles became an industrialized mass market in the mid-19th century, when James Young succeeded in distilling paraffin wax from coal and oil shales (Golan, 2004).

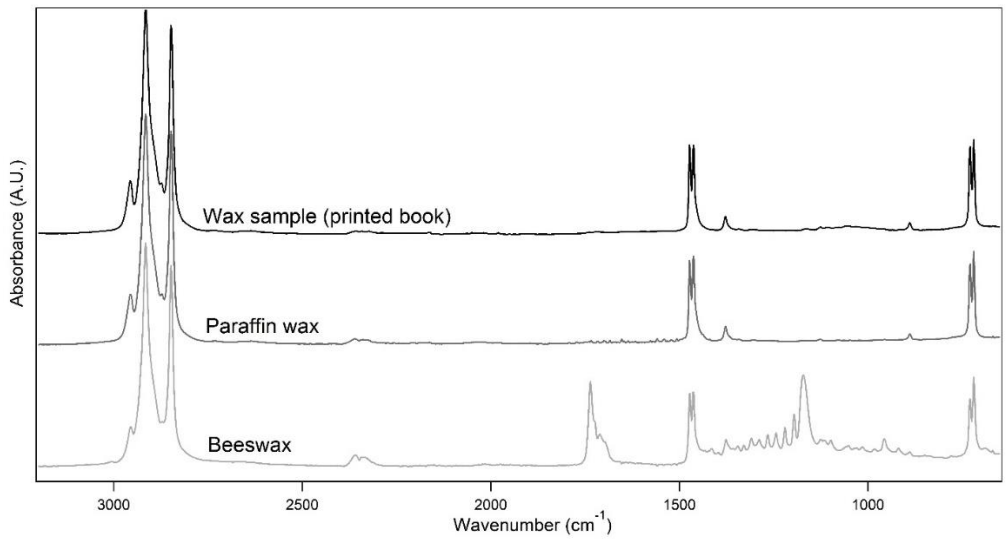

Figure 9.8. ATR-FTIR spectrum of wax sampled from printed book compared to spectra of paraffin wax and beeswax.

The comparison between the waxes' spectra indicated perfect overlap of sampled was with the spectrum of paraffin wax, as highlighted by the presence of bands at 2910 and 2846 cm^{-1} (ν CH), 1460 cm^{-1} (δ CH), 1380 cm^{-1} (δ CH_3), 728 and 719 cm^{-1} (ρ CH_2) (Fallahi et al., 2009; Meuse and Barker, 2009; Pouchert, 1997;Ludwig, 1965).

9.4 Preparation of the cleaning intervention

Before the intervention on artworks, several important steps are paramount. Beyond the physical-chemical characterization of materials and the assessment of conservative issues, investigations over composition of inks, dyes and pigments are fundamental for the selection of compatible tools and safe and suitable conservation treatments.

The most usual test is the assessment of the stability of paper substrate, inks, dyes and pigments when are wetted with water or other solvents.

In this context, diethyl carbonate and methyl ethyl ketone were tested on paper artworks before the application of PMMA organogels, in order to evaluate the solubility of inks, dyes and pigments in these organic solvents.

During the tests, which were carried out with DEC for Fellini's drawing and MEK for printed book, the solubilization of media was not observed: inks and dyes remained fixed over the paper support. Moreover, alterations of cellulose fibers seems to be avoided because of high volatility of both solvents.

It is important to recall that the selection of diethyl carbonate and methyl ethyl ketone for the removal of PSTs and waxes was due to their solubility parameters, their high volatility as well as their lower toxicity. Moreover, the confinement of DEC and MEK in a polymeric network broadens the applicability of gels for the removal of coatings found on the surface of paper artifacts.

9.5 Removal of pressure sensitive tapes: application of PMMA-DEC organogels

Preliminary tests on laboratory samples (not reported here), which simulate Fellini's drawing "*Anniversario"*, were performed in order to choose the best formulation among PMMA-DEC systems.

Therefore, the PMMA-DEC.3 organogel was selected as better performing cleaning tool for the removal of pressure sensitive tape of "*Anniversario"*. In fact, since this system was applied in correspondence of art media, a high retentiveness is required (see chapter 8, section 8.5).

Figure 9.9 shows the application of organogel on PST.

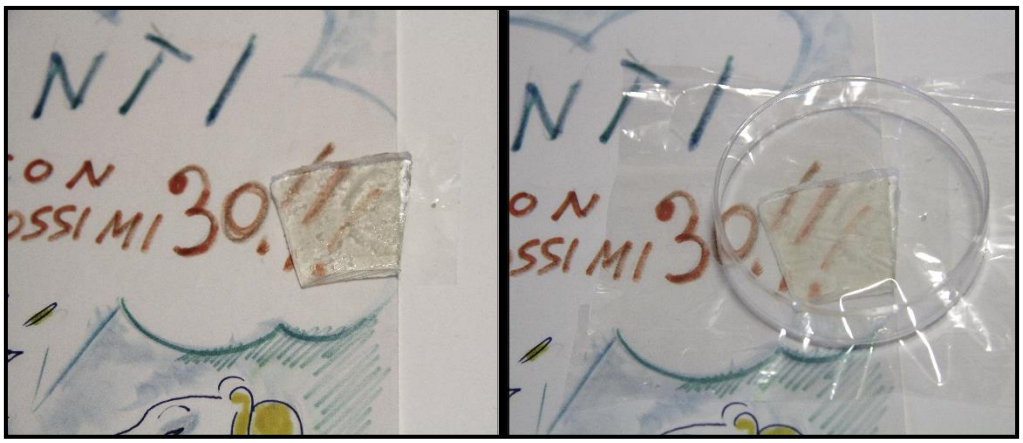

Figure 9.9. Application of PMMA-DEC.3 on PST (sheet's *recto*).

The PMMA-DEC.3 organogel was cut as the shape of PST (ca. 1x2 cm), to ensure a perfect adhesion and a controlled release of solvent on the defined area. As established during preliminary test, the application time was 10 minutes and, to avoid the solvent's evaporation, the gel was covered with a Mylar® foil and a petri dish. The PST was detached with a spatula, without strong mechanical action (figure 9.10)

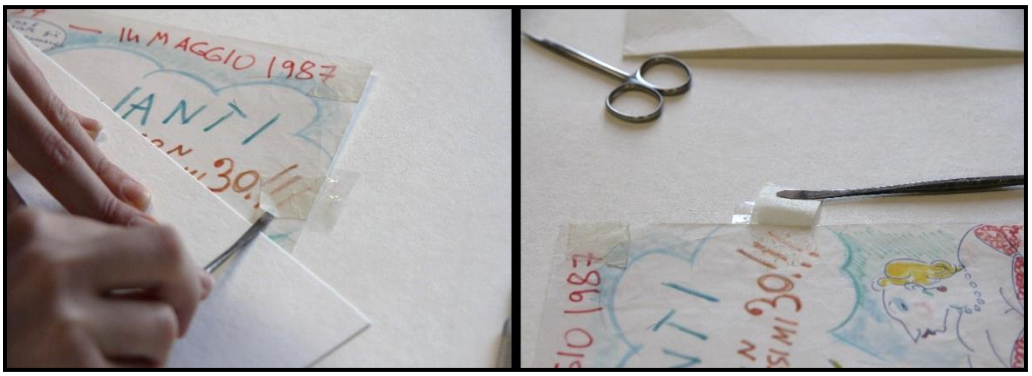

Figure 9.10. Removal of PST (sheet's *recto*).

In the same way, the application of PMMA-DEC.3 and the removal of PST were performed on the sheet's *verso* (figure 9.11).

Figure 9.11. Application of PMMA-DEC.3 and removal of PST (sheet's *verso*).

9.5.1 Results and discussion

The backing of PST was removed without mechanical action and only with the assistance of a spatula; however, some traces of adhesive are still remained on paper surface. Then, we decided to re-apply the PMMA-DEC.3 organogel directly on paper surface. The swollen adhesive was removed with a cotton swab, after 5 minutes.

At a first sight, the PST was successfully removed and alterations of cellulose-based support was not detected (figure 9.12).

Unfortunately, we were not able to check out the efficiency of treatment with ATR-FTIR analysis because of impossibility to move the drawing in our laboratories.

Figure 9. 12. Removal of PST (sheet's *verso*). Before (left) and after treatment (right).

9.6 Removal of wax: application of PMMA-MEK organogels

As discussed in chapter 5 (see section 5.4.4) methyl ethyl ketone is widely used industrial chemistry for solvent dewaxing process (Freund et al, 1982; Mohamed et al., 2008; As'Ad et al., 2015).

The preliminary tests performed on laboratory paraffin wax samples, which seem to be very similar to wax sampled from historical printed book (see section 9.3.1), were satisfactory: wax samples were completely dissolved in methyl ethyl ketone. Moreover, solubility tests of book's ink gave good results.

Also in this case, the better performing organogel, in terms of retentiveness (see chapter 8, section 8.5), was the PMMA-MEK.3 formulation. Figure 9.13 shows the comparison between the release effects of the PMMA-MEK system and the "free" solvent during a test, which carried out on a laboratory sample (paper sheet of 19th century).

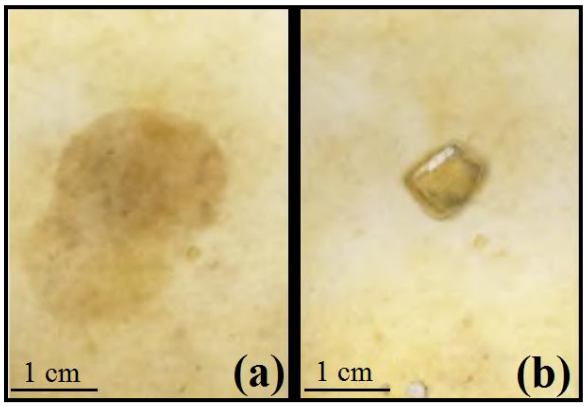

Figure 9. 13. Digital images of application of "free" solvent (left) and MEK confined in PMMA network (right).

The most effective cleaning procedure consisted in applying the PMMA-MEK.3 gel directly on wax spots in two successive applications, each of about 15 minutes (total application time of 30 minutes), in order to obtain a gradual and controlled removal of the wax layer.

The gel was covered with a Mylar® foil and a petri dish to avoid the solvent's evaporation.

Figure 9.14 shows the wax spot on the paper surface and its optical microscope image before the removal.

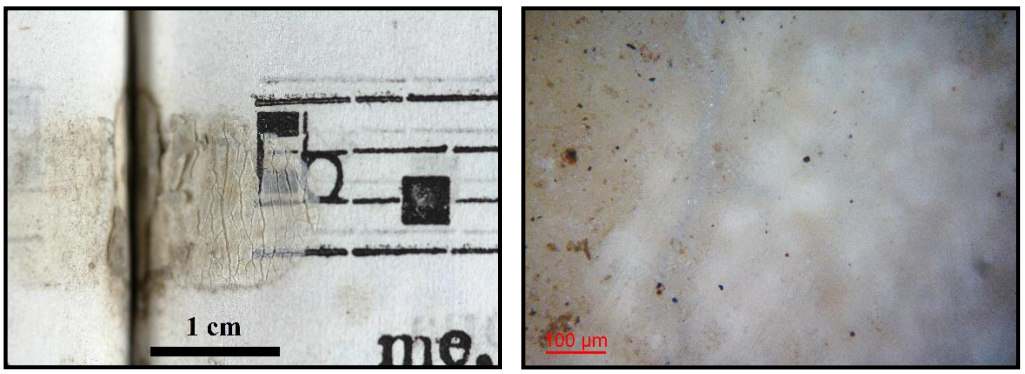

Figure 9. 14. Wax spot to be removed. Digital (left) and optical microscope (right) images.

After each application, the wax became swollen and softened and partially adhered to the gel detaching from the paper surface. After the second application, the swollen wax residues on paper surface were removed with gentle mechanical action using a dry cotton swab.

In figure 9.15 is shown the application of PMMA-MEK.3 organogel on wax spot.

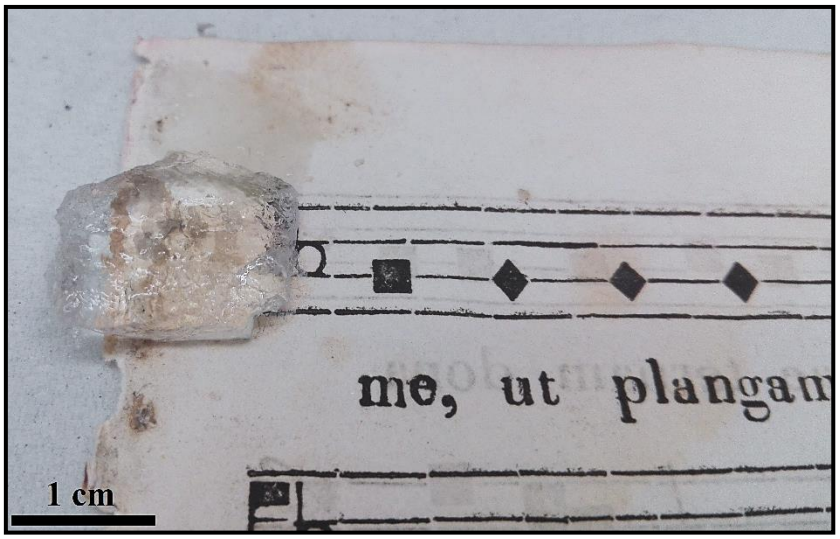

Figure 9.15.Digital image: application of PMMA-MEK.3 on wax spot.

9.6.1 Results and discussion

Digital and optical microscope images on the same spot, after the cleaning treatment, showed the disappearance of the matte waxy layer, to reveal the original paper fibers (see figure 9.16).

The efficiency of the treatment was checked using ATR-FTIR on the cleaning area (figure 9.17). Therefore, the spectrum of treated area was compared with the spectrum of PMMA-MEK.3 organogel to verify the absence of gel residues on cellulose substrate (figure 9.18).

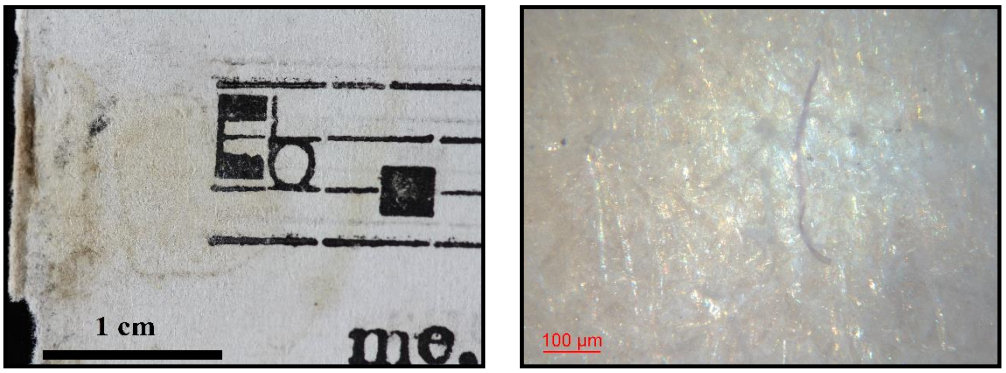

Figure 9. 16. Digital and optical microscope images of the paper surface of the 19th century missal: spot after removal of the wax using the PMMA-MEK.3 organogel.

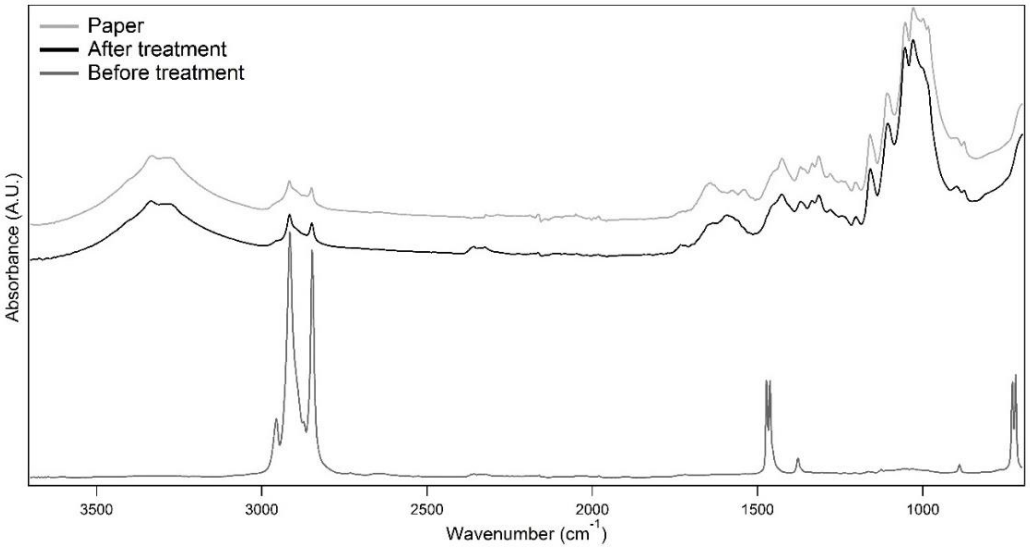

Figure 9.17. ATR-FTIR spectra: comparison between the spectra of paper before cleaning, paper after wax removal with the PMMA-MEK.3 gel, and paper that did not show any wax contamination.

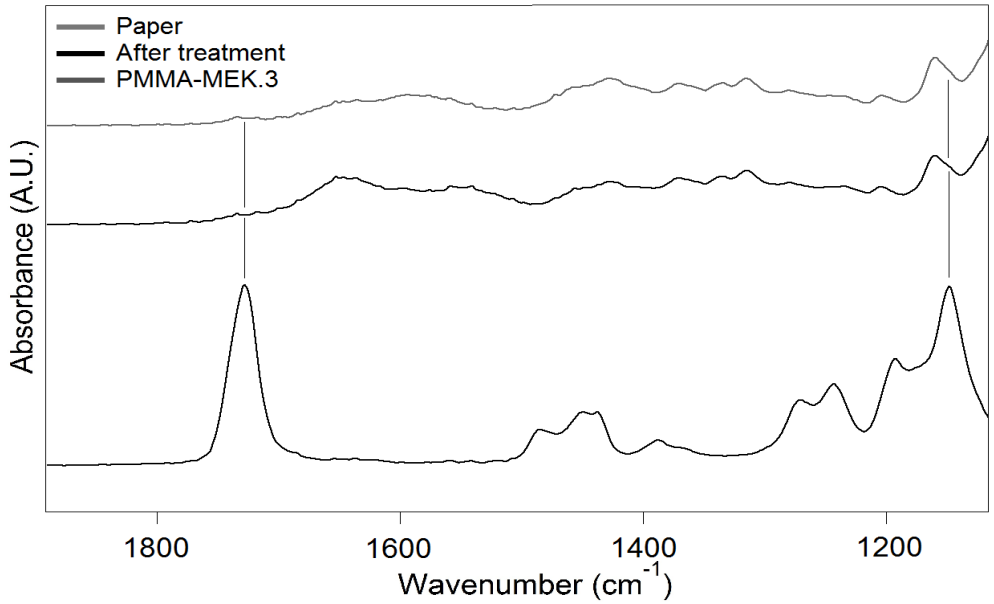

Figure 9.18. ATR-FTIR spectra: 1900-1100 cm^{-1} region. The bands of the gel are not observable in the spectrum of the paper cleaned with the gel.

The spectrum of treated area (see figure 9.17) confirms the removal of paraffin wax, whose bands are almost no longer observable.

The most intense bands of PMMA at 1726 cm^{-1} (ν C=O) and 1150 cm^{-1} (ν_a C-O-C) are not observable in the spectrum of the cleaned paper surface (see figure 9.18), confirming the absence of gel residues as detectable by ATR-FTIR.

Moreover, the spectrum of the cleaned area overlaps with that of spots that were not contaminated by wax; then we can assume that there are not alterations of cellulose substrate.

References

As'Ad, A.M.; Yeneneh, A.M.; Obanijesu, E.O. 2015. Solvent Dewaxing of Heavy Crude Oil with Methyl Ethyl Ketone. J. Pet. Environ. Biotechnol. 6, 213-217.

Benedek, I.; Feldstein, M.M. 2009. Technology of Pressure-Sensitive Adhesives And Products. CRC Press: Boca Raton, FL.

Bundy, W.M.; Ishley, J.N. 1991. Kaolin in paper filling and coating. Appl. Clay Sci. 5, 397-420.

Casoli, A.; Di Diego, Z.; Isca, C.; 2014. Cleaning painted surfaces: evaluation of leaching phenomenon induced by solvents applied for the removal of gel residues. Environ. Sci. Pollut. Res. 21, 13252-13263.

Creton, C. 2003. Pressure-Sensitive Adhesives: An Introductory Course. MRS Bulletin 28, 434-439.

Duràn, V.L.; Larsson. P.A.; Wagberg, L. 2016. On the relationship between fibre composition and material properties following periodate oxidation and borohydride reduction of lignocellulosic fibres. Cellulose,. doi:10.1007/s10570-016-1061-4.

Fallahi, e.; Barmar, M.; Kish, M.H. 2010. Preparation of phase-change material microcapsules with paraffin or camel fat cores: application to fabrics. Iran. Polym. J. 19, 277-286.

Freund, M.; Csikòs, R.; Keszthelyi, S.; Mozès, G.Y. 1982. Paraffin Prodoucts. Properties, technologies, applications. Elsevier.

Garside, P.; Wyeth; P. 2003. Identification of Cellulosic Fibres by FTIR Spectroscopy. Thread and single fibre analysis by attenuated total reflectance. Studies in Conservation 48, 269-275.

Golan, T. 2004. Laws of Men and Laws of Nature: The History of Scientific Expert

Testimony in England and America. Harvard University Press, pp. 89–91.

Gorassini, A.; Calvini, P.; Baldin, A. 2008. Fourier Transform Infrared Spectroscopy (FTIR) Analysis of Historic Paper Documents as a Preliminary Step for Chemometrical Analysis. Presented at Multivariate Analysis and Chemometry Applied to Environment and Cultural Heritage, 2nd ed., Ventotene Island, Italy.

Guzialowska, J. 2013. Description of raw materials for manufacturing candles and grave candles and their influence on the environment. Chemik 67, 1027–1034.

Hansen, C.M. 2007. Hansen Solubility Parameters: A User's Handbook, Second Edition. CRC Press.

IRUG database. [www document]. URL: http://www.irug.org/jcamp-etails?id=56. (accessed 05/11/2016).

Johnson, R. 1984. The removal of micro crystalline wax from archaeological ironwork. In Brommelle et al., pp.107-9.

Librando, V.; Minniti, Z.; Lorusso, S. 2011. Ancient and modern paper characterization by FTIR and Micro-Raman spectroscopy. Conserv. Sci. Cult. Herit. 11, 249-268.

Lojewska, J.; Miskowieca, P.; Lojewskia, T.; Proniewicza, L.M. 2005. Cellulose oxidative and hydrolytic degradation: In situ FTIR approach. Polym. Degrad. Stabil. 88, 512-520.

Lower, E.S. 1990. Calcium stearate-Part 3. Pigm. Resin Technol. 19, 8-10.

Meuse, C.W.; Barker, P.E. 2009. Quantitative infrared spectroscopy of formalin-fixed, paraffin-embedded tissue specimens: paraffin wax removal with organic solvents. Appl. Immunohistochem. Mol. Morphol. 17, 547-552.

Moffett, D. 1996. Wax coatings on ethnographic metal objects: Justifications for allowing a tradition to wane. J. Americ. Inst. Conserv. 35, 1-7.

Mohamed, N.H.; Zaky, M.T.; Farag, A.S.; Fahmy, A.F.M. 2008. Separation of Paraffin Wax Using Solvent Fractionation. Petrol. Sci. Technol. 26, 562–574.

Pouchert, C.J. 1997. The Aldrich Library of Infrared Spectra, 2nd ed., Aldrich Chemical, Milwaukee, Wisconsin.

Zervos, S.; Alexopoulou, I. 2015. Paper conservation methods: a literature review. Cellulose 22, 2859–2897.

CONCLUSIONS

Conclusions

This thesis presents the synthesis, characterization and application of new cleaning systems based on chemical organogels, specifically developed for the treatment of paper artifacts.

Paper artworks, such as drawings and books, may be classified as water/solvent sensitive materials due to their cellulose-based nature and to the presence of artistic media, e.g. inks, dyes and pigments. The list of unwanted materials to be removed from paper surfaces includes a varied group of substances, which may cause irreversible degradation processes, therefore the cleaning become a necessary intervention. In particular, the removal of pressure sensitive tapes (PST) and waxes from cellulose-based artifacts represents a challenge for paper conservator worldwide.

In this context, efficacy, high selectivity, controllable action and low toxicity are fundamental features that a system should have to allow an efficient and harmless cleaning performance.

The organogel systems developed during this study are principally designed for the removal of waxy layers and the detachment of pressure sensitive tapes from paper supports.

In particular, the properties of poly(methyl methacrylate) (PMMA) as polymer network were studied. Diethyl carbonate (DEC) and methyl ethyl ketone (MEK) were selected as solvents used for the synthesis of PMMA organogels and as cleaning fluid loaded within gels.

Diethyl carbonate, a non-toxic and biodegradable alkyl carbonate, was employed during this work as potential cleaning agents for cleaning of paper artifacts. In fact, it seems to be able to dissolving or swelling a wide range of

natural and synthetic resins. Here, PMMA-DEC organogels were used as cleaning tools for the removal of pressure sensitive tapes from water/solvent sensitive paper artworks.

Methyl ethyl ketone is an organic solvent characterized by good solubility, volatility and stability. It is widely used in various range of applications, for example as an extraction medium for oils, paraffin waxes and resins. In this context, PMMA-MEK organogels were specifically designed for the selective removal of degraded waxy coatings from the surface of water sensitive inked paper.

The physico-chemical and mechanical characterization of the selected polymeric formulations was performed through Attenuated Total Reflection Fourier Transform Infrared Spectroscopy (ATR-FTIR), gravimetric analysis, Thermogravimetry (TGA), Differential Scanning Calorimetry (DSC), Small-angle X-ray Scattering (SAXS) and rheological measurements.

ATR-FTIR analysis was employed to obtain information on the presence of unreacted monomer in the polymer networks. The results have shown that for PMMA-DEC and PMMA-MEK systems were necessary five and seven washing cycles, respectively, to obtain free-monomer gels.

In order to verify the affinity of the polymer gel to the liquid phase, the equilibrium solvent content, Q, was determined gravimetrically and through TGA analysis.

For all the PMMA formulations, the values of equilibrium solvent content demonstrated that both DEC and MEK have a high affinity for the PMMA polymer network, as confirmed by the results obtained through TGA measurements.

The free solvent index (FSI) was investigated in order to estimate the quantity of solvent within organogels structure acting as bulk liquid, being thus available for

the cleaning process. The measurements were performed with Differential Scanning Calorimetry (DSC).

The FSI values of the selected PMMA-DEC systems are all quite similar to each other, around 20-30 %.

The nano-scale structure of swollen PMMA organogels was studied through SAXS measurements and using the Debye-Bueche fitting model.

Regarding PMMA-DEC gels, the system that presents a higher mesh size is PMMA-DEC.2, according to its higher ESC value.

For what concerns the investigation of PMMA-MEK formulations, the size of gel inhomogeneities (*a*) is slightly higher for the PMMA-MEK.3 formulation. In fact, the increased amount of cross-linker used in the synthesis of this system led to a decrease in the mesoporosity, which could contribute to its higher retentiveness. Also in this case, the mesh size was influenced by the high solvent content.

Rheological measurements were performed in order to investigate the dynamic mechanical properties of the selected formulations of PMMA organogels. Both PMMA-DEC and PMMA-MEK systems have an analogous mechanical behavior: *G'* is always higher than the *G''* and both moduli, in the LVE range, are independent from the angular frequency of the applied shear stress.

The viscoelastic behavior can be described by critical strain (γ_c), which has been calculated for all organogel formulations. Moreover, the tanδ values indicate that the PMMA systems are strong chemical organogels.

The selection of best performing organogels was based on the results obtained during the physical-chemical and mechanical characterization and on preliminary tests achieved on paper laboratory samples (not reported here). Accordingly with obtained results, PMMA-DEC.3 and PMMA-MEK.3 formulations

were employed for the removal of pressure sensitive tapes and waxes from water/solvent sensitive paper surface.

The restoration of Federico Fellini's drawing, entitled "*Anniversario. 14 Maggio 1957-14 Maggio 1987"*, was performed in collaboration with Opificio delle Pietre Dure (Florence). The artwork is characterized by the presence of aged PST.

The PMMA-DEC organogel systems, developed as innovative cleaning tools, are tested for the first time for the removal of adhesives tapes from paper surface.

ATR-FTIR measurements were performed in order to characterized the paper support and the PSTs. The obtained results suggested that pressure sensitive tape used in Fellini's drawing could be Masking Tape.

The PMMA-DEC.3 organogel was selected as better performing cleaning tool for the removal of pressure sensitive tape. In fact, since PST was applied in correspondence of art media, a highly retentive gel is required

The backing of PST was removed without mechanical action and only with a spatula and the traces of adhesive still remained on paper surface were removed with a second application of gel. Unfortunately, we were not able to check-out the efficiency of treatment with ATR-FTIR analysis because of impossibility to move the drawing in our laboratories.

During this work we focused our attention also on a historical printed book, entitled "*In officio et Missa solemni pro defunctis*", of the mid-19th century. It represents an interesting case study because of the abundance of waxy spots that cover the surface of the paper sheets.

Before the cleaning treatment, wax was identified as paraffin wax through ATR-FTIR analysis.

Also in this case, the better performing organogel, in terms of retentiveness and applicability, was the PMMA-MEK.3 formulation. The shaped gel was applied directly on wax spots in two successive times (total application time of 30

minutes). The swollen wax residues on paper surface were removed with gentle mechanical action using a dry cotton swab. The successful of the treatment was checked with the optical microscopy and confirmed by ATR-FTIR measurements.

The innovative PMMA organogel systems allowed a safer and more gradual release of solvent on the paper surface, which led to the gradual swelling and detachment unwanted layers. After the cleaning intervention, the gel can be removed without leaving polymer residues on the surface. Overall, this work validated the tunable synthesis of PMMA-based organogels as a process to produce versatile cleaning tools that can be used on different artistic surfaces, decreasing the risks of altering the original properties of the artifacts.
The obtained results may open new perspectives in the cleaning and protection of cellulose-based artifacts.

Acknowledgments

I would like to start expressing my gratitude to my supervisor and tutor, Prof. Rodorico Giorgi, without whom I would not had the chance of doing this experience; his expertise and understanding of the materials for the conservation of Cultural Heritage has allowed me to fully express the concepts in this dissertation.

At the same time, my special gratitude goes to Dr. David Chelazzi for his support, assistance and patience during this research project.

I would like to thank my apprenticeship tutor, Father Sisto (Vincenzo) Giacomini, for his constant support and precious teachings during the training at Book Restoration Laboratory of Certosa di Firenze.

I wish also to thank Dr. Giovanna Poggi, Dr. Michele Baglioni and Dr. Nicole Bonelli, whom have collaborated with me actively and helped me to attain my research goals.

I would like to acknowledge Letizia Montalbano, director of the advanced training school of Opificio delle Pietre Dure (Florence), who gave me the possibility of carrying out applicative tests on some original drawings of Federico Fellini.

Furthermore, I wish to thank Dr. Pedro Daniel Dalio, the pastor of Sant'Ilario's Church, who provided interesting case studies ("*In officio et Missa solemni pro defunctis*"–1850 AD and "*Roman Missal"*-1725 AD), to test the versatility of the cleaning systems on historical paper artifacts.

Almost the entire work presented in this dissertation was carried out at the laboratories of the Chemistry Department, University of Florence. The interaction with my colleagues of the CSGI group, gave me the possibility of

increase my professional experience and of establishing good relationships with everyone, especially Chiara and Martina.
Special thanks also goes to Pamela Ferrari, for her personal and professional involvement in every step throughout the fulfillment of this work. She patiently helped and supported me over the past years.

Finally, I want to thank my family: my dad, who always encouraged me to begin this adventure but unfortunately has gone away too soon; my mom and my brother, for their encouragement, support and patience.
Special thanks to my best friends, Elena and Valentina, who supported, reassured and helped me over these years, despite the distance.

ANNEX

List of publications

Baglioni, M.; Bartoletti, A.; Bozec, L.; Chelazzi, D.; Giorgi, R. Odlyha, M.; Pianorsi, D.; Poggi, G.; Baglioni, P. 2016. Nanomaterials for the cleaning and pH adjustment of vegetable-tanned leather. Appl. Phys. A 122: 114.

Pianorsi, M.D.; Raudino, M.; Bonelli, N.; Chelazzi, D.; Giorgi, R.; Fratini, E.; Baglioni, P. 2017. Organogels for the cleaning of artifacts. Pure Appl. Chem., doi:10.1515/pac-2016-0908.
Paper in publishing.

Appl. Phys. A (2016) 122:114
DOI 10.1007/s00339-015-9553-x

Applied Physics A
Materials Science & Processing

INVITED PAPER

Nanomaterials for the cleaning and pH adjustment of vegetable-tanned leather

Michele Baglioni[1] · Angelica Bartoletti[3] · Laurent Bozec[3] · David Chelazzi[1] · Rodorico Giorgi[1] · Marianne Odlyha[2] · Diletta Pianorsi[1] · Giovanna Poggi[1] · Piero Baglioni[1]

Received: 20 July 2015 / Accepted: 15 December 2015 / Published online: 2 February 2016

Abstract Leather artifacts in historical collections and archives are often contaminated by physical changes such as soiling, which alter their appearance and readability, and by chemical changes which occur on aging and give rise to excessive proportion of acids that promote hydrolysis of collagen, eventually leading to gelatinization and loss of mechanical properties. However, both cleaning and pH adjustment of vegetable-tanned leather pose a great challenge for conservators, owing to the sensitivity of these materials to the action of solvents, especially water-based formulations and alkaline chemicals. In this study, the cleaning of historical leather samples was optimized by confining an oil-in-water nanostructured fluid in a highly retentive chemical hydrogel, which allows the controlled release of the cleaning fluid on sensitive surfaces. The chemical gel exhibits optimal viscoelasticity, which facilitates its removal after the application without leaving residues on the object. Nanoparticles of calcium hydroxide and lactate, dispersed in 2-propanol, were used to adjust the pH up to the natural value of leather, preventing too high alkalinity which causes swelling of fibers and denaturation of the collagen. The treated samples were characterized using scanning electron microscopy, controlled environment dynamic mechanical analysis, and infrared spectroscopy. The analytical assessment validated the use of tools derived from colloid and materials science for the preservation of collagen-based artifacts.

1 Introduction

Leather has been used by mankind since ancient times, yet the preservation of this collagen-based material represents a challenge for conservators worldwide [1, 2]. Leather objects are made from mammalian skin and hide, which are then transformed into a material that is resistant to mechanical abrasion, microbial attack, and heat. This is achieved through the tanning process, where either vegetable tannins or salts of metals (e.g., chromium, aluminum) are commonly applied to improve the stability of collagen. In particular, tannins have been used since Neolithic time to retard decay, and vegetable-tanned leather was indeed one of the most important materials in Western and Mediterranean Europe until the end of the nineteenth century, when chromium mineral tanning gradually came into use [3, 4]. Tannins form a complex with collagen, mainly through hydrogen bonds between free amino side groups of the collagen protein and hydroxyl groups from the polyphenolic tannin molecules, as well as through hydrophobic bonds [5]. Moreover, covalent bonds can be formed via quinoid structures between the protein and aromatic carbon in the molecules of condensed tannins, i.e., polymeric flavonoids consisting of flavan-3-ol (catechin) unit.

Michele Baglioni and Piero Baglioni: No kinship exists among the authors.

✉ Piero Baglioni
baglioni@csgi.unifi.it

David Chelazzi
chelazzi@csgi.unifi.it

[1] Department of Chemistry Ugo Schiff and CSGI, University of Florence, Via della Lastruccia 3, 50019 Sesto Fiorentino, Florence, Italy

[2] Department of Biological Sciences, Birkbeck, University of London, London, UK

[3] UCL Eastman Dental Institute, University College London, London, UK

Leather artifacts in historical collections and archives are often contaminated by soiling, salts, biocontamination, or coatings that alter their appearance and readability. Moreover, degradation is promoted by the presence of acidic compounds, coming either from manufacturing processes (tannery) or from the absorption of air pollutants such as sulfur and nitrogen oxides. Acidity increases the rate of hydrolysis of bonds within the collagen structure, reducing the polymer's structural integrity and eventually turning collagen into a gelatin colloidal solution. The tanning agents break down in turn under oxidative and acid hydrolytic conditions, forming products that can promote the degradation of collagen [1, 6].

The traditional materials and methods used for the cleaning and pH adjustment of collagen-based works of art involve risks to the artifacts, owing to the sensitivity of both collagen and the collagen–tannin complex to the action of solvents, water-based formulations, and alkaline chemicals. In fact, traditional moist-/water-based cleaning treatments of leathers that exhibit low pH (<3) and shrinkage temperature ($T_s < 35$ °C) may cause shrinkage or gelatinization of the collagen. Likewise, both pre-gelatinized and gelatinized collagen fibers are very sensitive to water even at room temperature [7]. Organic solvents are less likely to cause detanning of leather, although their use can involve toxicity issues and the risk to dehydrate or degrease the leather, jeopardizing its structure and properties.

Alternatively, oil-in-water (o/w) microemulsions are systems where low quantities of organic solvents are dispersed as stable nanosized droplets in a continuous aqueous phase. These systems exhibit high efficacy in removing layers of grime and aged coatings (varnishes, adhesives, etc.), and their low solvent content reduces the environmental impact. In fact, throughout the last decade, nanostructured fluids have been widely tested for the cleaning of mural paintings, and the results obtained have demonstrated that these systems are a valid alternative to the use of neat solvents [8–11]. However, for their use on water-sensitive substrates, o/w microemulsions must be confined within a retentive network that allows their controlled release, so as to grant the removal of unwanted layers without excessive wetting of the surface. For this purpose, o/w microemulsions have been recently used where they have been loaded in chemical hydrogels for the selective removal of adhesives from canvas paintings [12]. In particular, chemical gels formed by semi-interpenetrating (IPN) poly(2-hydroxyethyl methacrylate) (pHEMA) and polyvinylpyrrolidone (PVP) have emerged as advantageous systems for cleaning works of art, because they exhibit high retentiveness and optimal mechanical properties that allow their feasible application and their removal without leaving residues [12, 13].

Based on these results, we decided to test and report here the use of semi-IPN pHEMA/PVP gels loaded with an o/w nanostructured fluid for the cleaning of collagen-based artifacts.

As a matter of fact, the removal of dirt, salts, surface coatings, or patinas is also important because it facilitates the access to collagen fibers by any treatment applied successively to the artifact, such as the application of chemicals for the pH control of collagen.

Traditional methodologies for pH adjustment show several limitations, and their effectiveness on substrates such as vegetable-tanned leather has been debated. Alkaline aqueous solutions are risky owing to the aforementioned sensitiveness of collagen to water. Moreover, any excess alkalinity in the form of free, highly mobile hydroxide ions could damage either the collagen fibers [14] or the collagen–tannin complex in leather. On the other hand, salts of lactate and citrate have been shown to provide some protection against acidic degradation of leather during both natural aging in heavily polluted environments and strong accelerated aging, and it was found that treatment of new leathers with buffer salts can be effective without causing blooming [15]. It must be noticed that the pH of aqueous solutions of calcium lactate can range ca. from 6 to 8, which is milder and less risky to collagen than to strong alkalis. Moreover, lactic acid was used in the past for leather decalcination also because it favors the penetration of tannins [16].

Based on these considerations, in the present study we opted for the application of calcium lactate in the form of nanoparticles dispersed in a nonaqueous medium, for pH adjustment. The use of nanoparticles for the deacidification of works of art has been explored in the last decade, and alkaline earth hydroxides dispersed in short-chain alcohols have been used on cellulose-based artworks such as inked paper, canvas, and waterlogged archaeological wood. The particles grant the safe neutralization of acids and leave mild alkaline buffers against recurring acidity [17–20]. For instance, calcium hydroxide nanoparticles have been used to stabilize the pH of paper and canvas around 7–8, which is an optimal value for cellulose-based artifacts. However, in the case of collagen substrates the pH needs to be adjusted to lower values. Therefore, dispersions of calcium lactate nanoparticles in 2-propanol were prepared here for the first time and used either as pure or as mixed with calcium hydroxide nanoparticles to obtain a milder alkaline system. In fact, the goal was to tune the treatment so as to reach a final pH of ca. 4.5, which is the "natural" acidic value of leather objects in stable conditions, avoiding too high pH values such as 7 or more. The nanoparticles dispersions were characterized using scanning electron microscopy (FE-SEM), Fourier transform infrared spectroscopy (FTIR), X-ray diffraction (XRD), dynamic light

scattering (DLS), and turbidimetry measurements through UV–Visible spectroscopy.

The hydrogel, o/w nanostructured fluid, and nanoparticles dispersions were all tested on both modern and historical leather samples.

In order to monitor the effect of the cleaning and pH adjustment treatments on the artifacts, a set of analytical techniques was used, including attenuated total reflection Fourier transform infrared spectroscopy (ATR-FTIR), pH measurements, SEM, and controlled environment dynamic mechanical analysis (DMA-RH).

2 Experimental details

2.1 Chemicals

Lactic acid (90 %, Sigma-Aldrich, impurities of residual water), ethanol absolute (99.9 %, Fluka), 2-propanol (≥99.8 %, Sigma-Aldrich), and metal granular calcium (99 %, Aldrich) were used for the syntheses of nanoparticles and the preparation of nanoparticles dispersions. Sodium dodecyl sulfate (SDS) (≥99 %, Sigma-Aldrich), 1-pentanol (≥98.5 %, Merck), ethyl acetate (ACS reagents, ≥99.5 %, Sigma-Aldrich), and propylene carbonate (99 %, Sigma-Aldrich) were used for the preparation of the EAPC o/w nanostructured fluid. 2-Hydroxyethyl methacrylate (HEMA) (97 %, Sigma-Aldrich), polyvinylpyrrolidone (PVP) (average Mw ≈ 1300 kDa, Sigma-Aldrich), α,α′-azoisobutyronitrile (AIBN) (98 %, Fluka) and *N,N*-methylene-bis(acrylamide) (MBA) (99 %, Fluka) were used for the synthesis of the pHEMA/PVP hydrogels. Water was purified by a Millipore MilliRO-6 Milli-Q gradient system (resistivity >18 MΩ cm).

2.2 Preparation and characterization of nanoparticles dispersions, o/w nanostructured fluid, and hydrogel

Calcium hydroxide nanoparticles were synthesized via a solvothermal process as reported in the literature [20]. This synthetic method lets us obtain colloidal calcium hydroxide already dispersed in ethanol.

Calcium lactate nanoparticles were synthesized starting from the aforementioned $Ca(OH)_2$ nanoparticles dispersions. Four milliliters of lactic acid was gradually added to the $Ca(OH)_2$ dispersion (500 mL, 10 g/L) and magnetically stirred in a flask at 25 °C for 1 h. The obtained slurry was sonicated and centrifuged, and then dried in oven at 110 °C for 72 h, under a N_2 atmosphere. The obtained powders were finally suspended in 2-propanol (4 g/L). The choice of 2-propanol as a dispersing medium for the nanoparticles is due to the fact that this solvent might be less prone to induce alterations of collagen as compared to ethanol because of the lower polarity, and some alteration of the leather surface was observed during spot tests using ethanol as opposed to 2-propanol.

The mixed calcium hydroxide–calcium lactate dispersions were prepared by dispersing $Ca(OH)_2$ powders (obtained by drying the $Ca(OH)_2$ nanoparticles dispersion in oven) in 2-propanol and mixing them with a calcium lactate nanoparticles dispersion in the same solvent. For practical applications, the hydroxide/lactate ratio was set to 2:1 (w/w, 2 g/L calcium hydroxide, 1 g/L calcium lactate).

SEM analysis on dried nanoparticles dispersions were carried out with a FEG-SEM ΣIGMA (Carl Zeiss, Germany), using an acceleration potential of 5 kV and a working distance of 5.3 mm.

FTIR analysis on the dried dispersions was carried out using a BIORAD FTS 40-PC spectrometer with a resolution of 4 cm^{-1} and 32 scans. The spectral range was 4000–400 cm^{-1}. Pellets were prepared by finely grinding and mixing the powders with KBr.

XRD on the dried dispersions was carried out using a XRD Bruker New D8 Da Vinci. The source is a Cu tube ($\lambda = 1.5418$ Å, 40 kV, 40 mA). Data were collected from 5° to 50° 2θ with a step size of 0.03° and a count time of 38.4 s. The XRD spectrum was analyzed using the database ICCD PDF-2.

Dynamic light scattering (DLS) measurements were taken directly on the nanoparticles dispersions with a 90Plus Particle Size Analyzer (Brookhaven Instrument Corporation). The light scattered from the sample was collected at 90° with the incident 659-nm laser light radiation. The measurements were taken at 25 °C. Particle size distributions were obtained from the fitting of the measured autocorrelation functions using the NNLS (nonnegatively constrained least squares) method [21].

Turbidimetry measurements were taken directly on the nanoparticles dispersions to evaluate their stability, using a Varian Cary 100 Bio Spectrophotometer, equipped with a Peltier Multi-block. The absorbance of the dispersion at 600 nm was measured as a function of time. Absorbance was assumed proportional to the system turbidity: The decrease in absorbance over time is due to particles aggregation and settling. Measurements were taken at 25 °C, using sealed quartz cuvettes with an optical path of 1 cm.

The EAPC o/w nanostructured fluid was prepared as reported in the literature [22]. The fluid is named EAPC after the two solvents contained in the system, i.e., ethyl acetate (EA) and propylene carbonate (PC).

The pHEMA/PVP gel was synthesized by free radical polymerization of HEMA monomer and the crosslinker MBA in a water solution containing linear PVP, as reported in the literature [13]. Hydrogel synthesis was carried out in

molds to obtain flat hydrogel films having 2 mm thickness. After polymerization, hydrogels were washed and placed in containers filled with distilled water. The water was renewed twice a day for 7 days to remove any residue of unreacted monomer and the free PVP. Then, the gels were loaded with the EAPC o/w fluid through immersion for 12 h before application on the artifacts.

2.3 Applicative tests on modern and historical samples

The gel, nanostructured cleaning fluid, and nanoparticles dispersions were tested on both modern and historical leather samples. The modern sample (M1) was a vegetable-tanned (sumac) leather made from calfskin. Leaves from sumac shrub (*Rhus coriaria*) were among the most important vegetable source for tanning leather [1]. The sample was tested as received. The first historical sample (H1) was the cover of a Luther Bible (1749 AD). The second historical sample (H2) was the cover of a *Missale Romanum* (Roman Missal, 1725 AD). The historical samples exhibited surface deposits of dirt, salts, or waxy (or lipid) materials, which needed to be removed.

The cleaning tests were carried out by applying sheets of the pHEMA/PVP gel, loaded with the EAPC fluid, directly on the surface of the samples. Application time was 20 min. During application, the gel was covered with a foil of Mylar®, to prevent evaporation of the volatile components of EAPC. After the application, the gel was removed, and no further mechanical action was carried out on the sample surface. Then, a gel simply loaded with water was applied for 20 min on the cleaned area to remove residues from the nonvolatile components of EAPC (i.e., SDS surfactant). The presence of gel residues over the surface was checked with ATR-FTIR performed on the leather samples after the application and removal of the gels. A Thermo Nicolet Nexus 870 FTIR spectrometer equipped with a Golden Gate diamond ATR was used. The spectra were obtained from 128 scans with 4 cm^{-1} of optical resolution, in the 4000–650 cm^{-1} range. For each sample, five spectra (from five different spots) were collected.

For each leather sample, the nanoparticles dispersions were applied on several areas of ca. 2 × 2 cm^2, dripping 30 μL in 2–3 steps over each spot, with a Gilson P200 pipette.

Surface pH measurements on leather samples were taken in situ using a WTW pH 3310 SET 2 pH meter, equipped with a SenTix®41 electrode. Each measurement spot (1 × 1 cm^2) was damped with a droplet of water using a pipette. After 2-min extraction, the electrode was placed on the surface and the pH of the water film was measured. The pH value was obtained as the average between 2 measurements (being the leather surface highly water sensitive, it was not possible to carry out numerous measurements on each spot).

Surface examination of the leather samples before and after treatments was made using a FEG-SEM (Philips XL30 FEG-SEM–FEI, Eindhoven, Netherlands). For each leather sample, a small piece (0.5 mm^2) was cut and fixed, with the grain side up, on a standard SEM Al stub and gold–palladium sputter coated at 20 mA and 1.25 kV for a minute and half (Palaron E5000 sputter coater). The images were obtained at 5 keV acceleration voltage and a spot size of 3 μm at three different locations for each sample.

Controlled environment dynamic mechanical analysis (DMA-RH) was used to evaluate the mechanical properties of the leather samples under selected conditions of RH using the Triton 2000 DMA together with the Triton Technology humidity generator and controller. DMA-RH measures the variation in elastic (or storage) modulus E' and inelastic (or loss) modulus E'' and changes in viscoelasticity with changes in RH, as moisture is taken in and lost by the material at a programmed rate. The samples were measured in tension, and this also gave a measure of the sample displacement (D %) under a selected strain and relative humidity. All the analyses were carried out on samples from a well-defined and small area for each leather object (modern leather, historical leathers). The same sample was not analyzed by DMA-RH before and after treatment; however, the samples came from the same location in the hide, and all were measured in the head to tail direction. Samples (15 mm × 5 mm) were pre-dried for 24 h before measurement and then mounted in the tensile mode in the DMA analyzer. The sample chamber was set to 20 % RH, and the sample remained at 20 % RH for at least 30 min. The RH was then increased at 1 %/min until it reached 80 % RH. More than one sample was measured (from same location and in the head to tail direction), and variability in calculated slope (D %/RH) was ±5 %.

3 Results and discussion

3.1 Characterization of the nanomaterials

The calcium hydroxide nanoparticles synthesized via a solvothermal process and used for the tests are hexagonal platelets that exhibit a bimodal size distribution, with one population having a mean hydrodynamic diameter of ca. 80 nm, and the second population having a mean of ca. 220 nm. The thickness of particles is 20–30 nm. The platelets are highly crystalline, the crystalline form being portlandite [20].

Calcium lactate was synthesized in the form of irregular particles with an average dimension of 400–500 nm as

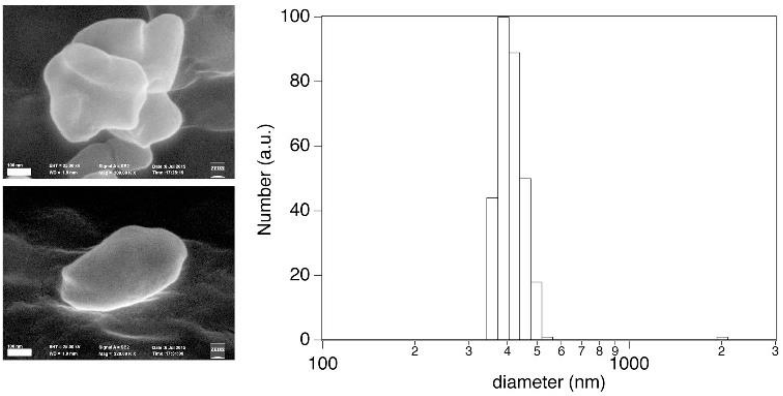

Fig. 1 *Left* SEM image of calcium lactate nanoparticles (dry powders). *Bar* is 100 nm. *Right* DLS analysis of a dispersion of calcium lactate nanoparticles in 2-propanol

shown by SEM analysis. The DLS analysis carried out on the particles dispersion in 2-propanol confirmed the presence of a main population with a size of 350–500 nm and a small portion of micrometric particles, consistently with SEM data (see Fig. 1). The FTIR spectrum of the dried dispersions shows all the characteristic peaks of calcium lactate: a broad band centered at 3360 cm^{-1} (νOH), and peaks at 2990, 2936, 2885 cm^{-1} ($\nu_s CH_3$, $\nu_{as} CH_3$, νCH), 1583 cm^{-1} ($\nu_{as} CO_2^-$), 1485, 1470, 1431 cm^{-1} ($\delta_{as} CH_3$, $\delta_{as} CH_3$, $\nu_s CO_2^-$), 1388, 1368, 1318 cm^{-1} (δ_{AL}OH, $\delta_s CH_3$, δC–H), 1270 cm^{-1} (δC–H), 1130 cm^{-1} ($\rho CH_3 + \nu_{AL}$C–O), 1090, 1047 cm^{-1} (ν_{AL}C–O), 930 cm^{-1} (rCH_3), 864 cm^{-1} (νC–CO_2^-), 778 cm^{-1} (δCO_2^-), 551 cm^{-1} (wCO_2^-), 434 cm^{-1} (rCO_2^-) [23, 24]. The band at 667 cm^{-1} is assigned to the Ca–O mode. The peak at 3642 cm^{-1} is characteristic of calcium hydroxide (νOH). Consistently, the XRD spectrum shows the peaks of crystalline $Ca(OH)_2$ (*portlandite*), as well as broad bands that indicate the presence of amorphous domains (see Fig. 2). Therefore, we hypothesize that the preparation method led to the formation of particles with a crystalline core of calcium hydroxide, and a shell consisting of amorphous calcium lactate. Turbidimetry measurements showed that the absorbance of the nanoparticles dispersion at 600 nm did not decrease significantly in the first 2 h after preparation. Moreover, no significant particles aggregation was observed even after days following the preparation of the dispersion, with only minimal aggregation that was reversible upon slight mechanical agitation.

Mixing the calcium hydroxide and calcium lactate nanoparticles dispersions (see Sect. 2.2) did not hinder their stability.

The o/w nanostructured fluid EAPC has been fully characterized in previous studies. The system's water content is ca. 73 %, the rest being solvents (ethyl acetate, propylene carbonate), surfactant SDS, and 1-pentanol (as a co-surfactant). A small-angle neutron scattering study recently detailed the structure of this system, showing that EAPC is neither a "classical" microemulsion (i.e., where the solvents are only found as confined in nanosized droplets dispersed in the aqueous phase) nor a simple micellar solution. In EAPC, both ethyl acetate and propylene carbonate are partitioned between the continuous phase (water) and the dispersed droplets, which also accounts for the

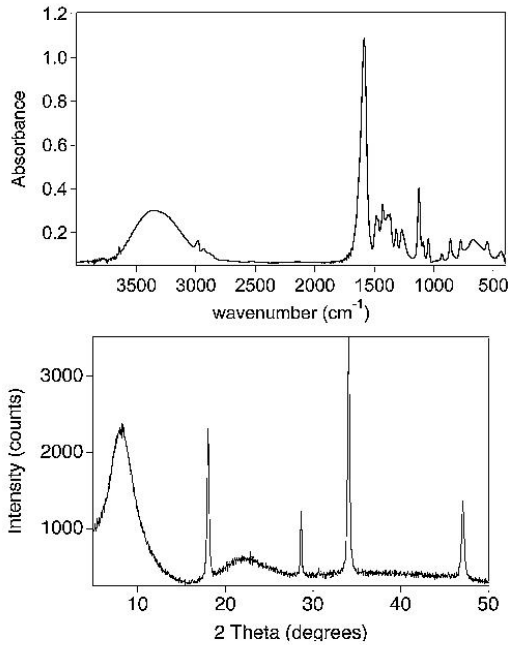

Fig. 2 FTIR spectrum (*top*) and XRD pattern (*bottom*) of calcium lactate nanoparticles (dry powders)

versatility and the effectiveness of this fluid in removing different types of coatings from the surface of works of art [22].

Three formulations of semi-IPN pHEMA/PVP chemical hydrogels have also been characterized in the literature [12, 13]. The formulations differ in the monomer/crosslinker and pHEMA/PVP ratios, which result in different porosities (both macro-porosity and micro-porosity), equilibrium water content, and water release rate. The formulation selected for this study ("H58") represents a balance that was deemed optimal for application on collagen-based artifacts. The formulation with the highest release rate could be risky in that it might cause excessive wetting, which is detrimental to collagen. The formulation with the lowest release rate was not selected as it might prove too slow in removing hydrophilic surface dirt or other unwanted layers.

3.2 Application of the nanomaterials to leather

Sample M1 (see Fig. 3) is vegetable-tanned modern leather that was tested exclusively to investigate the effects of the treatment with the H58 gel (loaded with EAPC) and with dispersions of alkaline nanoparticles in 2-propanol on collagen in pristine conditions, i.e., one that did not undergo natural aging. The gel was applied on the sample grain side, i.e., the external side normally exposed to aging and pollution. Then, the mixed calcium hydroxide–calcium lactate nanoparticles dispersion was applied by dripping. The FEG-SEM analysis of the sample shows that the nanoparticles are homogeneously distributed on the leather surface following the treatment (see Fig. 4).

Fig. 3 M1 sample (modern leather, vegetable tanned, 10 cm × 15 cm) before (*bottom*) and after (*top*) treatment with a H58 gel (loaded with EAPC) and a mixed calcium hydroxide–calcium lactate nanoparticles dispersion in 2-propanol

The applied quantity was finely tuned to adjust the pH from 3.6 up to 4.5, which is considered to be an optimal value for leather substrates. It must be noticed that when only calcium lactate nanoparticles were used (i.e., not mixed with calcium hydroxide), significantly larger quantities of dispersion or highly concentrated dispersions were needed to reach the ideal pH values (ca. 4.5), which might not be feasible in practical applications, for instance due to the risk of forming white veils on the surface.

ATR-FTIR was carried out before and after the treatment with the H58 gel and the nanoparticles (see Fig. 5). The spectrum of the untreated sample shows the following bands, assigned either to collagen or to tannins: 3414 cm^{-1} (νOH tannins), 3279 cm^{-1} (νN–H), 3075 cm^{-1} (δNH_2 overtone), 2921, 2852 cm^{-1} ($\nu_{as}CH_3$, ν_sCH_3, ν_sCH_2), 1712 cm^{-1} (νC=O tannins), 1650 cm^{-1} (amide I), 1621 cm^{-1} (aromatic ring stretch vibrations, tannins), 1548 cm^{-1} (amide II), 1513 cm^{-1} (aromatic ring skeletal vibration, tannins), 1448 cm^{-1} (δCH_2, δCH_3, aromatic ring stretch vibrations, tannins), 1320 cm^{-1} (ν_sC–O, tannins), 1174 cm^{-1} (νC–O, tannins), 1112, 1077 cm^{-1} (ethereal C–O asymmetric stretching, tannins), 1030 cm^{-1} (νC–O, tannins) [25–28]. The bands at 923, 910, 867, and 755 cm^{-1} are also ascribed in the literature to the presence of tannins and might be assigned to aromatic C–H out-of-plane and C–H rocking vibrations. The bands at 2950 cm^{-1} (νCH) and the shoulder at 1736 cm^{-1} (νC=O) might be ascribed to the presence of waxy or lipid material, which can be found as a finish layer on leather.

In the spectrum of the treated sample, the band at 3642 cm^{-1} (νOH, $Ca(OH)_2$) confirms the presence of the alkaline nanoparticles. The increased intensity of bands at 3011 cm^{-1} (not clearly observable before treatment) and 1467 cm^{-1} (νC–H aromatics, tannins) [25] suggests that the treatment resulted in the partial removal of a surface finish coating originally laid over the tanned leather surface. This is also suggested by the discoloration (darkening) of the sample following the treatment (see Fig. 3). It must be noted that in this case the aesthetic alteration due to the finish removal is not of concern, as the model leather sample was treated exclusively to check the compatibility between the applied nanomaterials and the collagen, as verified through FTIR and DMA-RH (see below).

The amide II band is hidden by two peaks at 1577 ($\nu_{as}CO_2^-$, calcium lactate) and 1542 cm^{-1} ($\nu_{as}COO$ carboxylate), which can be ascribed to the presence of calcium lactate nanoparticles and of carboxylate groups, the latter

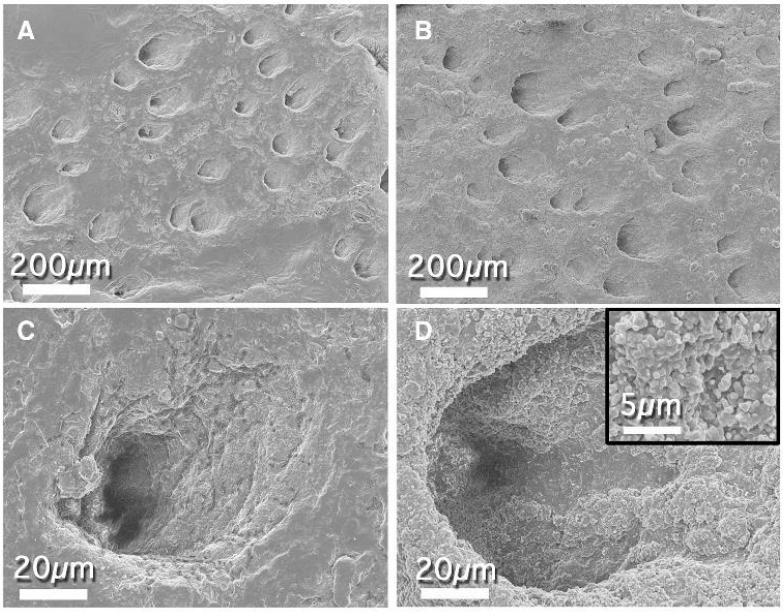

Fig. 4 FEG-SEM images of the M1 sample (modern leather, vegetable tanned). **a**, **c** Before treatment with nanomaterials. **b**, **d** After treatment with a H58 gel (loaded with EAPC) and a mixed calcium hydroxide–calcium lactate nanoparticles dispersion in 2-propanol. The *inlet* in panel **d** shows a detail of the nanoparticles distributed on the leather surface

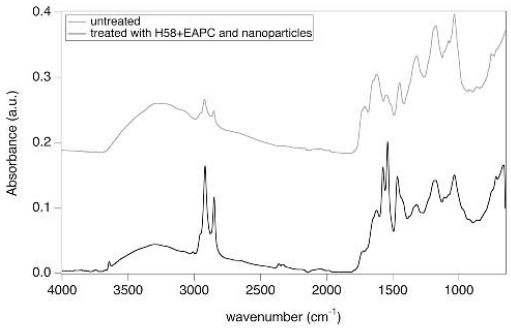

Fig. 5 ATR-FTIR spectrum of the M1 leather sample. *Top* untreated sample. *Bottom* sample treated with a H58 gel (loaded with EAPC) and then with a mixed dispersion of calcium lactate–calcium hydroxide nanoparticles in 2-propanol

possibly formed following the partial neutralization of acids present in the tannins.

No bands ascribable to SDS (1084 cm^{-1}, $\nu_s SO_2$) or to the H58 gel (1724 cm^{-1}, νC=O of HEMA) are observable in the spectrum, confirming that the application of the gel loaded with EAPC did not leave any residue (as detectable via FTIR) on the surface of the sample.

DMA-RH analysis was used to obtain the rate of sample displacement (*D* %) with RH, a useful damage marker for collagen-containing materials. The procedure was

Fig. 6 H1 sample (Luther Bible cover, 1749 AD) before (*bottom*) and after (*top*) treatment with the pHEMA/PVP H58 gel (loaded with EAPC) and a mixed calcium hydroxide–calcium lactate nanoparticles dispersion in 2-propanol. The area on the *bottom* shows the dull grayish surface patina of dirt, salts, and pollutants. The area on the *top* shows the removal of the patina to reveal the underlying heterogeneous leather surface

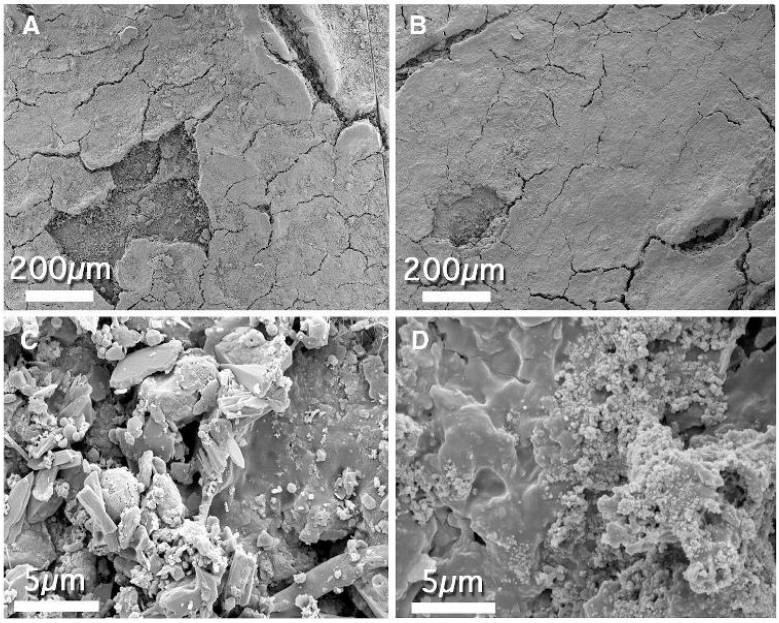

Fig. 7 H1 sample (Luther Bible cover, 1749 AD). **a**, **c** Before treatment. Panel **c** details the presence of salts, dirt deposits, and signs of biological contamination on the surface. **b**, **d** Images of the sample after treatment with the pHEMA/PVP H58 gel (loaded with EAPC) and a mixed calcium hydroxide–calcium lactate nanoparticles dispersion in 2-propanol. Panel **d** shows the reduction of salts, dirt, and biological contamination after the treatment, as well as the presence of nanoparticles on the surface

originally developed in the IDAP project for damage assessment of collagen in collagen-containing parchment samples [29]. There it was demonstrated that samples that underwent natural or accelerated aging exhibited a lower rate of displacement (expansion) than undamaged samples [29]. Elsewhere, a correlation has been demonstrated between the shrinkage temperature (T_s) and D % for thermally aged parchment samples. Lower T_s values and therefore lower D % values indicate damage to collagen [30]. Reduction in D % values was also correlated with

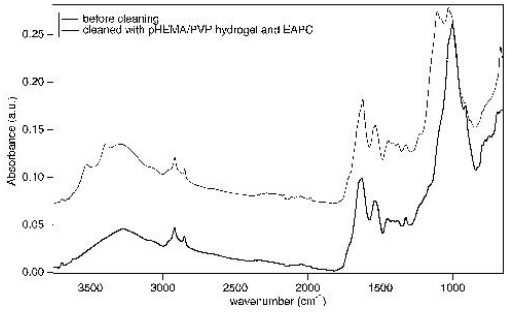

Fig. 8 ATR-FTIR spectrum of H1 sample (Luther Bible cover, 1749 AD). *Top* untreated sample. *Bottom* sample treated with a pHEMA/PVP H58 gel (loaded with EAPC)

Fig. 9 H2 sample (Roman Missal cover, 1725 AD) before (*bottom*) and after (*top*) treatment with the pHEMA/PVP H58 gel (loaded with EAPC) and a mixed calcium hydroxide–calcium lactate nanoparticles dispersion in 2-propanol. The area on the *bottom* shows the presence of surface dirt. The area on the *top* shows the removal of the *white–gray* surface patina of dirt enhancing the underlying leather surface

reduction in extent of coverage of sample with intact *D*-banding (as observed from AFM studies), which indicates loss of structure in the collagen fibrils [30].

DMA-RH data obtained on the M1 sample showed that there were no significant changes in the rate of displacement, before and after the treatment with gel and nanoparticles. Where minor changes were observed, they occurred in a direction opposite to that which typically occurs in aged samples.

The H1 sample (Luther Bible cover, 1749 AD) exhibited a grayish surface patina of gypsum, biological contaminants (spores and hyphae), and dirt deposits, which was removed using the H58 gel loaded with EAPC (see Figs. 6, 7). The presence of waxy or lipid surface material cannot be excluded, even though it was not possible to detect it clearly through FTIR.

In fact, using the gel simply loaded with water did not allow the effective removal of the patina. It is also possible to load the gel with ethanol or with ethanol/water mixtures [12]; however, cleaning tests carried out in the present work showed that the use of ethanol is detrimental to the leather surface, producing small cracks across the treated area.

The patina was removed applying the gel loaded with the EAPC fluid, with no additional mechanical action required. After the removal of the patina, the subsequent application of the mixed calcium lactate–calcium hydroxide nanoparticles dispersion adjusted pH from 4.0 to 4.6. It is important to notice that the surface patina must be removed prior to application of the nanoparticles dispersion to favor the penetration of particles and avoid the formation of white veils.

The ATR-FTIR spectrum of the sample before treatment (Fig. 8) clearly shows the absorption bands of gypsum at 3525, 3398 cm^{-1} (νOH), 1619 cm^{-1} (δOH), 1111 cm^{-1} (asymmetric stretching vibrations of SO_4^{2-}), and 669 cm^{-1} (symmetric bending of SO_4^{2-}) [31, 32]. These absorptions are no longer observable in the spectrum of the sample after treatment with the gel, while the bands of collagen and tannins can be clearly observed, which confirmed the effective removal of the surface patina. Also in this case, no bands ascribable to SDS (1084 cm^{-1}, $\nu_s SO_2$; 1227 cm^{-1} $\nu_{as} SO_2$; 1471 cm^{-1}, δCH_2) or to the H58 gel are observable in the spectrum.

The DMA-RH analysis on sample H1 showed that the rate of displacement (*D* %) versus RH is the same for the untreated sample and the sample treated with the gel and the nanoparticles, indicating that there is no further damage to the collagen resulting from the treatment.

Sample H2 (Roman Missal cover, 1725 AD) exhibits a white–gray surface patina of dirt, which was removed using the H58 gel loaded with EAPC (see Fig. 9). Also in this case, the use of the gel simply loaded with water was not effective, and the use of ethanol or ethanol/water mixtures proved detrimental to the leather surface. The FEG-SEM analysis showed a smoother surface following

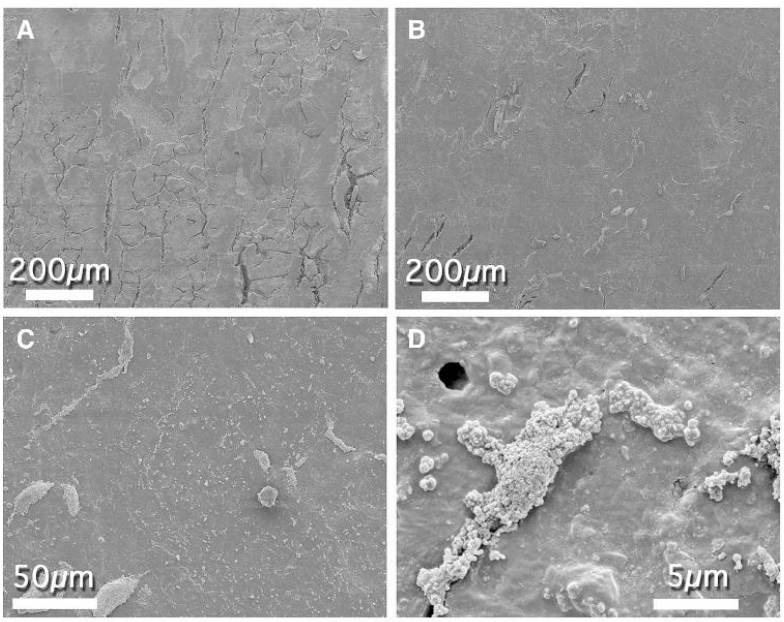

Fig. 10 FEG-SEM images of H2 sample (Roman Missal cover, 1725 AD). **a** Before treatment. **b–d** After treatment with the pHEMA/PVP H58 gel (loaded with EAPC) and a mixed calcium hydroxide–calcium lactate nanoparticles dispersion in 2-propanol. Panel **c** and **d** detail the presence of the particles on the surface

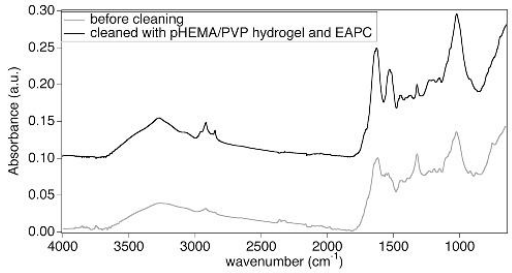

Fig. 11 ATR-FTIR spectrum of leather sample H2 (Roman Missal cover, 1725 AD). *Top* untreated sample. *Bottom* sample treated with a pHEMA/PVP H58 gel (loaded with EAPC)

the treatment, where dirt deposits are reduced and nanoparticles are distributed on the surface, in some cases also forming clusters (see Fig. 10).

In the ATR-FTIR spectrum of the sample after treatment with the H58 gel (Fig. 11), the increased intensity of bands at 2921 and 2852 cm^{-1} ($\nu_{as}CH_3$, ν_sCH_3, ν_sCH_2), and peaks at 1650 cm^{-1} (amide I), 1530 cm^{-1} (amide II), and 1029 cm^{-1} (νC–O, tannins) confirmed the removal of the surface patina that covered the original tanned leather surface.

After the removal of the patina, the subsequent application of the mixed calcium lactate–calcium hydroxide nanoparticles dispersion adjusted pH from 4.1 to 4.7. The removal of the surface patina favored the penetration of the particles, avoiding the formation of white veils.

DMA-RH data for sample H2 showed an increase in the measured rate of displacement over the RH range (40–60 %). The increase in the *D* % value for the treated samples as compared to the untreated one indicates an improvement in the mechanical properties and confirms that the treatment did not cause damage to the collagen.

4 Conclusions

Chemical hydrogels loaded with an o/w nanostructured cleaning fluid were used for the first time to remove surface patinas of dirt and salts (possibly including waxy or lipid material) from the surface of historical leather objects. The use of gels allows the controlled release of water-based cleaning fluids, avoiding damage to the collagen.

After the removal of the unwanted surface layers, it is possible to apply dispersions of alkaline nanoparticles (calcium lactate mixed with calcium hydroxide) to adjust the surface pH of leather to its typical value of ca. 4.5, avoiding excessive alkalinity that might be detrimental to collagen and the collagen–tannin complex.

Results from DMA-RH show that for the treated samples there is no decrease in the *D* %/RH parameter, indicating that there is no negative effect of the treatment on the state of the collagen.

In some cases, the increase in the *D* %/RH value shows improvement in the mechanical performance of the leather samples, as the frictional resistance to the movement of the fibers with moisture uptake is reduced.

The obtained results may open new perspectives in the conservation of collagen-based artifacts.

Acknowledgments CSGI, MIUR, and European Union (project NANOFORART, FP7-ENV-NMP-2011/282816) are acknowledged for financial support.

References

1. M. Kite, R. Thomson, *Conservation of Leather and Related Materials* (Elsevier, Oxford, 2006)
2. P. Fratzl, *Collagen: Structure and Mechanics* (Springer, Berlin, 2008)
3. R. Thomson, Leather, in *Conservation Science: Heritage Materials*, ed. by E. May, M. Jones (The Royal Society of Chemistry, Cambridge, 2006), p. 92
4. E. Haslam, Vegetable tannins, in *Encyclopedia of Life Sciences* (Wiley, 2001). 10.1038/npg.els.0001913
5. A.D. Covington, *Tanning Chemistry: The Science of Leather* (The Royal Society of Chemistry, Cambridge, 2009)
6. Improved Damage Assessment of Parchment—IDAP. Assessment, Data Collection and Sharing of Knowledge. European Commission Research Report No. 18. Edited by René Larsen, The Royal Danish Academy of Fine Arts, School of Conservation, Copenhagen, Denmark, © European Communities, 2007
7. K.M. Axelsson, R. Larsen, D. Sommer, J. Cult. Herit. **13**, 128 (2012)
8. R. Giorgi, M. Baglioni, D. Berti, P. Baglioni, Acc. Chem. Res. **43**, 695 (2010)
9. M. Baglioni, R. Giorgi, D. Berti, P. Baglioni, Nanoscale **4**, 42 (2012)
10. P. Baglioni, E. Carretti, D. Chelazzi, Nat. Nanotechnol. **10**, 287 (2015)
11. M. Raudino, G. Selvolini, C. Montis, M. Baglioni, M. Bonini, D. Berti, P. Baglioni, A.C.S. Appl, Mater. Interfaces **7**, 6244 (2015)
12. J. Domingues, N. Bonelli, R. Giorgi, P. Baglioni, Appl. Phys. A **114**, 705 (2014)
13. J. Domingues, N. Bonelli, R. Giorgi, E. Fratini, F. Gorel, P. Baglioni, Langmuir **29**, 2746 (2013)
14. J.H. Bowes, R.H. Kenten, Biochem. J. **46**, 1 (1950)
15. R. Larsen, in *Environment Leather Project. European Commission DG XII. Research Report No. 6* (The Royal Danish Academy of Fine Arts, School of Conservation, Copenhagen, 1996). ISBN 87 89730 07 0, p. 174
16. H. Benninga, *A History of Lactic Acid Making: A Chapter in the History of Biotechnology* (Springer, Berlin, 1990)
17. R. Giorgi, L. Dei, M. Ceccato, C. Schettino, P. Baglioni, Langmuir **18**, 8198 (2002)
18. R. Giorgi, D. Chelazzi, P. Baglioni, Langmuir **21**, 10743 (2005)
19. G. Poggi, R. Giorgi, N. Toccafondi, V. Katzur, P. Baglioni, Langmuir **26**, 19084 (2010)
20. G. Poggi, N. Toccafondi, L.N. Melita, J.C. Knowles, L. Bozec, R. Giorgi, P. Baglioni, Appl. Phys. A **114**, 685 (2014)

21. P.A. Hassan, S. Rana, G. Verma, Langmuir **31**, 3 (2015)
22. M. Baglioni, D. Rengstl, D. Berti, M. Bonini, R. Giorgi, P. Baglioni, Nanoscale **2**, 1723 (2010)
23. G. Cassanas, M. Morssli, E. Fabrègue, L. Bardet, J. Raman Spectrosc. **22**, 409–413 (1991)
24. Y. Chen, Y. Lin, Z. Peng, J. Lin, J. Phys. Chem. C **114**, 17720–17727 (2010)
25. E. Malea, S.C. Boyatzis, M. Kehagia, Cleaning of tanned leather: testing with Infra Red spectroscopy and SEM-EDAX, in *Joint Interim-Meeting of Five ICOM.CC Working Groups, Rome 2010*, ed. by M. Paris (ICOM-CC, 2010), p. 1
26. Chemical testing of textiles, ed. by Q. Fan (Woodhead Publishing Limited in association with The Textile Institute, CRC Press, Boca Raton, 2005)
27. N.M. Puica, A. Pui, M. Florescu, Eur. J. Sci. Theol. **2**(4), 49–53 (2006)
28. L. Falcão, M.E.M. Araùjo, J. Cult. Herit. **14**, 499–508 (2013)
29. M. Odlyha, C. Theodorakoulos, J. de Groot, L. Bozec, M. Horton, Thermoanalytical (macro to nanoscale) techniques and non-invasive spectroscopic analysis for damage assessment of parchment, in Improved Damage Assessment of Parchment—IDAP. Assessment, Data Collection and Sharing of Knowledge. European Commission Research Report No. 18. Edited by René Larsen, The Royal Danish Academy of Fine Arts, School of Conservation, Copenhagen, Denmark, © European Communities, 2007, p. 73
30. M. Odlyha, C. Theodorakoulos, J. de Groot, L. Bozec, M. Horton, e-PS **6**, 138–144 (2009)
31. V. Stefov, G. Jovanovski, B. Soptrajanov, B. Minceva-Sukarova, S. Dimitrovska, B. Boev, Geologica Macedonica **14**, 61–66 (2000)
32. G. Anbalagan, S. Mukundakumari, K. Sakthi Murugesan, S. Gunasekaran, Vib. Spectrosc. **50**, 226–230 (2009)